N° d'ordre NNT : 2018LYSE1117

THÈSE DE DOCTORAT DE L'UNIVERSITÉ DE LYON

opérée au sein de

l'Université Claude Bernard Lyon 1

en cotutelle avec

l'Université de Montréal

École Doctorale ED 476 Neurosciences et Cognition

En vue de l'obtention du grade de Docteur en Neurosciences

Faculté des Études Supérieures et Postdoctorales, École d'optométrie

En vue de l'obtention du grade de Philosophiae Doctor (Ph.D) en Sciences de la vision, option Neurosciences de la vision et psychophysique

Soutenue publiquement à Lyon le 28/06/2018, par :

Laura MIKULA

Intégration multisensorielle pour les mouvements de pointage chez les sujets sains et les patients avec ataxie optique

---

Devant le jury composé de :

VIGHETTO Alain	PU-PH, Université Lyon 1	Président du jury
VERCHER Jean-Louis	DR, Aix-Marseille Université	Rapporteur
MALFAIT Nicole	CR, Aix-Marseille Université	Rapporteure
FAUBERT Jocelyn	Professeur, Université de Montréal	Examinateur
MAMASSIAN Pascal	DR, Ecole Normale Supérieure Paris	Examinateur
PISELLA Laure	CR, Université Lyon 1	Co-directrice de thèse
KHAN Aarlenne	Professeure, Université de Montréal	Co-directrice de thèse

UNIVERSITÉ CLAUDE BERNARD - LYON 1

Président de l'Université	**M. le Professeur Frédéric FLEURY**
Président du Conseil Académique	M. le Professeur Hamda BEN HADID
Vice-président du Conseil d'Administration	M. le Professeur Didier REVEL
Vice-président du Conseil Formation et Vie Universitaire	M. le Professeur Philippe CHEVALIER
Vice-président de la Commission Recherche	M. Fabrice VALLÉE
Directrice Générale des Services	Mme Dominique MARCHAND

COMPOSANTES SANTÉ

Faculté de Médecine Lyon Est – Claude Bernard	Directeur : M. le Professeur G.RODE
Faculté de Médecine et de Maïeutique Lyon Sud – Charles Mérieux	Directeur : Mme la Professeure C. BURILLON
Faculté d'Odontologie	Directeur : M. le Professeur D. BOURGEOIS
Institut des Sciences Pharmaceutiques et Biologiques	Directeur : Mme la Professeure C. VINCIGUERRA
Institut des Sciences et Techniques de la Réadaptation	Directeur : M. X. PERROT
Département de formation et Centre de Recherche en Biologie Humaine	Directeur : Mme la Professeure A-M. SCHOTT

COMPOSANTES ET DÉPARTEMENTS DE SCIENCES ET TECHNOLOGIE

Faculté des Sciences et Technologies	Directeur : M. F. DE MARCHI
Département Biologie	Directeur : M. le Professeur F. THEVENARD
Département Chimie Biochimie	Directeur : Mme C. FELIX
Département GEP	Directeur : M. Hassan HAMMOURI
Département Informatique	Directeur : M. le Professeur S. AKKOUCHE
Département Mathématiques	Directeur : M. le Professeur G. TOMANOV
Département Mécanique	Directeur : M. le Professeur H. BEN HADID
Département Physique	Directeur : M. le Professeur J-C PLENET
UFR Sciences et Techniques des Activités Physiques et Sportives	Directeur : M. Y.VANPOULLE
Observatoire des Sciences de l'Univers de Lyon	Directeur : M. B. GUIDERDONI
Polytech Lyon	Directeur : M. le Professeur E.PERRIN
Ecole Supérieure de Chimie Physique Electronique	Directeur : M. G. PIGNAULT
Institut Universitaire de Technologie de Lyon 1	Directeur : M. le Professeur C. VITON
Ecole Supérieure du Professorat et de l'Education	Directeur : M. le Professeur A. MOUGNIOTTE
Institut de Science Financière et d'Assurances	Directeur : M. N. LEBOISNE

"It always seems impossible until it's done."

— Nelson Mandela

Résumé

Afin d'effectuer un mouvement de la main, le système nerveux doit mettre en commun des informations issues de plusieurs sens : c'est l'intégration multisensorielle. Le cortex pariétal postérieur est une interface sensorimotrice qui est impliquée dans le processus d'intégration multisensorielle. Si cette région est endommagée, les patients présentent un trouble visuomoteur dénommé ataxie optique qui se caractérise par une difficulté à réaliser des mouvements visuellement guidés de la main. À ce jour, les mécanismes qui sous-tendent l'intégration multisensorielle pour l'action ne sont pas encore totalement connus. Le premier axe de ma thèse consiste à définir, chez les sujets sains, comment les informations visuelles et somatosensorielles sont intégrées pendant la planification d'un mouvement de pointage. Le deuxième axe s'intéresse aux troubles sensorimoteurs associés à l'ataxie optique qui permettent une meilleure compréhension des fonctions du cortex pariétal postérieur dans la planification motrice et le contrôle du mouvement.

Mots-clés : vision, proprioception, intégration multisensorielle, ataxie optique, cortex pariétal postérieur

Intitulés et adresses des laboratoires :

- Centre de recherche en Neurosciences de Lyon (CRNL), Inserm U1028, CNRS UMR 5292, équipe ImpAct. 16 avenue du Doyen Lépine, 69676 Bron Cedex, France.
- École d'Optométrie de l'Université de Montréal, laboratoire VISATTAC. Pavillon 3744, rue Jean-Brillant, Montréal, QC H3T 1P1, Canada.

Abstract

To execute reach movements, the central nervous system needs to combine information from different sensory modalities, a process knows as multisensory integration. The posterior parietal cortex is a sensorimotor interface implicated in multisensory integration processes. Patients with a damage to this region exhibit a visuomotor deficit called optic ataxia. Patients with optic ataxia present difficulties in performing hand visually-guided movements. To date, the mechanisms underlying multisensory integration are still not fully understood. The first aime of my thesis is to determine how visual and somatosensory information are integrated in healthy participants, during the planning of pointing movements. I will then focus on the sensorimotor deficits observed in optic ataxia which enable a better understanding of the functions of the posterior parietal cortex in motor planning and online control.

Key-words : vision, proprioception, multisensory integration, optic ataxia, posterior parietal cortex

Remerciements

Cette thèse a reçu le soutien financier du Groupe de Recherche en Sciences de la Vision (GRSV), de la Faculté des études supérieures et postdoctorales et de l'École d'optométrie de l'Université de Montréal. Le Programme Avenir Lyon Saint-Étienne (PALSE) et le LabEx CORTEX ont également contribué à la réalisation de ce projet de thèse grâce aux bourses de mobilité qui m'ont été octroyées.

Je tiens tout d'abord à remercier les membres de mon jury de thèse : Alain Vighetto, Jocelyn Faubert, Pascal Mamassian ainsi que Nicole Malfait et Jean-Louis Vercher qui ont accepté d'endosser le rôle de rapporteurs et d'évaluer mon travail.

C'est ensuite tout naturellement que je me tourne vers vous, Laure et Aarlenne. Merci Laure d'avoir fait confiance à l'étudiante de M2 peu loquace que j'étais à mon arrivée au labo. Merci pour ta force tranquille qui m'a permis d'arriver plus sereinement que je ne l'aurais pensé jusqu'à la soutenance. Many thanks for all your support, Aarlenne. I am especially grateful for all the opportunities you offered me during these past four years now. Finally, thank you Gunnar for your valuable help in data analyses and your clever feedbacks on the papers. I was pleased to work with you three and I could not have imagined better mentoring. Thank you for making me a scientist and not just a student anymore.

Un grand merci aux ingénieurs de l'équipe ImpAct : Olivier, Roméo et Éric car sans vous pas d'expériences et pas de thèse... ou alors j'y serais encore ! Merci également à Romain qui m'a grandement aidée dans la mise en place de l'expérience et l'analyse des données à Montréal.

Je souhaiterais remercier chaleureusement l'ensemble de l'équipe ImpAct, en particulier les chercheurs et gestionnaires. Une pensée aux post-docs qui sont déjà passés par là : Delphine, Dollyane, Ouazna, Selene, Olga, Carole, Luke, Elvio et Moussa. Merci pour vos conseils, vos remarques bienveillantes ou simplement vos encouragements. Amélie, qui aurait cru 5 ans plus tôt qu'on suivrait la même voie ? Dans le même labo ?! Merci pour les bons moments de rigolade et de discussion. Un grand merci à Silvia, Éric, Clément, François, Alexis, Audrey D, Audrey V, Simon, Leslie, Margaux, Anne et Grégoire pour les

repas et conversations du midi disons animés ! Sans oublier Judith, Salam (et ses pâtisseries libanaises), Samy et Lisa.

One of the best things about the cotutelle is getting to meet people that make Canada feel kinda like home. I would like to thank my vision sciences buddies : Bruno, my girl Robyn, Thomas, Umit, Reza, Jimmy, Khash, Azadeh, Will and Nelson. Thanks for your friendship and all the food, birthday cakes and laughs you have brought into my Montreal life. Un immense merci à Marilyn, Trang et Sofia avec qui j'ai pu travailler au laboratoire VISATTAC et une pensée pour Anton, Julie, Paul et Romain que j'ai pu rencontrer plus tard et qui ont su mettre de la vie dans un lab pratiquement vide à mon arrivée.

Du côté personnel, je souhaiterais remercier tout particulièrement Steven, ma Lau, Mö , Coco, Wai, Gui, ma miniona Vaea et Tommy. La team gros lardos ! Merci de m'avoir supportée pendant ces nombreuses années d'études et d'être toujours là, fidèles au poste. Les amis sont la famille que l'on choisit et vous êtes ma famille de tahitiens-lyonnais, ceux avec qui je passe mes week-ends et mon temps libre hors du labo. Sans oublier ceux avec qui on a aussi fait un bout de chemin à Lyon : Cocotte, Djenna, Nadège, notre Bruno Tamars, le mei'a Lloyd et Cédric le black swan.

Qu'aurait été l'université sans danse ni atelier chorégraphique ? Beaucoup de belles rencontres : Jaouad, Emmanuel, Sonia, Thomas, Smael, Sylvain, Louise, Morgane, Octave, Aymeric et tous les autres, parce qu'en 8 ans j'en ai croisé des personnes ! Enfin merci Dom d'avoir encadré tout ce joyeux monde et de m'avoir donné l'opportunité de m'exprimer à travers la danse en cours, sur scène ou dans des endroits plus insolites !

Et pour finir, mention spéciale pour ma famille. Mon frère qui « m'encourage » à sa façon, ma soeur avec qui j'ai pu passer plus de temps à Montréal et mes grands-parents qui sont toujours fiers de moi quoi que j'entreprenne. Et enfin merci Papa et Maman de vous intéresser à mon travail pas toujours très compréhensible, de m'avoir toujours soutenue et encouragée à faire ce que j'aime et surtout de m'avoir laissée partir à l'autre bout de monde, littéralement, pour réaliser tout ça !

Liste des abréviations

AIP Aire intrapariétale antérieure
aIPS Partie antérieure du sillon intrapariétal
CGL Corps géniculé latéral
CPP Cortex pariétal postérieur
CS Colliculus supérieur
IPS Sillon intrapariétal / *Intraparietal sulcus*
IRMf Imagerie par résonance magnétique fonctionnelle
JPO Jonction pariéto-occipitale
LIP Aire intrapariétale latérale
LPI Lobule pariétal inférieur
LPS Lobule pariétal supérieur
M1 Cortex moteur primaire
MIP Aire intrapariétale médiane
mIPS Partie médiane du sillon intrapariétal
pIPS Partie postérieure du sillon intrapariétal
PM Cortex prémoteur
PRR *Parietal reach region*
SMT Stimulation magnétique transcrânienne
SNC Système nerveux central
SPOC Cortex pariéto-occipital supérieur / *Superior parieto-occipital cortex*
STCC Stimulation transcrânienne à courant continu
TEP Tomographie par émission de positons
V1 Cortex visuel primaire

Liste des figures

Sommaire

1 Introduction

1.1 Les sens et l'intégration multisensorielle

1.1.1 Qu'est-ce qu'un sens ?

Un sens désigne la faculté grâce à laquelle une forme d'énergie particulière (appelée **stimulus**) est perçue. Les organes sensoriels possèdent des capteurs capables de répondre à un stimulus spécifique. Si l'on prend l'exemple de la vision, les récepteurs qui lui sont spécifiques sont les cônes et les bâtonnets. Ces cellules réceptrices tapissent la rétine et captent l'énergie lumineuse. Une fois absorbée, l'énergie est convertie en signaux électriques, appelés **potentiels d'action**, afin que l'information puisse se propager en direction du système nerveux. En fonction de leur nature, les stimuli sensoriels sont aiguillés vers différentes régions du cerveau qui sont chacune spécifique d'une modalité sensorielle donnée ; on parle de **cortex sensoriels primaires**. Les informations sensorielles sont traitées et interprétées par le cortex sensoriel primaire qui leur est dédié afin de donner naissance à une perception.

Depuis l'Antiquité, il est admis que l'Homme possède cinq sens que sont la vision, l'audition, le toucher (ou tact), l'odorat et le goût. Bien que ces sens soient les plus communément décrits, on s'accorde maintenant à penser que nous en possédons davantage. La nociception, par exemple, est le sens qui nous permet de percevoir la douleur. La thermoception correspond à notre aptitude à percevoir la température tandis que l'équilibrioception fait référence au sens de l'équilibre. Enfin, la **proprioception** désigne notre capacité à pouvoir situer les parties de notre propre corps les unes par rapport aux autres. La proprioception est un sens de position étroitement lié avec la motricité et fera par conséquent l'objet d'une description détaillée plus loin dans le manuscrit.

Les informations collectées au travers de nos différents sens, ou modalités sensorielles,

servent à construire une représentation du monde dans lequel nous évoluons. Cette représentation interne est indispensable pour avoir un comportement adapté et interagir de façon adéquate avec notre environnement.

1.1.2 Plusieurs sens mais une représentation unique

Un même objet présent dans l'environnement peut être perçu par différentes modalités sensorielles. Or chaque sens apporte une information particulière, qui lui est propre, à propos des caractéristiques de l'objet en question. De plus, les stimuli sont acheminés vers le cerveau via différentes voies spécifiques à chaque modalité. Malgré la relative ségrégation des informations sensorielles, notre perception n'est pour autant pas morcelée entre les différents sens. Ces observations suggèrent l'existence d'un mécanisme permettant de mettre en commun plusieurs stimuli sensoriels afin de former une représentation unique et cohérente de notre environnement.

Dès l'Antiquité, le philosophe Aristote proposa le terme de « sens commun » (*sensus communis*) afin de désigner la capacité à rassembler et coordonner les cinq sens qui étaient alors décrits à l'époque. Ainsi, le sens commun permettrait de combiner plusieurs informations sensorielles et les synthétiser pour former une **perception unifiée** du monde. De façon assez intéressante, il semblerait que le sens commun soit localisé au niveau du cerveau (Figure 1.1).

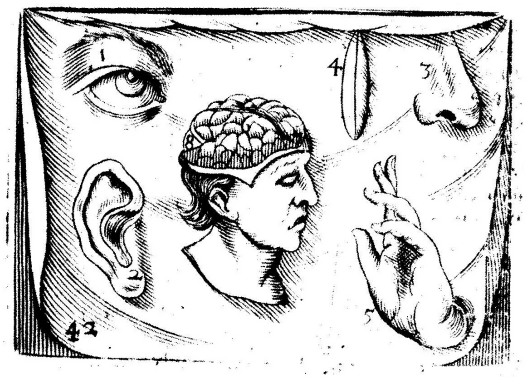

Figure 1.1 – Illustration de la notion de « sens commun » proposée par Aristote. Le sens commun permet de rassembler et coordonner l'ensemble des autres sens, il serait situé dans le cerveau. Reproduit depuis *Orbis Sensualism Pictus* (p.71), Johann Amos Comenius, 1659.

Dans le domaine des neurosciences, l'**intégration multisensorielle** est le terme utilisé pour faire référence à la combinaison d'informations issues de deux sens ou plus. Ainsi, les différentes modalités sensorielles interagissent entre elles et mettent en commun

les informations dont chacune dispose. L'intérêt de synthétiser les informations issues de plusieurs sens est de multiplier la quantité d'informations disponibles et utilisables par le système nerveux central (SNC). Au final, la représentation de l'environnement qui résulte de diverses informations sensorielles est beaucoup plus fiable, précise et donc robuste (Ernst & Bülthoff, 2004). L'intégration multisensorielle confère un certain nombre d'avantages comportementaux : elle permet de résoudre des ambiguïtés perceptives, d'augmenter la probabilité de détection des stimuli et de diminuer les temps de réaction moteurs (Bell et al., 2005 ; Gleiss & Kayser, 2012 ; Rowland et al., 2007).

1.1.3 L'intégration multisensorielle à l'échelle cellulaire

Historiquement, les modalités sensorielles ont d'abord fait l'objet de recherches séparées. Ce n'est donc que relativement récemment que les bases neuronales de l'intégration multisensorielle ont été explorées, notamment grâce à l'électrophysiologie. Au sein du système nerveux, on trouve des neurones dits **multisensoriels** qui répondent non pas à une mais à plusieurs modalités sensorielles. L'existence de ces neurones a d'abord été mise en évidence dans le colliculus supérieur (CS), une structure sous-corticale située dans le mésencéphale. Le CS est particulièrement impliqué dans les changements d'orientation du regard en réponse à des stimuli visuels. Les couches superficielles du CS sont principalement visuelles alors que dans les couches profondes, les neurones reçoivent et répondent à des stimulations visuelles, auditives et/ou somatosensorielles (Sparks & Hartwich-Young, 1989 ; Wallace et al., 1996). De ce fait, le CS fut le premier modèle pour l'étude de l'intégration multisensorielle

L'ensemble des neurones multisensoriels présente la particularité suivante : la réponse à une stimulation multimodale est drastiquement différente de celle évoquée par chacune des modalités sensorielles présentées séparément. Dans certains cas, la réponse neuronale multisensorielle peut surpasser la réponse unimodale la plus importante, voire même la somme arithmétique des réponses unisensorielles : on parle alors de **supra-additivité** (Meredith & Stein, 1986). À l'inverse, une réponse multisensorielle est qualifiée de **sub-additive** dans le cas où elle est inférieure à la somme des réponses unimodales (B. E. Stein

& Meredith, 1993). Les enregistrements électrophysiologiques des neurones du CS, principalement menés par Stein et son équipe, ont permis d'identifier certaines règles qui régissent les interactions multisensorielles.

Le but de l'intégration multisensorielle est de combiner les signaux originaires d'un même objet et de garder séparés ceux qui proviennent de sources distinctes. Pour cette raison, les processus d'intégration sont soumis à des contraintes à la fois spatiales et temporelles : deux modalités sont mises en commun s'il y a une **coïncidence spatiale et temporelle** entre les informations sensorielles (Meredith et al., 1987 ; Meredith & Stein, 1996). En effet, lorsque deux stimuli sont proches dans le temps et dans l'espace, ils sont davantage susceptibles d'appartenir à une même entité. L'intégration multisensorielle est également sujette à la règle d'**efficacité inverse**. Selon ce principe, la magnitude de la réponse multisensorielle est inversement proportionnelle à l'efficacité des stimuli qui sont intégrés (Meredith & Stein, 1986 ; B. E. Stein & Meredith, 1993). Autrement dit, les effets sont d'autant plus importants que les signaux sensoriels sont ambigus ou de faible intensité. Cette propriété permettrait au SNC de détecter et traiter les stimuli les moins saillants (B. E. Stein & Stanford, 2008).

Bien que particulièrement abondants dans le CS, les neurones possédant des champs récepteurs multisensoriels sont présents dans la majorité, si ce n'est la quasi-totalité des structures corticales et sous-corticales (Ghazanfar & Schroeder, 2006). En effet, il se trouve que des régions longtemps considérées comme unimodales (comme les cortex sensoriels primaires) comptent également des neurones capables de répondre à plusieurs modalités sensorielles (Sadato, 2005 ; Watkins et al., 2006 ; Zhou & Fuster, 2004). Cependant le nombre de neurones multisensoriels présents dans les aires primaires est nettement inférieur à celui dans les **aires associatives**, telles que le cortex pariétal, qui reçoivent des informations en provenance de plusieurs systèmes sensoriels (Colby & Duhamel, 1996 ; Duhamel et al., 1998 ; Murata et al., 2000).

1.1.4 Comment sont combinées les informations sensorielles ?

Selon le principe de l'intégration multisensorielle, les informations issues de chaque sens sont traitées par le SNC afin de maximiser la fiabilité de la perception (Ernst & Bülthoff, 2004 ; B. E. Stein & Meredith, 1993). Le problème qui se pose alors c'est que chaque modalité encode les informations sensorielles dans un format qui lui est propre. Par conséquent, l'intégration ne peut pas se faire par une simple moyenne des entrées sensorielles (Deneve & Pouget, 2004). En revanche, le **modèle bayésien** permettrait de décrire la manière dont les informations sensorielles sont combinées afin d'obtenir une estimation multimodale optimale (Battaglia et al., 2003 ; Ernst, 2006 ; O'Reilly et al., 2012).

Selon le modèle bayésien, le SNC combine les informations sensorielles redondantes en les pondérant par leurs fiabilités (ou précisions) respectives. Afin d'illustrer ce principe, prenons un exemple. Lorsque l'on doit estimer la position d'un objet dans l'espace sur la base d'une modalité sensorielle, l'estimation unimodale peut être représentée par une distribution de probabilité suivant une loi normale. Cette distribution est caractérisée par une moyenne $\overline{S}$ et une variance σ^2 (Figure 1.2A).

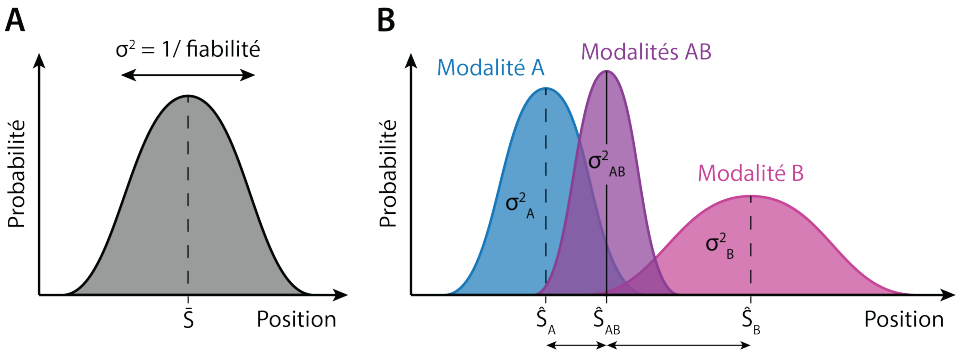

Figure 1.2 – Distributions de probabilité de la position d'un objet en fonction d'une ou plusieurs modalités sensorielles. A. Estimation unimodale. $\overline{S}$ correspond à la position de l'objet la plus probable tandis que σ^2 reflète l'incertitude de l'estimation et est inversement proportionnelle à la fiabilité de la modalité sensorielle. B. Estimation bimodale selon le modèle bayésien. La modalité A est plus précise et moins variable que la modalité B, par conséquent l'estimation bimodale $\hat{S}_{AB}$ est plus proche de l'estimation unimodale $\hat{S}_A$. De plus, la largeur et donc la variabilité de la distribution bimodale est réduite par rapport aux deux modalités A et B. Figure adaptée de O'Reilly et al. (2012).

$\overline{S}$ est associé à la probabilité la plus élevée (maximum de vraisemblance) et correspond à la position réelle de l'objet lorsque l'estimateur n'est pas biaisé. σ^2 représente l'incertitude de l'estimation et est inversement proportionnelle à sa fiabilité. Ainsi plus une distribution est large, plus la variance associée à la modalité correspondante est élevée. Supposons maintenant que non pas une, mais deux modalités sensorielles A et B informent sur la position de l'objet. Conformément au modèle bayésien, l'estimation multimodale $\hat{S}_{AB}$ est le résultat d'une moyenne pondérée des estimations unimodales ($\hat{S}_A$ et $\hat{S}_B$) en fonction de leurs fiabilités respectives, autrement dit l'inverse de leurs variances $\left(\frac{1}{\sigma_A^2} \text{ et } \frac{1}{\sigma_B^2}\right)$:

$$\hat{S}_{AB} = w_A \hat{S}_A + w_B \hat{S}_B$$

$$\text{avec } w_A = \frac{\frac{1}{\sigma_A^2}}{\frac{1}{\sigma_A^2} + \frac{1}{\sigma_B^2}} \quad \text{et} \quad w_B = \frac{\frac{1}{\sigma_B^2}}{\frac{1}{\sigma_A^2} + \frac{1}{\sigma_B^2}} \tag{1.1}$$

Le poids (w) attribué à chaque sens tient compte de sa fiabilité intrinsèque et permet d'accorder davantage d'importance aux informations sensorielles les plus précises. De ce fait, l'estimation bimodale $\hat{S}_{AB}$ est biaisée en direction de la modalité qui fournit l'estimation la moins variable, ici en l'occurrence la modalité A (Figure 1.2B). En effet, lors de la présentation d'indices visuels et auditifs légèrement décalés dans l'espace, il se trouve que les réponses perceptives sont biaisées vers la vision qui est considérée comme plus fiable (Bertelson & Aschersleben, 1998). En plus du biais perceptif, la théorie bayésienne prédit une variance de l'estimation bimodale (σ_{AB}^2) inférieure à celle associée à la modalité sensorielle la plus fiable :

$$\sigma_{AB}^2 = \frac{\sigma_A^2 \sigma_B^2}{\sigma_A^2 + \sigma_B^2} \tag{1.2}$$

Conformément à cette prédiction, on peut observer que la distribution de probabilité multimodale est moins large que celles des deux estimations unimodales (Figure 1.2B).

Question

L'intégration multisensorielle selon le modèle bayésien pondère chaque modalité sensorielle en fonction de sa variabilité intrinsèque. Ainsi, la modalité la plus fiable (la moins variable) se voit attribuer plus d'importance dans l'estimation multimodale. L'étude n°1 se place dans le contexte de la programmation motrice. Elle se propose d'examiner si, dans le cas de l'estimation de la position de la main avant un mouvement de pointage, les informations sensorielles sont pondérées en fonction de leur fiabilité comme le suggère le modèle bayésien.

Le cerveau fonctionne comme un estimateur du maximum de vraisemblance (maximum likelihood estimator) : il augmente la précision de l'estimation bimodale par le biais la pondération des signaux qui prend en compte le bruit, l'incertitude, la variabilité associée à chaque modalité sensorielle (Ernst & Banks, 2002). Les informations sont intégrées de manière « **statistiquement optimale** » puisque dès qu'une modalité est bruitée (diminution de la fiabilité), le poids qui lui est associé dans la moyenne pondérée diminue. Dans la mesure où chaque sens possède son propre domaine d'expertise, leur contribution relative dans l'intégration multisensorielle dépend non seulement de la tâche à effectuer mais également des autres signaux sensoriels disponibles.

1.2 Les mouvements de la main

1.2.1 Généralités

Les **mouvements volontaires**, sur lesquels je me concentrerai dans cet ouvrage, supposent l'intention et la décision d'agir. À la différence des mouvements réflexes qui sont sous le contrôle de circuits spinaux et peuvent être initiés en une dizaine de millisecondes, les mouvements volontaires font intervenir des réseaux corticaux supplémentaires. De ce fait, ils présentent des temps de réaction plus longs, généralement compris entre 200 et 500 ms. Les mouvements intentionnels sont sous le contrôle conscient du système nerveux mais sont gérés en grande partie par des processus de contrôle automatique. Il existe un large éventail de mouvements volontaires mais je ne décrirai ici en détail que les **mouvements dirigés** (c'est-à-dire vers un but spatial) de la main. Ces mouvements comprennent les gestes d'atteinte, de pointage mais également de saisie (préhension).

Le plus souvent, nous réalisons les gestes de la vie quotidienne sans avoir à y penser et avec une certaine aisance. Pourtant plusieurs étapes sont nécessaires à la réalisation d'un mouvement de la main, comme par exemple attraper une tasse de café (Figure 1.3). Tout d'abord, les informations sensorielles visuelles et proprioceptives sont utilisées pour localiser la tasse et la main. Puis une **commande motrice** est élaborée au niveau du cortex pariétal (Mountcastle et al., 1975) et des régions motrices du lobe frontal (Roland, 1993). Le cortex pariétal participe à la conversion des informations sensorielles en commandes motrices. Le cortex préfrontal est le siège de la planification abstraite et de la prise de décision, le cortex prémoteur coordonne les séquences motrices et enfin le cortex moteur envoie la commande qui permet l'exécution du mouvement. La commande motrice passe par la mœlle épinière via les **motoneurones** qui vont permettre la contraction des muscles nécessaires au déplacement du bras et de la main. Alors que le mouvement se déploie, des neurones sensoriels envoient des signaux ascendants au cerveau, appelés **retours** ou ***feedbacks*** sensoriels. Les retours sensoriels renseignent le cerveau sur ce qui se passe en périphérie, ce qui permet d'effectuer des corrections pendant l'exécution motrice si nécessaire ; on parle alors de **contrôle en ligne** du mouvement.

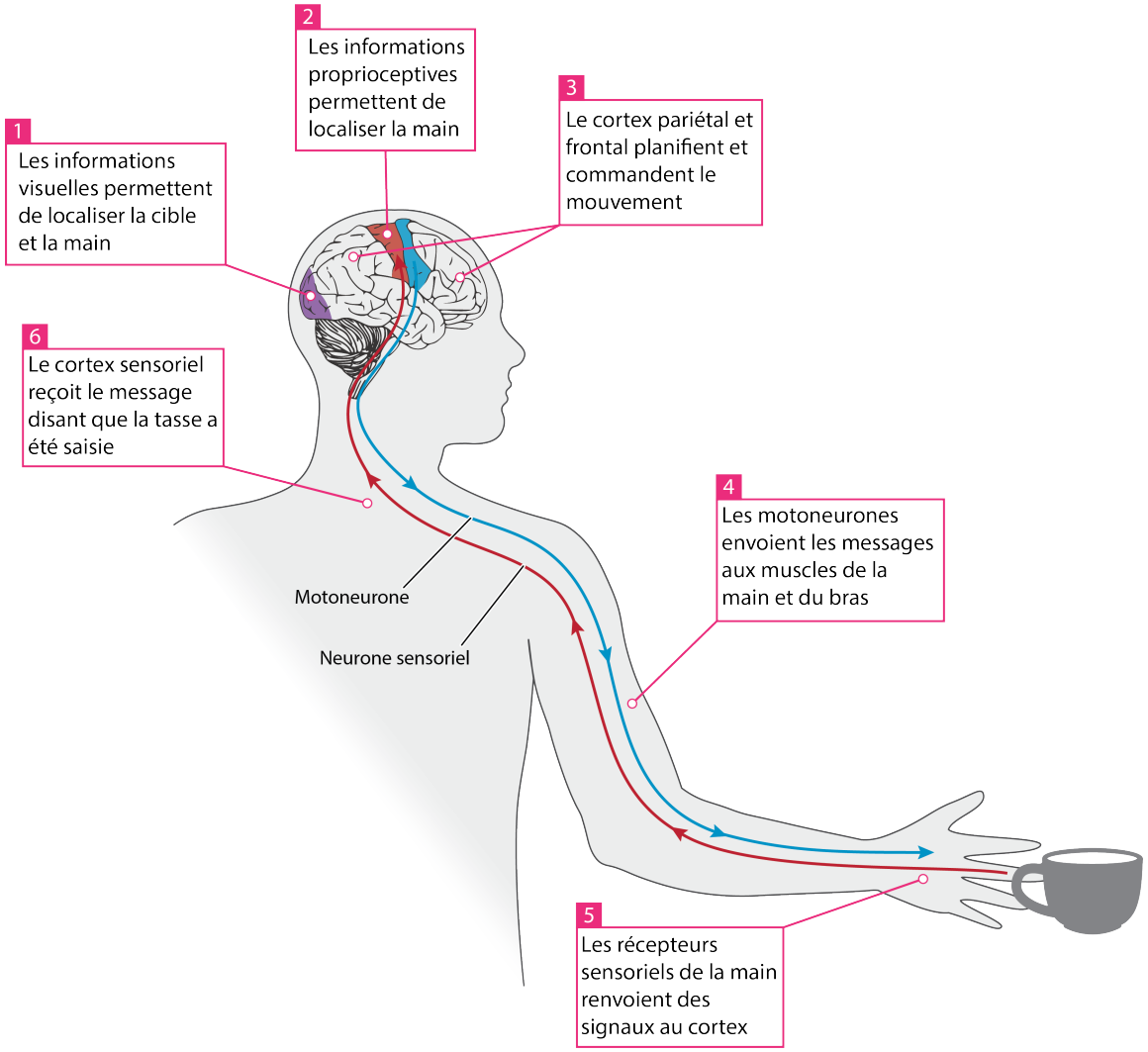

Figure 1.3 – Réalisation d'un mouvement volontaire de la main. Une fois la tasse et la main localisées grâce aux informations sensorielles, le cortex pariétal et les régions motrices du lobe frontal programment le mouvement. La commande motrice est envoyée aux muscles via les motoneurones. Au cours du mouvement, les informations sensorielles ascendantes informent le cerveau du déroulé de l'action.

1.2.2 La programmation du mouvement

La notion de **programmation motrice** regroupe l'ensemble des étapes précédant immédiatement l'initiation du mouvement, telles que la mise en place des paramètres initiaux du mouvement et l'élaboration de la commande motrice. La programmation motrice implique notamment le cortex pariétal postérieur (CPP). Dans cette partie, seront développées trois étapes essentielles à la programmation du mouvement à savoir 1) la localisation de la cible, 2) la localisation de la main et 3) les transformations des informations sensorielles en commandes motrices.

La localisation de la cible

L'intention d'agir nécessite d'abord la détection puis la localisation de la cible dans l'espace. La plupart du temps, la cible apparaît dans le champ visuel et ce sont donc les informations visuelles qui sont utilisées pour la localiser.

Les voies ascendantes visuelles. La rétine capte et transforme l'énergie lumineuse au moyen des cônes et des bâtonnets. Les signaux transitent via les cellules bipolaires et ganglionnaires jusqu'au nerf optique avant d'emprunter deux voies distinctes (Figure 1.4). La première est la **voie rétino-géniculo-striée** qui regroupe la majorité (80 à 90%) des fibres du nerf optique. Les informations visuelles font un relais dans le corps géniculé latéral (CGL) du thalamus puis les radiations optiques projettent sur le cortex visuel primaire (V1), qui constitue le premier niveau du traitement cortical de l'information visuelle. Le reste des fibres du nerf optique emprunte la **voie rétino-tectale** et passe par le colliculus supérieur (CS) puis le pulvinar avant d'atteindre les aires extrastriées, qui regroupent les aires visuelles autres que V1. Une fois que les informations visuelles sont arrivées à V1, elles se subdivisent à nouveau en deux voies anatomiques distinctes : la voie dorsale et la voie ventrale.

Les voies visuelles dorsale et ventrale. La **voie visuelle dorsale** se dirige vers le lobe pariétal et la **voie visuelle ventrale** s'étend vers la partie inférieure du lobe

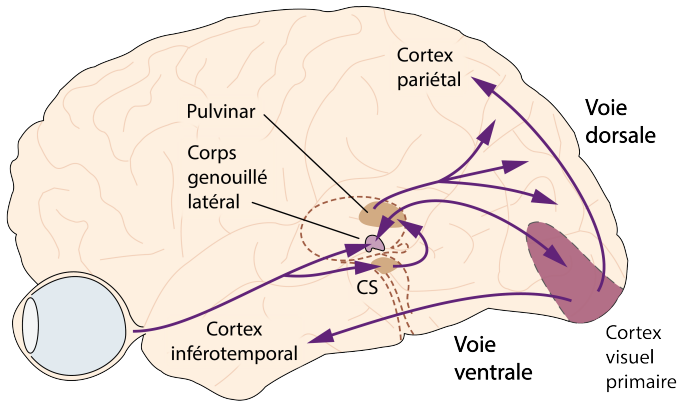

Figure 1.4 – Les voies ascendantes visuelles. Les informations visuelles peuvent suivre deux voies différentes. La voie rétino-géniculo-striée transite par le corps genouillé latéral avant de projeter sur le cortex visuel primaire. La voie rétino-tectale passe par le colliculus supérieur et le pulvinar pour aller vers les aires extrastriées. *CS* colliculus supérieur. Figure adaptée de Kandel et al. (2013).

temporal (Figure 1.4). La portion de V1 dédiée à la vision centrale est plus importante que celle allouée à la vision périphérique, ce phénomène correspond à la **magnification corticale** (Pointer, 1986). La sur-représentation de la vision centrale se poursuit dans la voie ventrale alors que la voie dorsale représente à la fois la vision périphérique et centrale (Colby et al., 1988). En outre, la voie ventrale représenterait préférentiellement le champ visuel supérieur et la voie dorsale plutôt le champ inférieur (Previc, 1990).

À l'origine, les deux voies furent tout d'abord différenciées par le type d'informations traité (Livingstone & Hubel, 1988 ; Mishkin et al., 1983 ; Ungerleider & Mishkin, 1982). La voie ventrale correspond à la **voie du « quoi »**, elle traite les informations permettant l'identification des objets et de leurs attributs (forme, couleur, texture). La voie dorsale est spécialisée dans le traitement des informations visuelles spatiales telles que la position des objets, leur taille, leur orientation ainsi que la direction des mouvements ; ces caractéristiques lui ont valu le terme de **voie du « où »**. Cette théorie fut reprise et affinée par Goodale et Milner qui distinguèrent les voies visuelles selon l'utilisation qui est faite de l'information (Goodale & Milner, 1992 ; Milner & Goodale, 1995). Selon eux, la voie ventrale (« quoi ») permet de construire une représentation du monde externe et sous-tend la vision pour la perception. La voie dorsale participe au traitement des informations visuelles en vue de guider les mouvements : elle est en charge de la vision pour l'action et fut donc renommée **voie du « comment »**.

La dissociation entre voie ventrale et dorsale est également observable en pathologie humaine. Les lésions qui affectent le cortex inférotemporal (voie ventrale) provoquent

des **agnosies visuelles**. Les patients présentent un trouble des fonctions perceptives et n'arrivent pas à reconnaître des objets qui leur sont présentés visuellement. En revanche, leur capacité à réaliser un mouvement vers ces mêmes objets est intacte (Goodale et al., 1994). À l'inverse, les lésions du cortex pariétal (voie dorsale) engendrent un trouble visuomoteur : l'**ataxie optique**. Chez les patients ataxiques, la reconnaissance visuelle des objets en vision centrale est relativement préservée mais ils présentent des difficultés à effectuer des mouvements visuellement guidés, notamment en vision périphérique (Perenin & Vighetto, 1988).

Bien que les informations visuelles soient traitées par deux voies distinctes, elles ne sont pas cloisonnées et interagissent entre elles (Cloutman, 2013). Chez le singe, des connexions entre les régions pariétales et inférotemporales ont été mises en évidence par injection de traceurs (Borra et al., 2010 ; Distler et al., 1993 ; Zhong & Rockland, 2003), ce qui suggère que les informations communiquent entre les voies dorsale et ventrale.

La localisation de la main

Utilisation des informations proprioceptives. La proprioception, littéralement la **perception de soi**, est un sens de position qui provient de signaux au niveau des muscles, des articulations et des tendons. Ces informations permettent de localiser les différentes parties du corps les unes par rapport aux autres, ainsi que leurs mouvements. Il existe des patients dits **désafférentés** qui, à la suite d'une neuropathie, se retrouvent privés d'afférences proprioceptives. Bien que capables d'effectuer des mouvements dirigés, ces patients démontrent des mouvements moins précis que les sujets sains (Nougier et al., 1996 ; Sainburg et al., 1995). C'est également le cas pour des singes ayant subi une désafférentation chirurgicale (Polit & Bizzi, 1979). La proprioception contribuerait donc à la construction d'un **modèle** ou **représentation interne** de la main nécessaire à la planification motrice (J. Gordon et al., 1995). Chez les participants sains, les perturbations proprioceptives affectent la localisation de la main au départ du mouvement (Lackner & Shenker, 1985 ; Larish et al., 1984). L'ensemble de ces observations démontrent que la proprioception est utilisée pendant la phase de programmation motrice pour estimer la

position de la main.

Les voies ascendantes proprioceptives. Les principaux récepteurs proprioceptifs comprennent les **fuseaux neuromusculaires**, les **organes tendineux de Golgi** et les **récepteurs articulaires** (Tuthill & Azim, 2018). Les fuseaux neuromusculaires sont formés de fibres musculaires contractiles encapsulées dans du tissu conjonctif. Ils renseignent sur le niveau d'étirement et donc la longueur du muscle. Les organes tendineux de Golgi se trouvent à l'endroit où les fibres musculaires s'insèrent dans les tendons et sont sensibles à la force de contraction du muscle. Les récepteurs articulaires sont présents dans la capsule articulaire et les ligaments, ils indiquent au SNC la position angulaire l'articulation (Figure 1.5A).

Les informations proprioceptives gagnent le cortex en empruntant la **voie lemniscale** (ou voie des colonnes dorsales) qui comporte une chaîne de 3 neurones (Figure 1.5B). Le premier neurone, situé dans le ganglion spinal, pénètre et monte dans la racine dorsale de la mœlle épinière. Au niveau du tronc cérébral, il fait un relais avec un neurone du bulbe rachidien. Le neurone de deuxième ordre passe la ligne médiane et projette sur le thalamus. Le troisième et dernier neurone envoie les informations proprioceptives vers le cortex somatosensoriel primaire qui occupe le gyrus postcentral. Comme pour le système visuel, il semblerait que les informations proprioceptives soient traitées par deux voies différentes. La première se termine dans le cortex pariétal postérieur et serait impliquée dans le guidage de l'action sur la base d'informations somatosensorielles. La seconde, plus ventrale, rejoint l'insula et sous-tendrait les mécanismes perceptifs (Dijkerman & de Haan, 2007).

Utilisation des informations visuelles La vision peut aussi être utilisée comme source d'informations pour localiser la main afin de préparer un mouvement. En effet, les imprécisions de pointage observées chez les patients désafférentés sont réduites lorsqu'ils voient leur main avant d'initier leur mouvement (Ghez et al., 1995). Des résultats similaires sont rapportés chez les sujets sains (Desmurget et al., 1997 ; D. Elliott et al., 1991 ; Ghilardi et al., 1995 ; Prablanc et al., 1979 ; Rossetti et al., 1994), suggérant que les

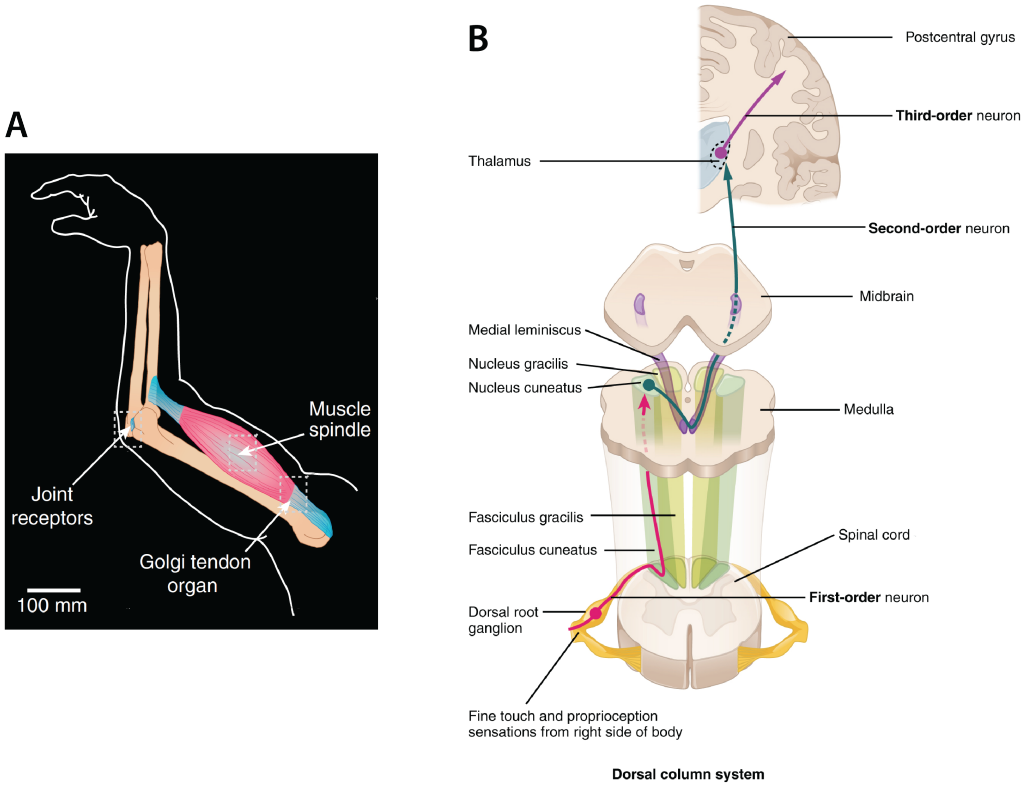

Figure 1.5 – Le système proprioceptif. A. Localisation des principaux récepteurs proprioceptifs : les fuseaux neuromusculaires (*muscle spindles*), les organes tendineux de Golgi (*Golgi tendon organ*) et les récepteurs articulaires (*joint receptors*). Modifié d'après Tuthill et Azim (2018). B. Les voies ascendantes proprioceptives. La voie des colonnes dorsales achemine les informations proprioceptives au cortex via 3 neurones. Le premier relais se fait dans le bulbe rachidien (*medulla*) et le deuxième au niveau du thalamus avant que les informations soient transmises au cortex somatosensoriel primaire (*postcentral gyrus*). Modifié d'après https ://openstax.org/details/books/anatomy-and-physiology

informations visuelles de la main au départ s'ajoutent aux informations proprioceptives et permettraient d'améliorer la planification motrice.

En effet, il a été montré que la position de la main avant un mouvement est encodée par la vision et la proprioception (Rossetti, Desmurget, & Prablanc, 1995). Dans cette étude, des **prismes** induisant un décalage entre la position « vue » et la position « sentie » (réelle) de la main furent appliqués pendant la phase de programmation motrice. Les erreurs de pointage résultantes mirent en évidence que le vecteur de mouvement avait pour origine une position intermédiaire entre les deux positions « vue » et « sentie » de la main. Les auteurs en conclurent que les informations visuelles et proprioceptives étaient combinées

afin d'obtenir une seule estimation de la position de la main. L'intégration multisensorielle de la vision et de la proprioception permettrait une estimation plus précise de la position de la main, conformément aux prédictions de la théorie bayésienne (Desmurget et al., 1997 ; van Beers et al., 1996, 1999b). De plus, il semblerait que les signaux visuels et proprioceptifs soient pondérés par leur fiabilité intrinsèque (van Beers et al., 1999a).

Question

La position de la main est généralement codée par des informations proprioceptives et visuelles. L'intégration visuo-proprioceptive permet de construire une estimation de la position de la main plus précise qu'en utilisant la proprioception seule. L'étude n°2 vise à déterminer si les bénéfices de l'intégration multisensorielle en termes de localisation spatiale sont également observés lorsque la position de la main est renseignée par la proprioception et une source d'informations additionnelles, à savoir le toucher.

Les transformations sensorimotrices

Pour réaliser un mouvement dirigé de la main, les informations visuelles et proprioceptives sont utilisées pour localiser la cible et l'effecteur. Cependant ces signaux ne peuvent pas être utilisés tels quels par le système moteur, ils doivent subir des **transformations sensorimotrices** qui permettent de convertir les informations sensorielles en commandes motrices (Flanders et al., 1992 ; Soechting & Flanders, 1992). Cette étape implique principalement des changements de coordonnées puisque les informations visuelles sont au départ représentées dans un référentiel centré sur la rétine ou rétinocentré (Y. E. Cohen & Andersen, 2002), les informations proprioceptives dans un référentiel centré sur tout ou une partie du corps (N. P. Holmes & Spence, 2004) et les commandes motrices sont définies dans un système de coordonnées musculaires.

Les mécanismes qui sous-tendent les transformations sensorimotrices sont encore débattus et plusieurs modèles ont été proposés. Parmi eux, le **modèle séquentiel** (Figure 1.6A) consiste en une succession de transformations d'un système de coordonnées à un

autre. À chaque étape, le SNC intègre un signal de position afin de passer au référentiel suivant (Flanders et al., 1992 ; McIntyre et al., 1997, 1998). Alors que selon le **modèle direct** (Figure 1.6B), la position de la main et de la cible sont toutes deux codées dans un référentiel commun qui serait **oculocentré** (Buneo et al., 2002), c'est-à-dire dont les coordonnées sont remises à jour à chaque mouvement oculaire. Par la suite, un vecteur de mouvement peut être généré directement en soustrayant les deux positions entre elles.

Le modèle direct a l'avantage de compter moins d'étapes computationnelles. On pourrait penser qu'il n'est applicable que lorsque la cible et la main sont toutes deux visibles mais c'est sans compter que des modalités autres que visuelles peuvent être représentées dans un référentiel oculocentré (Pouget et al., 2002).

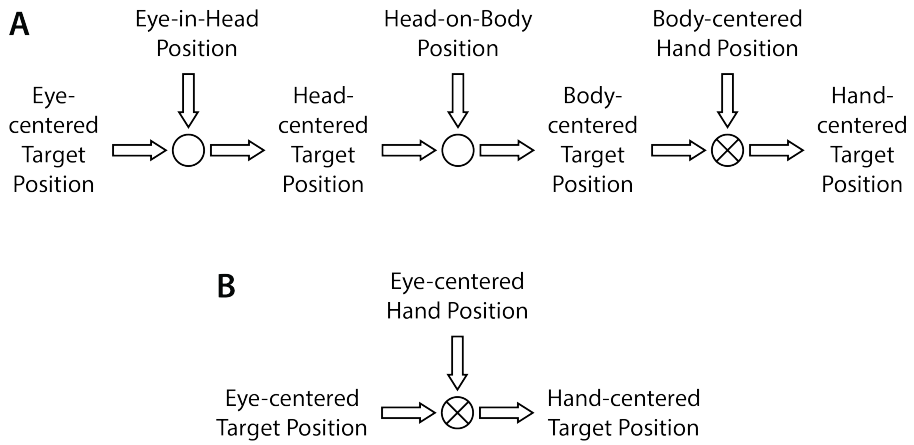

Figure 1.6 – Transformations sensorimotrices pour les mouvements de la main. A. Le modèle séquentiel suppose une succession de transformations. La position de la cible en coordonnées oculocentrées est combinée avec la position des yeux par rapport à la tête pour représenter la position de la cible en coordonnées crâniocentrées centrées sur la tête et ainsi de suite jusqu'à obtenir la position de la cible dans un référentiel centré sur la main. B. Le modèle direct transforme directement la position de la cible et de la main en coordonnées utilisables par le système moteur. Modifié d'après Buneo et al. (2002).

1.2.3 Le contrôle en ligne du mouvement

Suite à la phase de programmation, le SNC génère une commande motrice. Toutefois, à cause du bruit inhérent aux systèmes moteur et sensoriel, cette commande n'est pas parfaite et le SNC doit faire des ajustements pendant l'exécution motrice. Ces corrections

sont le résultat du **contrôle en ligne du mouvement** qui permet d'atteindre l'objectif initialement fixé. En laboratoire, de telles corrections en ligne ont été observées en réponse à des perturbations imprévisibles telles qu'un déplacement de la cible à atteindre (Bard et al., 1999 ; Goodale et al., 1986 ; H. Johnson et al., 2002 ; Pélisson et al., 1986 ; Prablanc & Martin, 1992) ou l'application de forces externes sur le bras en mouvement (Cordo, 1990 ; Smeets et al., 1990). L'étude de patients désafférentés a révélé ces derniers présentaient des déficits dans le contrôle de la trajectoire de la main (Sainburg et al., 1995). Par ailleurs, les participants sains effectuent des modifications du mouvement plus importantes en réponse à un déplacement de la position visuelle de la cible et ces ajustements sont plus rapides lorsque la main est visible pendant le mouvement (Sarlegna et al., 2003). L'ensemble de ces résultats démontrent que les informations visuelles et proprioceptives de la cible et de la main sont utilisées pour le contrôle en ligne du mouvement.

Le SNC est capable de développer des **modèles internes** permettant de modéliser les interactions entre les systèmes sensoriels, moteurs et environnementaux (Wolpert & Ghahramani, 2000). L'implémentation des corrections en ligne suppose l'utilisation d'un système en boucle fermée avec deux types de modèles internes (Figure 1.7) : un modèle direct, ou prédictif, et un modèle inverse, ou contrôleur (Kawato, 1999 ; Wolpert, Miall, & Kawato, 1998). Le **modèle inverse** permet de déterminer les commandes motrices appropriées pour produire un mouvement désiré (Atkeson, 1989 ; Kawato & Gomi, 1992). La commande motrice est envoyée vers les muscles et une copie de cette commande, appelée **copie d'efférence**, est générée. Le **modèle direct** a pour fonction de prédire les retours sensoriels du mouvement désiré, sur la base de la copie d'efférence reçue (Desmurget & Grafton, 2000 ; von Holst, 1954 ; Wolpert & Miall, 1996). Les retours sensoriels prédits sont ensuite comparés aux retours sensoriels véritables provoqués par le mouvement généré. Si une différence est détectée, un signal d'erreur est généré afin que le mouvement soit corrigé en conséquence.

Le modèle direct anticipe les conséquences d'une action et permet donc de **compenser** le délai avec lequel les réafférences visuelles et proprioceptives arrivent au SNC. En effet, les retours somatosensoriels et visuels mettent respectivement environ 30 et 90 ms

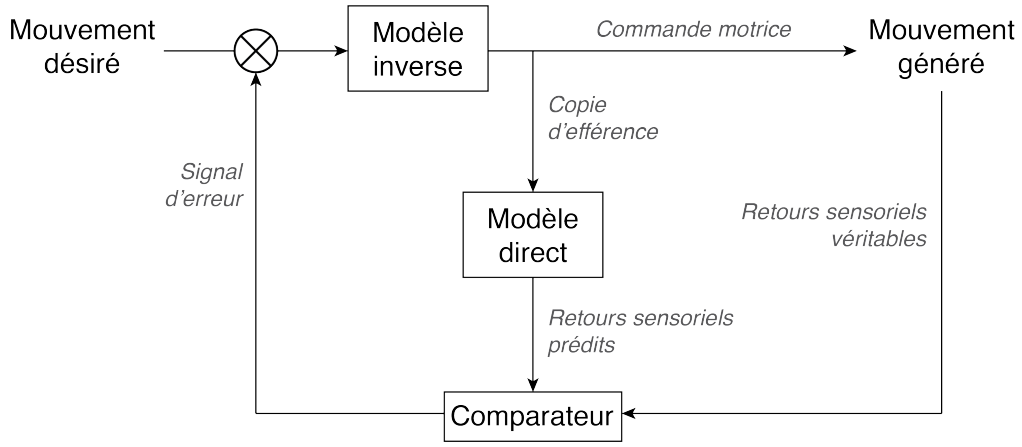

Figure 1.7 – Circuit permettant le contrôle en ligne du mouvement. Le modèle inverse transforme l'intention de l'action en commande motrice. Le modèle direct prédit les retours sensoriels qui sont ensuite comparés aux retours sensoriels véritables provenant de la périphérie. Si le système détecte une erreur, un signal d'erreur est envoyé afin de corriger le mouvement.

pour atteindre le cortex sensorimoteur (Allison et al., 1991 ; Raiguel et al., 1999). Les mécanismes prédictifs du modèle interne direct permettent donc d'expliquer les corrections motrices extrêmement rapides pouvant être observées suite à des perturbations visuelles (Cooke & Diggles, 1984 ; Goodale et al., 1986 ; Pélisson et al., 1986 ; Soechting & Lacquaniti, 1983) ou proprioceptives (Reichenbach et al., 2009 ; Smeets et al., 1990). Ces résultats suggèrent que certaines corrections sont possibles **en l'absence** d'informations sensorielles périphériques, conformément à ce qui a pu être rapporté chez une patiente désafférentée capable de modifier la trajectoire de ses mouvements dans le noir pour atteindre la position mémorisée de cibles non visibles pendant le pointage (Sarlegna et al., 2006). Par conséquent, le contrôle en ligne du mouvement repose, du moins en partie, sur les prédictions des modèles internes et l'utilisation de la copie d'efférence.

1.3 Le cortex pariétal postérieur

1.3.1 Anatomie du cortex pariétal

Le cortex pariétal est délimité en avant par le sillon central, sa limite arrière est constituée par le sillon occipital transverse sur la face externe et le sillon pariéto-occipital sur la face interne de l'hémisphère. En avant du sillon postcentral, se situe le **gyrus postcentral** qui correspond au cortex somatosensoriel primaire et comprend les aires 1, 2 et 3 de Brodmann (Figure 1.8). En arrière du sillon post-central se trouve le **cortex pariétal postérieur** (CPP) sur lequel nous allons nous attarder dans ce chapitre.

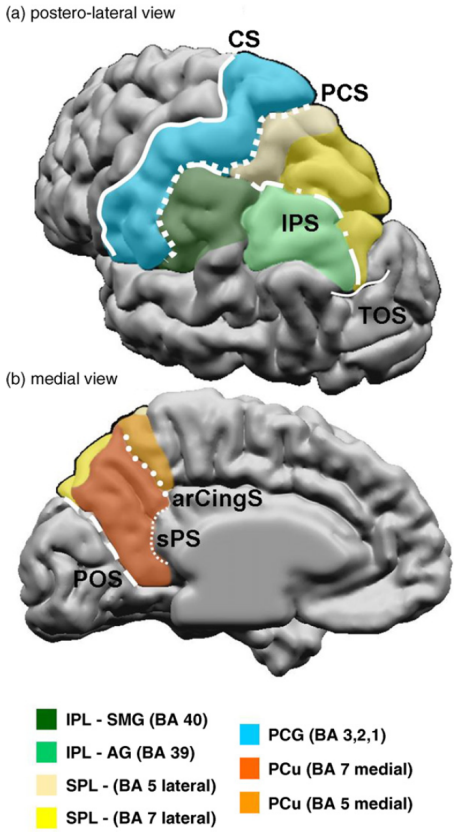

Figure 1.8 – Anatomie du cortex pariétal. Hémisphère gauche d'un cerveau humain vu par sa face externe (a) et interne (b). Les lignes blanches représentent les principaux sillons alors que les subdivisions anatomiques sont représentées par différentes couleurs. Les aires de Brodmann (*BA*) correspondantes sont indiquées entre parenthèses dans la légende. *CS* sillon central, *PCS* sillon postcentral, *IPS* sillon intrapariétal, *POS* sillon pariéto-occipital, *TOS* sillon occipital transverse, *arCingS* rameau ascendant du sillon cingulaire, *sPS* sillon subpariétal, *PCG* gyrus postcentral, *SPL* lobule pariétal supérieur, *IPL* lobule pariétal inférieur, *PCu* précunéus. D'après Culham et al. (2006).

Le CPP est séparé du lobe occipital par la jonction pariéto-occipitale (JPO). Le sillon intrapariétal (IPS, *intraparietal sulcus*) s'étend du sillon postcentral jusqu'à la JPO et est divisé en plusieurs aires fonctionnelles distinctes. L'IPS divise la face externe du CPP en deux régions : le **lobule pariétal supérieur** (LPS) et le **lobule pariétal inférieur** (LPI). Chez l'Homme, le LPS comprend les aires 5 et 7 de Brodmann alors que le LPI

contient les aires 39 et 40 (Figures 1.8 et 1.9). Les aires 5 et 7 s'étendent sur la face interne du lobe pariétal pour former le précunéus. Chez le macaque en revanche, l'aire 5 de Brodmann correspond au LPS et l'aire 7 au LPI (Figure 1.9).

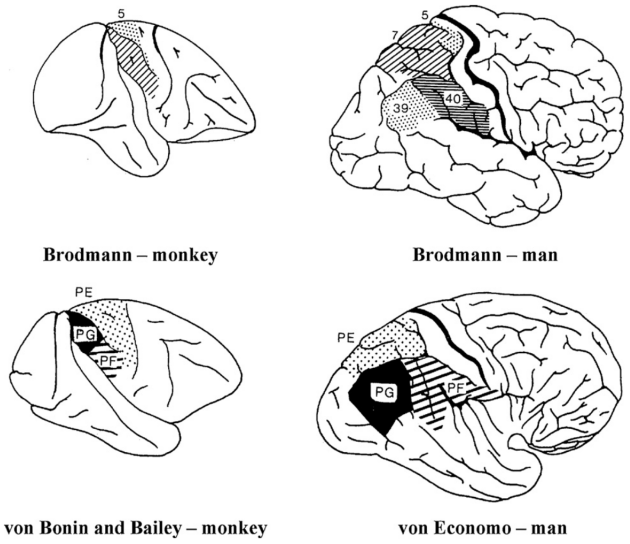

Figure 1.9 – Les subdivisions du CPP chez le singe (colonne de gauche) et l'Homme (colonne de droite) selon les nomenclatures de Brodmann, Von Bonin & Bailey et von Economo. D'après Singh-Curry et Husain (2009).

Différentes nomenclatures ont été utilisées pour dénommer les aires du cortex pariétal. La première fut celle de Brodmann qui repose sur la cytoarcitecture du cortex cérébral (Brodmann, 1909). Actuellement, la carte des aires de Brodmann demeure encore largement utilisée mais les divisions sont relativement grossières. von von Economo et Koskinas (1925) chez l'Homme et von Bonin et Bailey (1947) chez le singe proposèrent un découpage plus fin des régions. Bien qu'à prendre avec précaution, il existerait une certaine homologie entre les subdivisions du CPP chez le singe et l'Homme (Figure 1.9).

1.3.2 Le CPP : une interface sensorimotrice

L'intégration multisensorielle

Le CPP est une aire associative où convergent les informations provenant de diverses modalités sensorielles (Andersen et al., 1997 ; Y. E. Cohen, 2009). Il est connecté au pulvinar médian (Baizer et al., 1993) et au CS (Clower et al., 2001) qui sont deux structures connues pour jouer un rôle dans l'intégration multisensorielle (Stepniewska, 2003 ; Wallace et al., 1998). Ces éléments suggèrent fortement l'implication du CPP dans le traitement multisensoriel des informations. Cette hypothèse fut renforcée par le fait que la

stimulation transcrânienne à courant continu (STCC) et la stimulation magnétique transcrânienne (SMT) ciblées sur le CPP perturbent l'intégration visuo-auditive et visuo-tactile (Pasalar et al., 2010 ; Zmigrod, 2014).

Connexions avec le cortex frontal

Le cortex prémoteur (PM) et le cortex moteur primaire (M1) sont deux structures motrices situées au sein du lobe frontal. PM participe à la planification et l'organisation du mouvement alors que M1 commande directement l'exécution motrice en envoyant la commande motrice aux muscles via les motoneurones (Roland, 1993). Il se trouve que le CPP présente un grand nombre de connexions (Figure 1.10), directes ou indirectes, avec les régions motrices frontales notamment PM et M1 (Gharbawie et al., 2011 ; P. B. Johnson et al., 1996 ; Koch et al., 2010 ; Marconi et al., 2001 ; Petrides & Pandya, 1984 ; Wise et al., 1997). Le rôle du CPP consisterait à traiter les informations sensorielles avant qu'elles ne soient envoyées au cortex frontal pour l'élaboration de la commande motrice. L'abondance des connexions entre le cortex frontal et pariétal souligne l'importance du **réseau fronto-pariétal** dans les transformations sensorimotrices (Andersen & Cui, 2009 ; Rizzolatti et al., 1998). Enfin, les connexions bidirectionnelles entre M1 et le CPP permettraient à ce dernier de recevoir la copie d'efférence de la commande motrice (Kalaska et al., 1983 ; Mountcastle et al., 1975), il serait ainsi en mesure de construire une représentation interne de l'effecteur en mouvement.

Connexions avec le cervelet

Le cervelet est impliqué dans la coordination et le contrôle fin des mouvements volontaires. Par conséquent, les patients atteints d'une lésion au cervelet arrivent difficilement à réaliser des mouvements précis (Bastian et al., 2000 ; Manto et al., 1994). En outre, l'inactivation des noyaux cérébelleux par micro-injection de muscimol cause des déficits du contrôle moteur (Martin et al., 2000). Le CPP est connecté au cervelet via des projections qui transitent par le thalamus (Amino et al., 2001 ; Clower et al., 2001). De plus l'étude des réseaux cérébro-cérébélleux en imagerie par résonance magnétique fonctionnelle (IRMf)

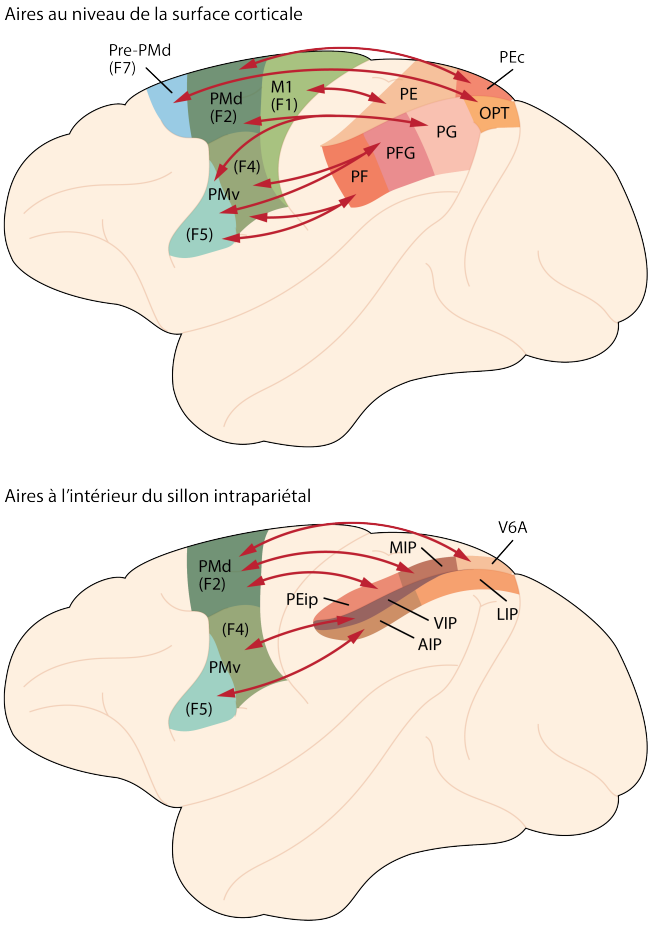

Figure 1.10 – Connexions entre les régions pariétales et frontales. Les régions fonctionnelles sont représentées sur une vue latérale de cerveau de singe. Sur la figure du bas, le sillon intrapariétal est ouvert pour visualiser les régions situées à l'intérieur. Les aires PE et PEc correspondent grossièrement à l'aire 5 de Brodmann et les aires PF, PFG, PG et OPT correspondent à l'aire 7 de Brodmann. *AIP* aire intrapariétale antérieure, *LIP* aire intrapariétale latérale, *MIP* aire intrapariétale médiane, *VIP* aire intrapariétale ventrale, *PEip* aire PE intrapariétale, *V6A* aire visuelle 6A, *M1* cortex moteur primaire, *OPT* cortex occipito-pariéto-temporal, *PMd* cortex prémoteur dorsal, *PMv* cortex prémoteur ventral, *Pre-PMd* cortex prémoteur prédorsal. Figure adaptée de Kandel et al. (2013).

de repos a pu mettre en évidence une **connectivité fonctionnelle**, c'est-à-dire une corrélation temporelle des activités neuronales, entre cervelet et cortex pariétal (Buckner et al., 2011). Ces observations tendent à faire penser que le CPP pourrait, avec le cervelet, participer à la correction des mouvements (Desmurget et al., 2001 ; Miall et al., 2007) notamment grâce aux copies d'efférence qu'il reçoit de M1 (Andersen et al., 1997).

Le CPP est qualifié de **structure sensorimotrice** car il constitue un carrefour entre les aires corticales sensorielles et motrices. Il est traditionnellement considéré comme important pour l'attention visuospatiale ainsi que pour la représentation multimodale de l'espace et des objets (Colby & Goldberg, 1999) mais il est maintenant admis que le CPP est également impliqué dans une grande variété de fonctions cognitives telles que la mémoire de travail ou la prise de décision (Koenigs et al., 2009 ; Murray et al., 2017). Le but n'est pas ici de dresser une liste exhaustive des fonctions du CPP mais de se focaliser, dans le cadre de cette thèse, sur ses fonctions multisensorielles et sensorimotrices qui

permettent de faire le lien entre perception et action.

1.3.3 Les subdivisions fonctionnelles du CPP

Le CPP est un site d'**intégration sensorimotrice** et est impliqué dans les actions dirigées vers un but. Nos connaissances actuelles sur l'organisation fonctionnelle du CPP proviennent en grande partie des études électrophysiologiques menées chez le macaque. Par la suite, des structures homologues ont été identifiées chez l'Homme, notamment grâce aux techniques de neuroimagerie. Le CPP est subdivisé en plusieurs aires spécialisées dans les mouvements oculaires, les mouvements de préhension et les mouvements d'atteinte et de pointage. Ces aires sont situées le long de l'IPS.

L'aire AIP. L'aire intrapariétale antérieure (AIP) est située dans la partie antérieure de la berge inférieure de l'IPS. Elle joue un rôle dans les mouvements de préhension (gestes de saisie) et comprend 3 types de neurones distincts : des neurones avec des propriétés visuelles, motrices et des neurones visuomoteurs (Sakata et al., 1995). Les neurones à dominance visuelle codent pour les caractéristiques 3D des objets alors que les neurones à dominance motrice coderaient pour la configuration spatiale de la main lors de la préhension. Les neurones visuomoteurs sont actifs à la fois pendant les mouvements de préhension et lors de la présentation d'objets (Murata et al., 2000). L'inactivation réversible de l'aire AIP par injection de muscimol altère la configuration de la main lors de la préhension mais sans affecter le geste d'atteinte en lui-même (Colby & Goldberg, 1999).

Chez l'Homme, la région antérieure du sillon intrapariétal (aIPS) a été identifiée comme étant impliquée dans les mouvements de saisie (Frey et al., 2005). De plus une lésion touchant aIPS provoque des déficits de saisie des objets (Binkofski et al., 1998), ce qui laisse penser que cette région serait l'équivalent de l'aire AIP chez le macaque (Grefkes et al., 2002).

L'aire LIP. L'aire intrapariétale latérale (LIP) se trouve dans la partie postérieure de la berge inférieure de l'IPS. Les neurones de l'aire LIP déchargent en réponse à des

stimulations visuelles ou à l'exécution de saccades oculaires (Colby & Duhamel, 1996). Avant l'exécution des saccades, les neurones de l'aire LIP subissent une réorganisation de leurs champs récepteurs afin de représenter les informations en coordonnées oculocentrées (Colby et al., 1995 ; Duhamel et al., 1992). L'aire LIP serait donc impliquée dans la transformation des signaux visuels en commandes oculomotrices.

Chez l'Homme, le champ oculomoteur pariétal (*parietal eye field*) serait l'homologue de l'aire LIP du macaque. Cette région possède des fonctions analogues à celles de l'aire LIP, cependant la localisation anatomique diffère légèrement entre ces deux régions. L'aire LIP est située sur la berge inférieure de l'IPS alors que le champ oculomoteur pariétal se trouve dans la partie postérieure de la berge supérieure de l'IPS (Koyama et al., 2004 ; Sereno et al., 2001).

La région PRR. La région PRR (*parietal reach region*) identifiée chez le singe comprend l'aire intrapariétale médiane (MIP) et l'aire V6A qui sont situées dans la partie postérieure de l'IPS, à proximité de la JPO (Andersen & Buneo, 2002 ; Chang et al., 2008 ; Y. E. Cohen & Andersen, 2002). Le PRR est spécialisé dans les mouvements d'atteinte et de pointage, il joue un rôle prépondérant dans la préparation et le contrôle en ligne du mouvement (Calton et al., 2002 ; Quian Quiroga et al., 2006). En effet, les neurones des aires MIP et V6A sont actifs avant et pendant les mouvements du bras (Batista et al., 1999 ; Snyder et al., 1997). De plus, leur taux de décharge est modulé par la direction du mouvement (Eskandar & Assad, 1999 ; Fattori et al., 2005). Les aires MIP et V6A contiennent différentes populations de neurones qui ont des propriétés purement visuelles, somatosensorielles ou qui répondent aux deux types de stimulations (Breveglieri et al., 2002 ; Colby & Duhamel, 1996). Par ailleurs, certains neurones reçoivent des signaux moteurs ce qui renforce l'idée selon laquelle le PRR est impliqué dans le contrôle des mouvements visuellement guidés du bras (Calton et al., 2002 ; Y. E. Cohen & Andersen, 2002 ; Eskandar & Assad, 2002).

Chez l'Homme, la partie médiane du sillon intrapariétal (mIPS) présente des fonctions similaires à l'aire MIP (Grefkes et al., 2004). Par ailleurs, le cortex pariéto-occipital supérieur (SPOC, *superior parieto-occipital cortex*) serait l'homologue humain de l'aire V6A

décrite chez le macaque (Pitzalis et al., 2013 ; Rossit et al., 2013).

Comme nous avons pu le voir, il existe certaines homologies entre le cortex pariétal du singe et celui de l'Homme (Culham et al., 2006 ; Vesia & Crawford, 2012). Toutefois, ces similarités sont à interpréter avec précaution car il existe également des différences entre les espèces (Figure 1.11).

1.3.4 Le CPP et les mouvements de pointage

La localisation de la main et de la cible

Le CPP est situé entre les cortex somatosensoriel et visuel, il occupe donc une position idéale pour mettre en lien les informations visuelles et proprioceptives renseignant sur la position de la cible et de la main. Les signaux visuels qui empruntent la voie dorsale passent par le CPP avant d'être acheminés vers les régions prémotrices et motrices (Goodale & Milner, 1992 ; Ungerleider & Mishkin, 1982). De plus, le CPP reçoit des informations proprioceptives depuis les noyaux de la colonne dorsale qui constituent le premier relais de la voie lemniscale assurant le transport ascendant des informations somatosensorielles (Prevosto et al., 2011).

Chez des singes, des neurones de l'aire 5 du CPP ont été enregistrés lors d'une tâche simple. Le bras des animaux était caché de leur vue tandis qu'un bras artificiel leur était présenté visuellement. La position du bras artificiel pouvait coïncider ou non avec celle du bras réel du singe. Les données électrophysiologiques montrent que l'activité des neurones est modulée à la fois par les informations proprioceptives du bras réel et par les informations visuelles du bras fictif (Graziano et al., 2000). Ces résultats démontrent que le CPP, et en particulier l'aire 5, intègre les signaux visuels et proprioceptifs en provenance du bras. Par ailleurs, des études en neurophysiologie chez le singe et en neuroimagerie chez l'Homme ont révélé que le CPP intégrait les informations relatives à la position de la main et celle de la cible (Beurze et al., 2007 ; Buneo & Andersen, 2012 ; Medendorp et al., 2005). Ces informations sont essentielles pour construire le vecteur de mouvement lors de la programmation motrice (Ghez et al., 1997 ; Vindras & Viviani, 1998).

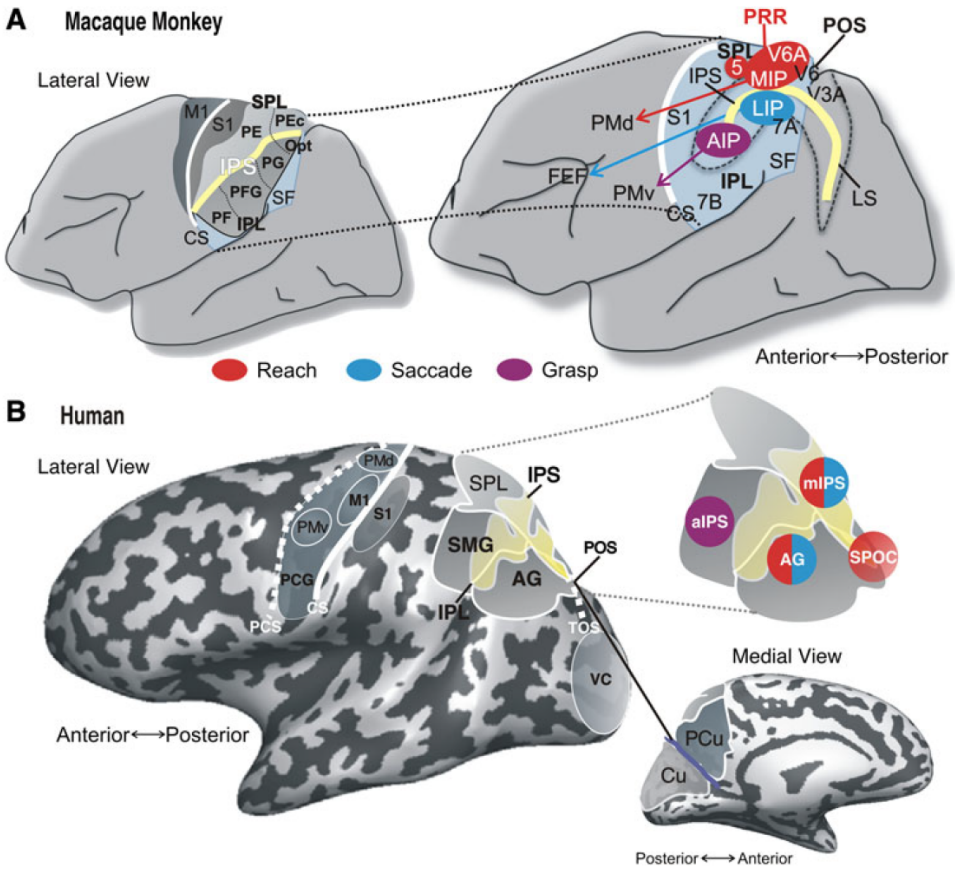

Figure 1.11 – Les subdivisions du CPP chez le singe et l'Homme. A. Illustration d'un cerveau de singe identifiant les régions spécialisées dans les saccades (en bleu), la préhension (en violet) et l'atteinte (en rouge). À droite, le sillon intrapariétal (*IPS*) et le sillon luné (*LS*) ont été ouverts pour représenter les régions situées dans l'IPS. B. Illustration d'un cerveau humain et représentation des régions homologues à celles du singe. *CS* sillon central, *SF* fissure sylvienne, *POS* sillon pariéto-occipital, *TOS* sillon occipital transverse, *PCS* sillon postcentral, *SPL* lobule pariétal supérieur (PE, PEc), *IPL* lobule pariétal inférieur (Opt, PG, PFG, PF), *S1* cortex somatosensoriel primaire, *M1* cortex moteur primaire, aires de Brodmann 5, 7A et 7B, aires visuelles V3A, V6A, *MIP* aire intrapariétale médiane, *LIP* latérale, *AIP* antérieure, *VC* cortex visuel, *AG* gyrus angulaire, *aIPS* partie antérieure de l'IPS, *mIPS* partie postérieure de l'IPS, *SPOC* cortex pariéto-occipital postérieur, *PMd* cortex prémoteur dorsal, *PMV* cortex prémoteur ventral, *FEF* champ oculomoteur frontal, *SMG* gyrus supramarginal, *PCG* gyrus postcentral, *PCu* précunéus, *Cu* cunéus. D'après Vesia et Crawford (2012).

Les transformations de coordonnées

Nous avons pu voir précédemment que les transformations sensorimotrices reposent en grande partie sur des transformations de coordonnées car chaque information sensorielle est encodée dans un référentiel qui lui est spécifique. Par conséquent, l'utilisation d'un sys-

tème de coordonnées commun permettrait de faciliter le calcul du vecteur de mouvement. Il semblerait que les premières étapes de la programmation des mouvements de pointage se fassent, au moins en partie, dans un référentiel oculocentré (Batista et al., 1999 ; Beurze et al., 2006). Ces résultats sont cohérents avec les données chez le singe montrant que l'aire 5 du CPP représente le vecteur moteur selon des coordonnées oculocentrées (Buneo et al., 2002).

Il se trouve que dans le CPP, les informations peuvent être représentées dans des coordonnées centrées sur le corps (Lacquaniti et al., 1995), la main (Ferraina et al., 1997), les yeux (Batista et al., 1999) ou encore dans un **système de coordonnées hybride** regroupant différentes coordonnées (Chang & Snyder, 2010 ; Mullette-Gillman et al., 2009). La multitude de systèmes de coordonnées au sein du CPP (Chang et al., 2008 ; McGuire & Sabes, 2009) lui permettrait transformer les coordonnées dans un référentiel commun afin de planifier un mouvement (Y. E. Cohen & Andersen, 2002). Ce référentiel serait dépendant du contexte, par exemple lorsque la cible présentée n'est pas visuelle mais proprioceptive, les régions du CPP utilisant un référentiel centré sur le corps sont préférentiellement recrutées (Bernier & Grafton, 2010).

La correction en ligne des mouvements

Le paradigme de **saut de cible** permet d'étudier les corrections en ligne du mouvement. Lors d'une tâche de pointage, la position de la cible est décalée pendant le mouvement de l'œil de sorte que le saut de cible ne soit pas perçu consciemment. Pour autant, les participants arrivent à corriger rapidement la trajectoire de leur mouvement en cours d'exécution (Prablanc et al., 1986 ; Prablanc & Martin, 1992). En revanche ces corrections en réponse au saut de cible sont perturbées lorsqu'une SMT est délivrée au niveau du CPP, juste avant l'initiation du mouvement (Desmurget et al., 1999). En utilisant la tomographie par émission de positons (TEP), ce même groupe de chercheurs a pu montrer que le CPP était spécifiquement recruté lors du guidage en ligne des mouvements dirigés (Desmurget et al., 2001). Ces résultats montrent que le CPP est nécessaire au contrôle en ligne des mouvements.

On suppose que le CPP travaille de concert avec le cervelet (Miall et al., 2007) qui est lui aussi impliqué dans le contrôle et la correction du mouvement (J. F. Stein & Glickstein, 1992). Tous deux construiraient une représentation interne du corps sur la base d'un modèle direct qui permettrait de détecter d'éventuelles erreurs et d'implémenter des corrections si nécessaire (Desmurget & Grafton, 2000). Le CPP jouerait plus spécifiquement un rôle dans le maintien de la représentation interne du corps (Sirigu et al., 1996), laquelle serait mise à jour au fur et à mesure du mouvement. C'est ce que semble suggérer le cas d'une patiente, avec une lésion du CPP, qui est incapable de maintenir une représentation interne de son bras (Wolpert, Goodbody, & Husain, 1998).

Question

Lors de pointages répétés sans vision de la main, on observe une déviation progressive des mouvements par rapport aux cibles (Brown et al., 2003 ; Cameron et al., 2015). Les mécanismes qui sous-tendent l'accumulation de ces erreurs feraient intervenir le CPP. L'étude n°3 se propose de déterminer l'impact de lésions du CPP dans la mise à jour de la représentation interne de la main qui requiert l'intégration de la copie d'efférence et des informations visuelles et proprioceptives.

1.4 L'ataxie optique

1.4.1 Historique

Le terme « ataxie optique » fut d'abord introduit par Bálint pour rendre compte de certains déficits observés chez un patient atteint d'une lésion bilatérale du cortex pariétal postérieur (Bálint, 1909). Ce patient manifestait une triade de symptômes associant une paralysie psychique du regard (incapacité à repérer et déplacer ses yeux vers des cibles périphériques), des troubles de l'attention spatiale et une **ataxie optique**. L'ataxie optique correspond à une difficulté à diriger des mouvements volontaires de la main vers des objets sous le contrôle de la vision. Pour Bálint, l'ataxie optique est indépendante de la paralysie psychique du regard car cette dernière affecte l'ensemble du champ visuel périphérique tandis que l'ataxie optique est restreinte au membre supérieur droit du patient. Selon l'interprétation de Bálint, l'ataxie optique résulterait de l'altération des connexions entre les centres visuels et moteurs.

En parallèle, Holmes rapporte plusieurs cas de « désorientation visuelle » chez des soldats blessés de guerre souffrant de lésions bilatérales étendues au niveau pariéto-occipital (G. Holmes, 1918). Le tableau clinique est relativement similaire à celui décrit par Bálint : les patients éprouvent des difficultés à réaliser des mouvements d'atteinte visuellement guidés, mais quelle que soit la main utilisée. Selon Holmes, ces déficits moteurs auraient pour origine un trouble global de la perception spatiale.

Ce n'est que plus tard que l'ataxie optique fut considérée comme une entité clinique distincte. En effet, Garcin et ses collaborateurs ont mis en évidence que l'ataxie optique pouvait se manifester de manière isolée, en l'absence de troubles oculomoteurs (Garcin et al., 1967). Dans le cas d'une lésion unilatérale du CPP, les patients présentent des déficits de mouvements visuellement guidés qui affectent uniquement la main contralésionnelle (du côté opposé à la lésion). La main ipsilésionnelle est qualifiée de saine, pourtant elle peut présenter des déficits lorsqu'elle est située dans le champ visuel opposé à la lésion (voir partie 1.4.3). Les symptômes de l'ataxie optique se manifestent en l'absence de déficits visuels, proprioceptifs ou moteurs primaires (Garcin et al., 1967 ; Vighetto, 1980) ce qui

montre que c'est bien un **trouble visuomoteur** (Perenin & Vighetto, 1988) comme le suggérait Bálint à l'époque.

1.4.2 Localisation des lésions

Bálint rapporte chez son patient des lésions bilatérales, très étendues englobant le cortex pariétal postérieur, la partie supérieure du lobe temporal et le lobe occipital. Les dommages sont plus importants dans la partie postérieure du LPS et du LPI. Les lésions chez l'Homme sont le plus souvent occasionnées par des accidents vasculaires cérébraux et sont identifiables par imagerie cérébrale. L'étude de plusieurs patients ataxiques laisse penser que l'ataxie optique est associée à des lésions unilatérales ou bilatérales du cortex pariétal affectant généralement le LPS, le sillon intrapariétal et parfois le LPI (Jeannerod & Rossetti, 1993 ; Perenin & Vighetto, 1988). Plus récemment, une étude en neuroimagerie s'est proposée d'identifier les structures anatomiques associées à l'ataxie optique. Pour ce faire, les auteurs ont comparé les lésions présentes chez un groupe de patients ataxiques unilatéraux avec celles d'un groupe contrôle de patients cérébrolésés, également unilatéraux, mais ne présentant pas d'ataxie optique. Le chevauchement des lésions suggère que les régions les plus couramment affectées chez les patients ataxiques sont la JPO (jonction entre le LPI et le cortex occipital supérieur), le précunéus et la jonction entre le cortex occipital et le LPS (Figure 1.12) (Karnath & Perenin, 2005). L'ataxie optique est donc le résultat de l'atteinte de la voie visuelle dorsale permettant de traiter les informations visuelles pour l'action (Milner & Goodale, 1995). L'ensemble de ces résultats permet d'avancer l'hypothèse que l'ataxie optique ne serait pas due à la lésion d'une région unique mais impliquerait plutôt un ensemble de régions, se situant au niveau du PRR (Andersen et al., 2014).

1.4.3 Les troubles de l'ataxie optique

Dans sa définition générale, l'ataxie optique se caractérise par des difficultés à réaliser des **gestes visuellement guidés**, c'est-à-dire sous le contrôle de la vision. Selon l'étendue des lésions, l'ataxie optique peut être restreinte aux mouvements d'atteinte

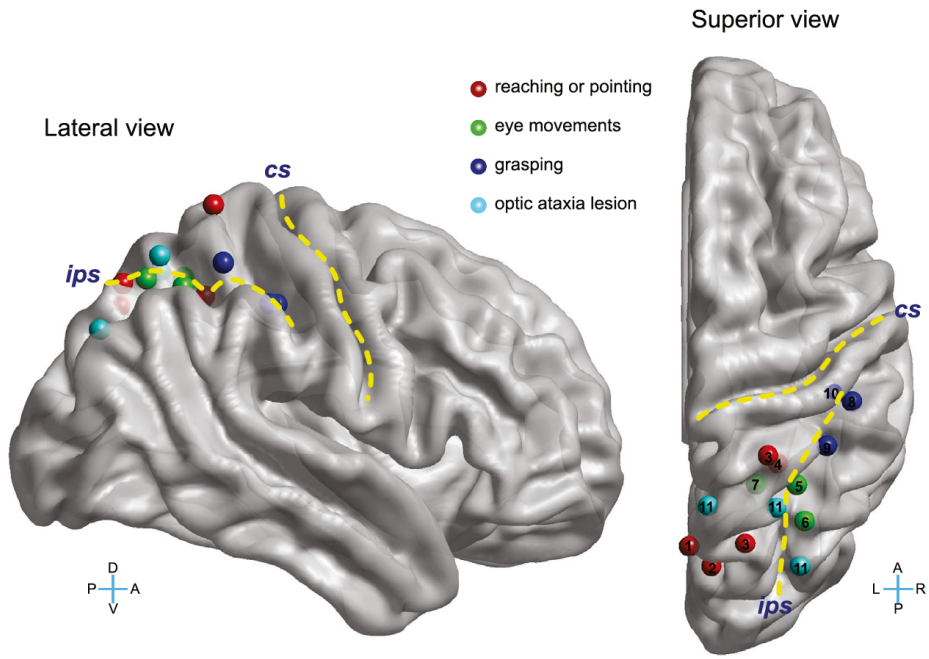

Figure 1.12 – Principaux sites lésionnels associés à l'ataxie optique sur une vue latérale et supérieure de cerveau humain. Les lignes pointillées jaunes représentent le sillon central (CS) et le sillon intrapariétal (IPS). Les sites représentés en bleu clair sont ceux identifiés par Karnath et Perenin (2005) dont la lésion serait responsable de l'ataxie optique. Ces régions sont proches celles impliquées dans les mouvements des yeux (en vert) et les gestes d'atteinte et de pointage (en rouge). D'après Andersen et al. (2014).

(Cavina-Pratesi et al., 2013) ou affecter à la fois les mouvements d'atteinte et de saisie (Jeannerod, 1986 ; Perenin & Vighetto, 1988). Traditionnellement, l'ataxie optique est décrite comme affectant de façon prédominante le membre supérieur. Cette interprétation serait cependant biaisée car les paradigmes expérimentaux utilisés pour étudier l'ataxie optique privilégient les mouvements du bras. En réalité, il semblerait que le membre inférieur puisse lui aussi être affecté puisque des imprécisions de pointage ont été observées chez un patient ataxique réalisant des mouvements avec le pied (Cavina-Pratesi et al., 2013). En revanche, les mouvements oculaires ne semblent pas affectés chez les patients avec ataxie optique et les saccades demeurent relativement précises pour des excentricités inférieures à 15° (Gaveau et al., 2008 ; Khan et al., 2009 ; Trillenberg et al., 2007). De même, l'inactivation du PRR chez le macaque produit des déficits semblables : les mouvements de pointage vers les cibles périphériques (environ 10°) sont imprécis alors que les

saccades ne sont pas impactées (Hwang et al., 2012).

Les patients ataxiques font relativement peu d'erreurs de pointage lorsque les mouvements des yeux ne sont pas restreints et qu'ils peuvent voir la cible à atteindre en vision centrale (Buxbaum & Coslett, 1998 ; Milner et al., 1999 ; Rossetti et al., 2003). Les troubles se manifestent surtout dans le champ visuel **périphérique** (Buxbaum & Coslett, 1998 ; Karnath & Perenin, 2005 ; Perenin & Vighetto, 1988). Par exemple, les patients ataxiques peuvent présenter une **aimantation du geste** dans la direction du regard (*magnetic misreaching*) : lors de la présentation de cibles périphériques, ils font des erreurs de pointage qui sont systématiquement dirigées vers leur point de fixation (Blangero et al., 2010 ; Carey et al., 1997 ; Jackson et al., 2005). Ces déficits peuvent s'expliquer par le fait que la vision périphérique serait sur-représentée au sein du CPP, en particulier dans l'aire V6A (Galletti et al., 1996, 1999 ; Pitzalis et al., 2013) afin de compenser la magnification corticale (Vindras et al., 2016). Par ailleurs, il a été montré que la JPO, dont la lésion serait à l'origine de l'ataxie optique, s'active de manière spécifique lors de mouvements de pointage vers des cibles périphériques (Prado et al., 2005).

En cas de lésion unilatérale du CPP, les déficits sont latéralisés en termes d'hémichamp visuel ou de main (Perenin & Vighetto, 1988 ; Vighetto, 1980). L'**effet champ** correspond aux erreurs faites dans le champ visuel contralésionnel (champ ataxique), quelle que soit la main utilisée. Ces erreurs proviendraient d'un déficit de localisation de la cible dans un référentiel oculocentré (Dijkerman et al., 2006 ; Khan, Pisella, Rossetti, et al., 2005 ; Khan, Pisella, Vighetto, et al., 2005). L'**effet main** caractérise les erreurs faites lorsque la main contralésionnelle (main ataxique) est utilisée, indépendamment du champ visuel. Ces erreurs sont spécifiquement réduites lorsque la vision de la main ataxique est disponible (Blangero et al., 2007), ce qui suggère que l'effet main aurait pour origine un déficit de la transformation des informations proprioceptives de la main ataxique en coordonnées spatiales. Les effets champ et main sont **indépendants** : ils peuvent se manifester isolément selon la localisation de la lésion. L'effet champ est principalement associé à une lésion de la région postérieure du CPP, au niveau de la JPO, alors que l'effet main résulte de dommages dans la partie antérieure du CPP (Blangero et al., 2009 ; Pisella et

al., 2009). Dans le cas de lésions plus larges, les deux effets coexistent et sont **additifs**. Les erreurs les plus importantes sont observées lorsque la main ataxique est utilisée pour atteindre une cible présentée dans le champ contralésionnel (Figure 1.13). En revanche, les mouvements sont relativement intacts lorsque la cible est présentée dans le champ sain et que le patient utilise sa main ipsilésionnelle, c'est-à-dire du même côté que la lésion (Blangero et al., 2010 ; Perenin & Vighetto, 1988 ; Vighetto, 1980).

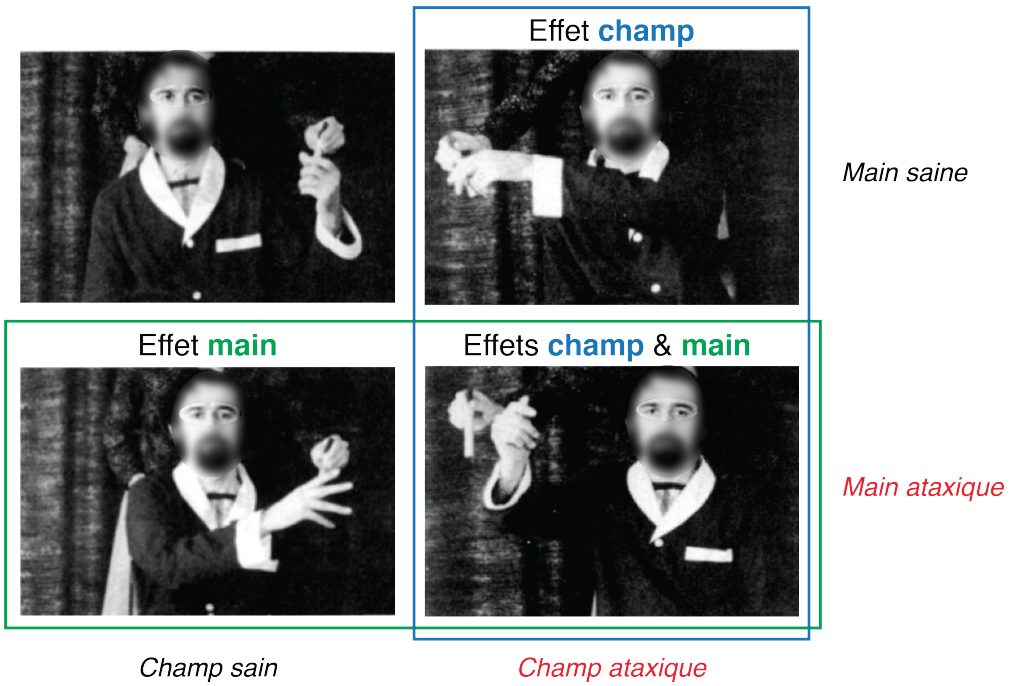

Figure 1.13 – L'effet champ et l'effet main. Un patient ataxique atteint d'une lésion unilatérale gauche du CPP saisit un objet présenté en vision périphérique. L'objet est présenté dans son champ visuel sain (champ gauche) ou son champ ataxique (champ droit) et il doit utiliser sa main saine (gauche) ou sa main ataxique (droite). Le patient présente des erreurs lorsqu'il utilise sa main ataxique (effet main) et quand l'objet se trouve dans son champ ataxique (effet champ). Les erreurs les plus importantes sont observées dans la condition combinant la main et le champ ataxiques. Modifié d'après Vighetto (1980).

Du fait de leur lésion du CPP, les patients avec ataxie optique présentent des déficits de contrôle en ligne des mouvements. Alors que les participants sains ajustent sans encombre la trajectoire de leur mouvement en réponse à un saut de cible, les patients ataxiques éprouvent des difficultés à effectuer de telles corrections motrices (Gréa et al., 2002 ; Pisella et al., 2000). Le contrôle en ligne reposerait plus particulièrement sur l'intégrité du LPS comme le suggère une étude menée chez le singe. En effet, après inactivation des aires

PE et PEc du LPS, les animaux présentent des troubles similaires à ceux observés chez les patients ataxiques lors du paradigme de double saut (Battaglia-Mayer et al., 2013). Il semble que les déficits de contrôle en ligne associées à l'ataxie optique soient spécifiques des transformations sensorimotrices rapides car les corrections lentes sont préservées (Pisella et al., 2000) et les performances des patients sont améliorées lorsque le délai entre la présentation de la cible et l'initiation du mouvement est rallongé (Milner et al., 1999 ; Revol et al., 2003). À l'inverse, les performances des participants sains chutent lorsqu'un tel décalage temporel est imposé. Ces résultats suggèrent qu'en cas de lésion du LPS, d'autres régions telles que le LPI seraient recrutées afin de permettre aux patients avec ataxie optique de compenser et d'implémenter des corrections hors ligne (Rossetti et al., 2005).

Question

Afin d'ajuster la trajectoire des mouvements en temps réel, une représentation interne de la main doit être construite. Celle-ci repose sur l'intégration des informations sensorielles et des copies d'efférence par le CPP. L'étude n°4 a pour objectif d'examiner les conséquences d'une lésion du CPP sur la représentation interne de la main lors du contrôle en ligne des mouvements de pointage.

2 Étude 1 Pondération de la vision et de la proprioception pour les mouvements de pointage

Learned rather than online relative weighting of visual-proprioceptive sensory cues

Laura Mikula, Valérie Gaveau, Laure Pisella, Aarlenne Z Khan, Gunnar Blohm

Article publié dans *Journal of Neurophysiology*

Points importants

- Selon la théorie bayésienne, les informations sensorielles sont combinées et pondérées en fonction de leur fiabilité (inverse de la variabilité) intrinsèque.
- L'objectif est ici de déterminer si le modèle bayésien s'applique à l'intégration visuo-proprioceptive de la position de la main, avant un mouvement de pointage.
- Pour la main droite et la main gauche, les poids attribués à la vision et la proprioception pendant la programmation motrice sont estimés et les variabilités sensorielles sont mesurées.
- Au niveau individuel, les poids sensoriels sont très similaires entre les deux mains, ce qui n'est pas le cas pour les variabilités sensorielles.
- Les poids attribués à la vision et la proprioception semblent être indépendants de leurs variabilités intrinsèques. Ces résultats suggèrent une pondération visuo-proprioceptive commune aux deux mains qui résulterait d'un apprentissage.

Abstract

When reaching to an object, information about the target location as well as the initial hand position is required to program the motor plan for the arm. The initial hand position can be determined by proprioceptive information as well as visual information, if available. Bayes-optimal integration posits that we utilize all information available, with greater weighting on the sense that is more reliable ; thus generally weighting visual information more than the usually less reliable proprioceptive information. The criterion by which information is weighted has not been explicitly investigated ; it has been assumed that the weights are based on task- and effector-dependent sensory reliability requiring an explicit neuronal representation of variability. However, the weights could also be determined implicitly through learned modality-specific integration weights. While the former hypothesis predicts different proprioceptive weights for left and right hand, we would expect the same integration weights if the latter hypothesis was true. We found that the proprioceptive weights for the left and right hands were extremely consistent regardless of differences in sensory variability for the two hands as measured in two separate complementary tasks. Thus, we propose that proprioceptive weights during reaching are learned across both hands and are independent of each effector's specific proprioceptive variability.

Introduction

The nervous system integrates information from different sensory modalities to form a coherent multimodal percept of the world (Ernst & Bülthoff, 2004), a process called multi-sensory integration. For example, to plan a reach, information about both the target and the hand location is necessary to form a desired movement vector. While the target position can be derived from visual information alone, hand position is typically determined by two sensory modalities : vision and proprioception. Proprioception is the sense of body position that allows us to know where the different parts of the body are located relative to each other. It has been demonstrated that the brain integrates the visual and the proprioceptive signals in order to form a unified estimate of the hand loca-

tion (Rossetti, Desmurget, & Prablanc, 1995 ; van Beers et al., 2002). However, it remains unclear what determines the criterion by which these signals are combined.

According to the Bayesian cue combination theory, during multi-sensory integration the sensory modalities are weighted proportional to their reliabilities ; the higher the reliability the more weight is given to that sense (Deneve & Pouget, 2004 ; Ernst & Bülthoff, 2004 ; Jacobs, 2002 ; Lalanne & Lorenceau, 2004 ; O'Reilly et al., 2012). This has been shown to be true for perception across many different modalities (Alais & Burr, 2004 ; Battaglia et al., 2003 ; Braem et al., 2014 ; Butler et al., 2010 ; Ernst & Banks, 2002) as well as for action, specifically to determine hand position (Burns & Blohm, 2010 ; McGuire & Sabes, 2009 ; Sober & Sabes, 2005, 2003 ; van Beers et al., 1999a). To date it has been assumed that multi-sensory weights are based on task-dependent (e.g. Sober & Sabes, 2005) and effector-dependent (e.g. Ren et al., 2007) sensory reliability requiring an explicit real-time neuronal representation of variability (Fetsch et al., 2011 ; Knill & Pouget, 2004 ; Vilares et al., 2012). Instead, sensory reliabilities could be learned through experience, which would predict a default weighting of different sensory modalities. The latter would predict that individual sensory reliabilities in specific uni-modal experimental conditions should be poor predictors for multi-sensory weightings, a prediction that is consistent with what has been observed in some visual-vestibular heading estimation experiments (Butler et al., 2010 ; Zaidel et al., 2011). On a similar note, within the perception domain, it has been demonstrated that the weights of multiple visual cues may not be entirely dependent on their variances (van Beers et al., 2011).

Here we tested which of the two above hypotheses (reliability-based integration vs. learned weights) best described visual-proprioceptive integration during reaching. To do so, we asked participants to carry out a reaching task in which we introduced a visual-proprioceptive conflict with shifting prisms (similar to Rossetti, Desmurget, & Prablanc, 1995) to measure multi-sensory weights. The prisms shift the perceived visual location of initial hand position before the reach, thus introducing a conflict between the visual (shifted) and proprioceptive (veridical) information about the hand position. This allowed us to estimate the weights attributed to the proprioceptive vs. the visual information

about the hand. We did so separately for the left and right hands as it has been shown that left and right arms have different sensory variabilities (Goble & Brown, 2008 ; Wong et al., 2014) predicting different multi-sensory weighting for reaching if reliability-based integration is used and predicting the same multi-sensory weights if modality-specific learned weights are used. Hand position estimation requires the integration of both visual and proprioceptive information. The proprioceptive variabilities are dependent on the hands whereas the visual variability is not (it should not change when using either hand). That is why proprioceptive variabilities should be assessed separately for left and right hands when estimating their respective position. To estimate uni-sensory reliabilities of vision and proprioception, we used two different tasks : a passive localization task without movements (perceptual) and an active localization task (motor). We collected both passive and active sensory reliability measures since it has previously been shown that multi-sensory integration can be different between perception and action (Knill, 2005). We found evidence supporting modality-specific learned weights rather than reliability-based estimation of hand position for reaching, i.e. we found the same proprioceptive weights for left and right hands despite large differences in proprioceptive reliabilities between the hands as measured in both the perceptual and motor contexts.

Methods

Participants

Sixteen participants between the ages of 22 and 55 (3 males, mean age = 32.8 $\pm$ 7.6 years old) took part in this study. All but three were naïve to the purposes of the study. All participants were neurologically healthy and all had normal or corrected-to-normal vision. They provided written informed consent to participate in the experiment which conformed to the Declaration of Helsinki for experiments on human subjects. All experimental procedures were approved by the health research ethics committee in France (CPP Nord-Ouest I, Lyon, 2017-A02562-51) and at the University of Montreal in Canada.

Apparatus and task design

Participants were seated on a height-adjustable chair, in front of a 30-degree-slanted table over which they performed reaching movements (Fig. 2.1A). Their forehead rested on a head support in order to minimize head movements and so that head position was the same for all participants. Eye movements were recorded through an electro-oculogram (EOG) by means of three electrodes placed on the left cheekbone, above the right eyebrow and on the first thoracic vertebra. The room was completely dark so that there was no visual information about hand position unless the initial hand position light was illuminated. Each participant completed two sessions, separated by a maximum of one week.

For the prism reach task as well as the active visual localization, red light-emitting diodes (LEDs) were projected onto the tabletop through a half-reflecting mirror (Fig. 2.1A). The half-reflecting mirror allowed participants to see their hand at the beginning of each trial (when the initial hand position light was illuminated) but not during the trial itself.

The reliability (variability) of visual and proprioceptive information was assessed in both a passive, perceptual (without reaching movements) and an active, motor localization task (see specific task descriptions below). Thereafter, participants performed a reaching task with shifting prisms to quantify the relative sensory weights given to vision and proprioception during motor planning.

A. Prism reach experiment – measuring multi-sensory weights. This task was used to assess the relative weights given to vision and proprioception during the planning of reaching movements. At the beginning of each trial, one of the three prisms (0, -10 or +10°) was pseudo-randomly selected and remained in place for the rest of the trial (sequence of the trial depicted in Fig. 2.1B). We used pseudo-random prism presentation to avoid adaptation to systematic prism-induced displacements of the visual field. After prism selection, hand lighting was switched on so that participants could align their index fingertip with the initial hand position (IHP), which was located 50 cm away from the

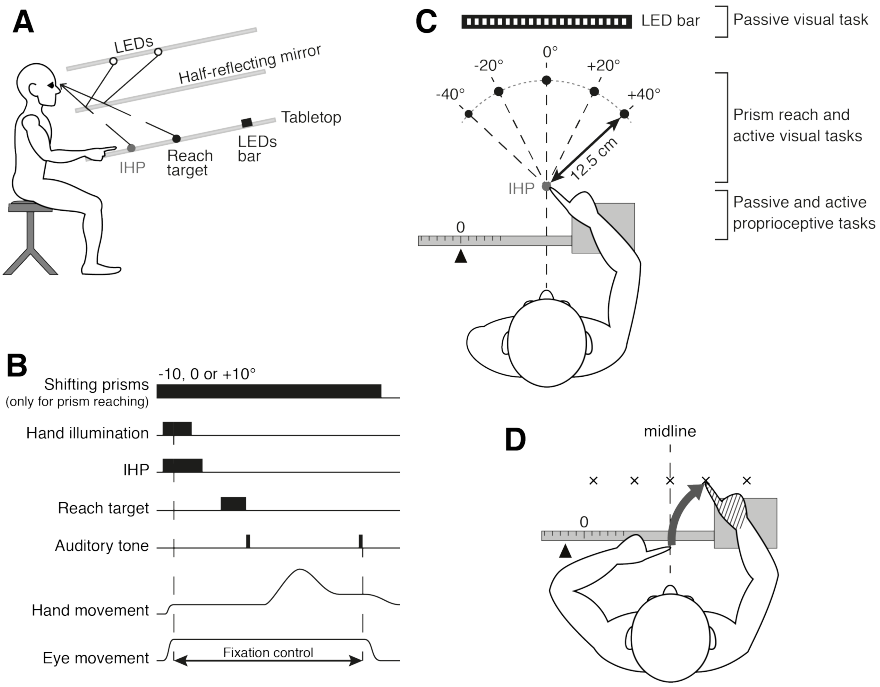

Figure 2.1 – A. Apparatus, side view. The participant executed pointing movements on the tabletop reflected from the top of the setup using a half-reflecting mirror. The grey dot represents the initial hand position (IHP) and the black dot, the reach target. The black rectangle represents the LED bar. B. Sequence of the prism reaching and the active visual localization. Hand movements were captured by the Optotrak motion-analysis system. Eye fixation on the IHP was controlled by EOG. The trial did not begin until the participant's eyes were on the IHP and the EOG calibration was completed. During the active visual localization task, only the 0° prism was presented throughout the block. C. Apparatus, bird's eye view. Five reach targets (black dots) were presented : one at the center (0°), two on the left side (-20 and -40°) and two on the right side (20 and 40°) compared to the cyclopean eye position. The distance from the participants' eyes to the LED bar was approximately 63.5 cm. The hand tested during the session (right hand here) was maintained on a sled that moved laterally. The 0 position on the ruler was set so that participants' index fingertip was aligned with the IHP. Where all tasks were performed within the workspace area is indicated on the right. D. Active proprioceptive localization. The target hand (hatched) was passively moved to one of the five target locations. Participants had their eyes closed and had to indicate where they thought their target index fingertip was by reaching with their opposite hand. Reaching errors relative to the target index fingertip were used to determine the variability associated with the target hand localization.

participants' eyes. Once the index finger remained still for 500 ms, hand lighting was extinguished. A 300-ms EOG calibration was performed while participants were looking at the IHP ; they had to maintain fixation at this position until the end of the trial. The IHP was then switched off and after a 500 ms gap, one of the five reach targets appeared for 700 ms before being extinguished ; targets were located on a radius 12.5 cm away from the IHP, at -40, -20, 0, 20 and 40° (Fig. 2.1C). A first auditory tone serving as a "go" signal was then heard. Participants were asked to make smooth, rapid movements to the remembered position of the target. After the movement ended (detected online), a second tone signaled to the participants to return to the IHP (remembered, not visible). Participants were asked to remain with eyes fixating on the remembered location of the IHP throughout the trial so all the reaching movements were made in peripheral vision. Eye position was monitored online and if eye fixation was broken, the trial was aborted and replayed later. The prism reaching task was performed in the middle workspace, between the IHP and the 5 visual reach target locations.

We used shifting prisms that displaced vision and created a conflict between visual and proprioceptive feedback of the hand (Fig. 2.2A-C). The horizontal pointing errors resulting from the visual displacement allowed us to compute the sensory weights of vision and proprioception. Three shifting prisms were used (Fig. 2.2D) : one that did not displace vision (0° prism), one inducing a rightward visual shift of 10° (+10° prism) and another inducing a leftward visual shift (-10° prism). With respect to the orthogonal distance between the participants' eyes and the tabletop on which targets were projected, a 10° prism shift displaced the visual positions of the hand and the central target by 70.5 mm. Due to their eccentricities, each of the four remaining targets had a slightly different displacement. Participants completed 12 trials for each of the 5 reach targets and the 3 prismatic conditions, totaling 180 trials per hand and participant. Trials were split in two 90-trial blocks. Participants performed two blocks in the first session with the right hand pointing and two blocks in the second session with the left hand pointing.

B. Passive, perceptual visual localization task. This task was designed to measure the reliability (variability) of the visual information through psychophysics without any

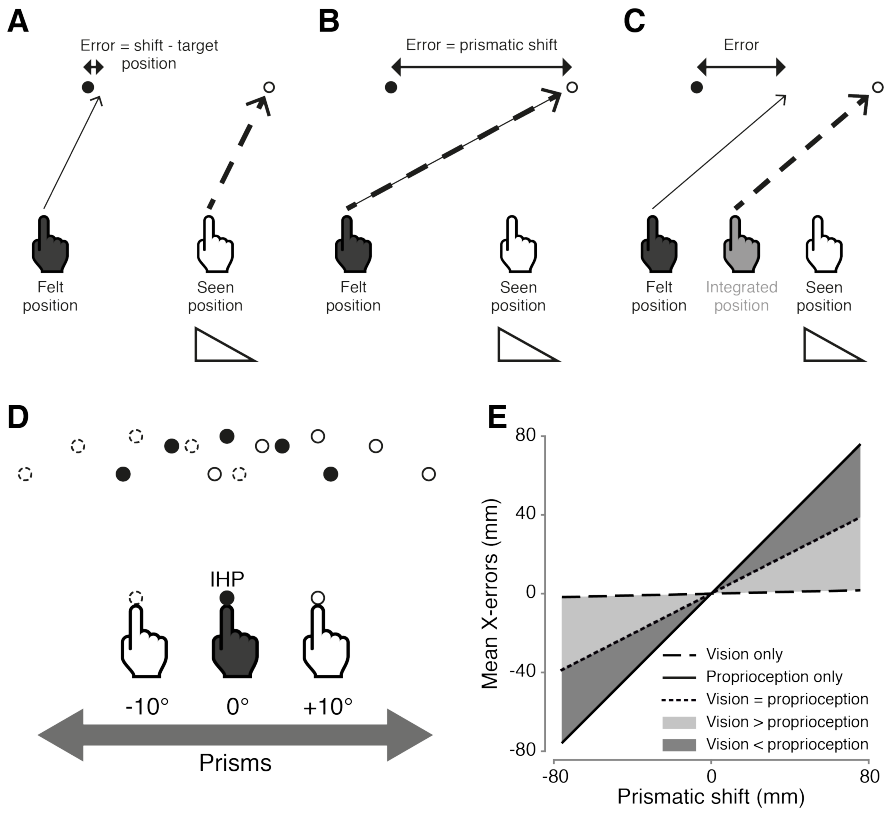

Figure 2.2 – A. Dark and white figures represent hand and targets' real positions and positions viewed through a rightward shifting prism, respectively. Dashed arrows correspond to programmed movements whereas solid arrows depict resulting movements, starting from the felt (i.e., real) hand position. Errors equal the target horizontal displacement minus the origin of the planning vector. When the reach is planned based on visual information only, the movement vector is encoded from the seen hand position. Since eccentricities are different for the hand and the target, they are subject to slightly different deviations and small errors are observed after the resulting movement. B. When using proprioceptive information only, the programmed and the resulting movements are the same because they both start from the felt/real hand position coded by proprioception. Pointing errors are equal to the prismatic shift for the corresponding target. C. When vision and proprioception are integrated, the programmed movement is encoded from an integrated position of the hand, located between the felt and the seen hand locations. Thus, based on the horizontal pointing errors, it is possible to compute the weights that a given participant assigns to vision and proprioception. D. Prisms used in our study induced a visual shift of 10° to the left (-10° prism, dashed targets) or to the right (+10° prism, white targets). E. Sensory weights' estimation. Individual mean X-errors were plotted as a function of the prismatic shift applied to each target. The slope of the linear regression was calculated. Participants with a slope close to .02 (horizontal dashed line) rely more on vision (light gray area). In contrast, the closer the slope to 1 (solid line), the more participants rely on proprioception (dark grey area).

reaching movements. We used 25 small red LEDs on the tabletop, aligned horizontally on a bar (Fig. 2.1C). LEDs were spaced at one degree intervals and covered a visual field from -12 to +12° (negative angles indicate leftwards relative to straight-ahead from the participant's point of view). The task of the participant was to respond (2-AFC) whether a presented LED was on the left or right of their midline (straight-ahead direction, 0°). Each trial consisted of a presentation of a randomly selected LED which remained visible until the end of the trial (i.e., until the participant verbally gave his/her answer to the experimenter). There was no constraint of time for the response. Each block was composed of 78 trials with central targets having more repetitions than peripheral ones (in order to construct psychometric functions). Each participant completed one block of trials during the first experimental session. The passive visual localization task was performed in the far workspace, the LED bar was located approximately 63.5 cm away from participants' eyes.

C. Passive, perceptual proprioceptive localization task. For the passive, perceptual proprioceptive localization task, the arm was held on a sled that could move from left to right (parallel to the torso) along a horizontal graduated ruler (Fig. 2.1C). Participants had to respond whether their index fingertip was located to the left or right of midline (2-AFC). The setup was built in such a way that a displacement of 1 cm indicated by the ruler was almost equivalent to a 1° displacement of the hand (12 cm = 11.89°). The distance of the hand from the body corresponded with the IHP used for the reaching experiment (see A above). Thirteen proprioceptive targets from -12° to +12° relative to midline and spaced in 2° intervals were randomly presented to the participant. The most eccentric proprioceptive targets (i.e. -12 and +12°) were tested twice and the more central targets were tested more often (up to 10 times for the 0° target). The experimenter passively moved the sled to align the fingertip to each of the different randomly selected locations. To prevent participants from estimating the position of their hand based on the duration and/or the magnitude of the movement, the experimenter switched from one position to another by moving the sled back and forth a number of times before arriving at the target position. Thereafter, the participants were asked to report whether their

index fingertip was on the left or on the right relative to their midline (straight-ahead direction, 0°). They kept their eyes closed during the entire block of 78 trials. Participants performed one block with the right hand placed on the sled during the first experimental session ; and another block with the left hand during the second session. This task was performed in the near workspace, in the area surrounding the IHP.

D. Active, motor visual localization task. This task was designed to assess visual reliabilities through visually-guided reaching movements to one of the 5 randomly presented targets (Fig. 2.1C). The trial sequence was the same as the prism reach task, except that the prism that did not displace vision (0° prism) was the only one that was presented at the beginning of the trial. Participants completed 10 trials for each of the 5 targets, totaling 50 trials per hand. They performed one block using each the left and right hands during the first and second experimental session respectively. As for the prism reach, the active visual localization task was performed in the middle workspace.

E. Active, motor proprioceptive localization task. This task was designed to assess proprioceptive reliabilities during active movements. We asked participants to match the location of a target hand (specifically index fingertip), that was moved passively on the sled, by reaching to it using the opposite hand (Fig. 2.1D). Five target hand positions were chosen : one at the center (0°), two on the left (-5 and -11°) and two on the right (+5 and +11°) with respect to the participants' midline and on the same horizontal plan as the IHP in the prism reach experiment described above. Positions were randomly determined, participants had their eyes closed and were asked to indicate where their target hand (index fingertip) was by reaching with their opposite hand slightly above the target hand's index fingertip from a central initial hand position (IHP). In this task, proprioceptive reliability for the left hand was assessed in the condition where left hand was the target and right hand was pointing. In the same way, right hand proprioceptive reliability was assessed when participants localized their right target hand by reaching with the left hand. As in the passive localization task, to prevent participants from estimating the position of their target hand based on the duration and/or the magnitude

of the movement, the experimenter switched from one position to another by moving the sled back and forth a number of times before arriving at the target position. Participants completed 10 trials for each of the 5 targets, totaling 50 trials per hand and participant. They performed one block in the first session with the right hand in the sled and the left hand pointing and vice versa for the second session. Just like the passive proprioceptive localization task, the active proprioceptive localization task was performed in the near workspace.

Data analysis

In the *prism experiments*, we were interested in horizontal errors (X-axis) since the prisms shift vision horizontally. First, the X-errors expected when using only vision or proprioception were computed for each target and prism. These errors were obtained by subtracting the origin of the planned movement vector from the horizontal target displacement induced by prisms. As shown in Fig. 2.2B, when using proprioception only, errors are equal to the prismatic deviation corresponding to the target presented. When relying only on vision (Fig. 2.2A), small errors are expected when applying prisms because eccentricities, and thus prismatic deviations, are not the same for hand position and targets. Then, X-errors were plotted as a function of the prismatic deviations (for all targets) and linear regressions were performed (Fig. 2.2E). A slope of 1 was found when using proprioception only ($\alpha_p = 1$) while the slope when using vision only was equal to .02 ($\alpha_v = .02$). To evaluate the proprioceptive weights for every participant, the slope (α) of the linear regression between the individual mean X-errors for each target and the corresponding prismatic deviations was first computed. The slope of the linear regression corresponds to the relative weights of vision and proprioception. Therefore, participants showing a slope close to .02 give more weight to vision, whereas those with a slope closer to 1 rely more on proprioception (Fig. 2.2E). Then, each participant's proprioceptive weight (W_p) was calculated as follows :

$$W_p = \frac{\alpha - \alpha_v}{\alpha_p - \alpha_v} \tag{2.1}$$

This allowed to correct for α_v which was different from 0. When W_p equals 0, the participant relies completely on vision whereas W_p is equal to 1 if he/she relies entirely on proprioception.

For the *passive, perceptual localization tasks*, the proportion of rightward choices was plotted as a function of target position. For each participant, three separate psychometric curves were calculated, one for vision, and one for right hand and left hand proprioception respectively. The data were fitted with cumulative Gaussians using the *psignifit* toolbox (Wichmann & Hill, 2001a, 2001b) for Matlab (The MathWorks, Natick, MA, USA). The psychometric model we used included a lapse rate which was set to 10%. The psychometric function for a representative participant is depicted in Fig. 2.3. The just-noticeable difference (JND) was computed as the inverse slope of the psychometric curve between 30% and 70% of rightward responses. We used the JND as a measure of variability ; the steeper the psychometric curve's slope, the smaller the variability.

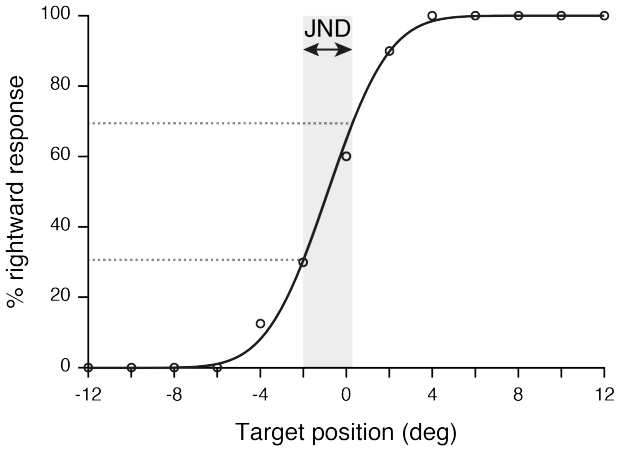

Figure 2.3 – Psychometric curve from one representative participant for the passive proprioceptive localization task. The percentage of rightward response is represented as a function of the target hand position (in deg). The participant's response data (open circles) is fitted with a psychometric function. The JND corresponds to the measure of the proprioceptive variability.

During *active, motor localization tasks*, positions and movements of both index fingers were recorded using the Optotrak motion-analysis system (NDI, Waterloo, Canada). Data were sampled at 1000 Hz and finger movements were measured in 3D space (in mm) relative to the IHP. Hand movements were detected using a velocity criterion (80mm/s). End positions of the index fingertip were recorded for each trial and pointing errors were computed using Matlab, by subtracting the end position of the finger from the target position. Errors in the horizontal X axis (X-errors) were thus calculated for each pointing movement and expressed in millimeters, such that a negative error would correspond to

an endpoint to the left of the target. The visual variability (σ_V^2) of each participant was defined as the standard deviation of the mean reach X-errors relative to the visual targets. Whereas left and right hand proprioceptive variabilities ($\sigma_{P_l}^2$ and $\sigma_{P_r}^2$) corresponded to the standard deviation of the mean X-errors when reaching to the left and right target hands, respectively.

Based on the measured estimates of uni-sensory variabilities, we predicted the multi-sensory proprioceptive weights (W) through simple Bayesian cue integration (Gaussian assumption) and calculated them for both the passive and active localization tasks as follows :

$$W_i = \frac{\sigma_{V\,i}^2}{\sigma_{V\,i}^2 + \sigma_{P\,i}^2} \tag{2.2}$$

with i corresponding to the hand that was tested (left or right). This was the same for the passive localization task, but since vision was tested without movements, only one visual variability was available. The two sets (active and passive) of predicted multi-sensory weights was then evaluated against the measured multi-sensory weights from the prism experiment.

For both left and right hands, normal distributions of the proprioceptive weights as well as the variabilities and the biases of vision and proprioception were assessed using Shapiro-Wilk tests. Given that some variables were not normally distributed, non-parametric tests were used for subsequent analyses. Correlations between parameters for the left and right hands were calculated and the strength of these relationships was assessed by Spearman's rank correlation coefficients and Wilcoxon signed rank tests. When a Wilcoxon test was found to be non-significant, equivalence testing was additionally performed to determine whether both correlated variables were similar. In traditional significance tests, the absence of an effect can be rejected but not statistically supported. Equivalence tests aim to provide support for the null-hypothesis (Lakens, 2016). We used the two one-sided test (TOST) procedure (Schuirmann, 1987), where equivalence is established at the α level if the $(1-2\alpha)\times 100\%$ confidence interval for the difference in means falls within the equivalence interval $[-\Delta;\Delta]$. In the TOST approach, two t-tests are used and equivalence is declared only when both tests are statistically rejected. The equivalence bounds were

based on the smallest effect size our study had sufficient power to detect ($d_z = .75$), such that $\Delta = d_z \times SD_{diff}$ where SD_{diff} is the standard deviation of the difference in means. Moreover, for each individual participant, we calculated whether the difference between the left and right hand parameters was significantly different from 0. In order to do that, the difference D between left and right hand parameters was first computed individually such that $D = left - right$. Then, the total standard deviation Σ_D was calculated for each participant as follows : $\Sigma_D = \sqrt{\Sigma_L^2 + \Sigma_R^2}$. D was considered significantly different from 0 when :

$$D \pm \Sigma_D > 0 \text{ if } D > 0 \quad \text{or} \quad D \pm \Sigma_D < 0 \text{ if } D < 0 \tag{2.3}$$

For all analyses, the statistical threshold was set at $p < .05$ (two-tailed tests) and $\alpha = .05$.

Results

The hand location during movement planning is determined through the integration of both visual and proprioceptive information. The visual variability should be the same regardless the hand that is tested, therefore the multi-sensory integration process requires the estimation of proprioceptive reliabilities for the left and right hands, independently. Visual-proprioceptive integration predicts that the visual and proprioceptive signals are combined and weighted according to their respective reliabilities. This is what is generally assumed to be true ; however, to our knowledge this has never been verified. To test this prediction explicitly, we first computed the relative contributions of vision and proprioception to reaching for both the left and right hands. We then independently evaluated the visual reliability as well as the left and right hand proprioceptive reliabilities in a passive and an active localization task. Finally, we used these independent measures to test whether multi-sensory integration weights could be predicted by the sensory reliabilities. The following section describe the results of these three steps in details.

Proprioceptive-visual weights

The relative contributions of vision and proprioception to reaching planning were assessed by pointing towards visual targets while shifting prisms were applied. Sensory weights were estimated for the left and right hands separately. As depicted for a typical participant in Fig. 2.4A, reach endpoints while using his right hand were deviated toward the direction of the shifting prisms that have been applied (e.g., endpoints on the left side of the target when the -10° prism is presented). As can be seen, this participant tended to undershoot the targets in depth (Y-direction), but this occurred across all targets and prism shifts. We presumed this was an overall bias and analysed only the horizontal reach error. To evaluate the proprioceptive weight, we performed a linear regression between observed mean reach errors (deviations in X-direction) for each target and the corresponding prismatic deviations (Fig. 2.4B). In Fig. 2.4B, the X-errors from Fig. 2.4A are shown as a function of the prismatic shift. Since the hand and the target had different eccentricities relative to midline, the horizontal displacement induced by prisms were not the same for both. Therefore, if only visual information was used, one would predict small reach errors across all three prisms conditions (Fig. 2.2A). In contrast, if vision was ignored, a reach endpoint displacement equivalent to the prism shift would be expected (Fig. 2.2B). Here, using equation 1, we calculated the proprioceptive weight for this participant for his right hand as .37. This weight can be interpreted as meaning that the participant relied on vision (1 - .37 = .63) more than on proprioception.

We calculated the proprioceptive weights in this manner for both hands separately for each of the sixteen participants. We then averaged the individual proprioceptive weights across all participants for each hand. The mean proprioceptive weights for left and right hands were equal to .55 (± .17) and .54 (± .16), respectively. A 1-sample Wilcoxon signed rank test showed that, for both hands, the average proprioceptive weights were significantly different from 0 and 1 (all $p < .001$). These results show that participants used a combination of visual and proprioceptive information, rather than just one or the other, when planning a reaching movement. Importantly, we directly compared individual proprioceptive weights for the left and right hands (Fig. 2.5). Left and right proprioceptive

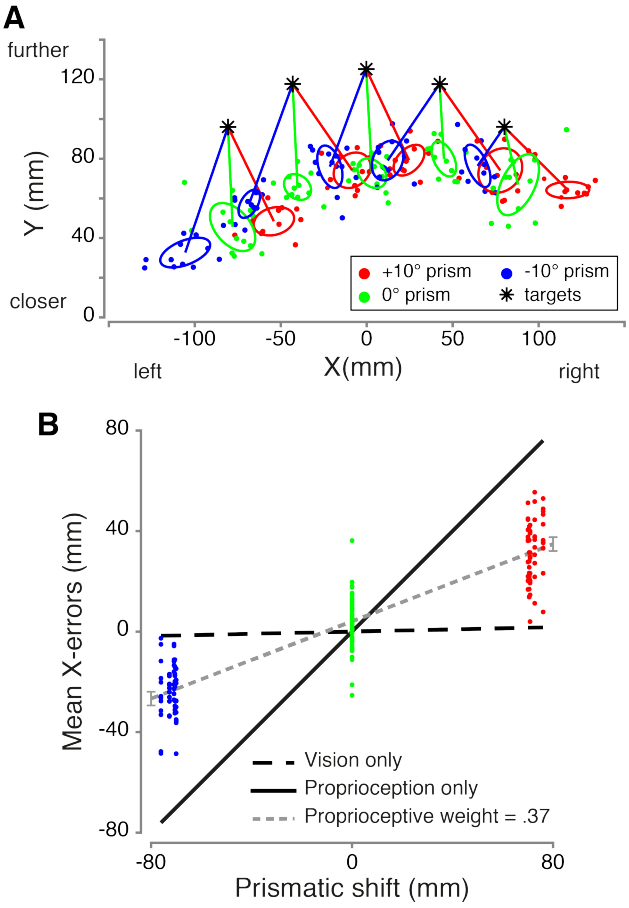

Figure 2.4 – A. Reach endpoints of one participant using his right hand, in the three prismatic conditions : 10-degree rightward, neutral and 10-degree leftward shifting prisms (in red, green and blue, respectively). The one-standard-deviation ellipses were computed for each target and each prism. The center of the ellipses corresponds to the mean error in each condition. B. Estimation of the participant's sensory weights when using the right hand. Data points for the -10° and +10° prisms (in blue and red) are more scattered because each of the 5 targets is displaced slightly differently depending on its eccentricity. The slope of the linear regression is .38. Thus, according to equation 1, the proprioceptive weight equals .37 whereas the visual weight is .63.

weights were highly correlated ($r = .94, p < .001; R^2 = .75, p < .001$), suggesting that the sensory reliabilities determining these weights were very similar across both hands within each participant. Moreover, the 95% confidence interval for the linear regression between left and right proprioceptive weights was [.63 ; 1.25]. Additionally, we tested whether there were overall differences in weights between left and right hands across all participants. A Wilcoxon test comparing the left and right hand weights showed no significant difference ($Z = .98, p = .33$), so an equivalence test was then performed. The equivalence region was set at $\Delta = d_z \times SD_{diff} = .75 \times .084 = .06$. The 90% confidence interval for the difference in the means was [-.02 ; .05] and was significantly within the equivalence bounds ($t(15) = -2.95, p = .01$). These results indicate that, across the population, the weights for the left and right hands were equivalent. In other words, the range of proprioceptive (and visual) weights were similar for the left and right hands across participants (ranging from .37 to .94 for the left and .37 to .91 for the right hand). Finally, the difference between the left and right proprioceptive weights was computed for each individual participant and

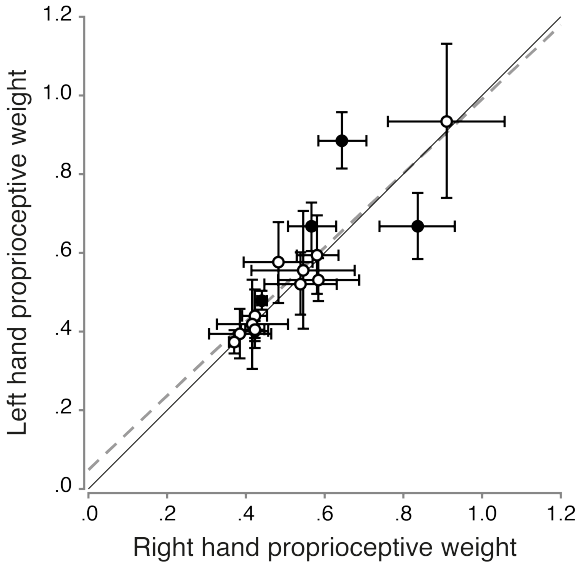

Figure 2.5 – Correlation between left and right hand proprioceptive weights. The error bars illustrate the 95% confidence intervals for the regression coefficients calculated individually for left and right hands (vertical and horizontal bars, respectively). The dashed grey line represents the line of best fit for the significant correlation for the sixteen participants ($r = .94, p < .001; R^2 = .75, p < .001$), that is very close to the perfect positive correlation. The solid black line corresponds to the line of unity, open circles represent participants who do not show left/right difference and filled circles represent participants showing a significant left/right difference.

compared to 0. As depicted in Fig. 2.5, four participants showed a significant difference while the 12 remaining participants showed no significant difference between the left and right proprioceptive weights.

We also investigated whether fast and slow movements had different weights. In order to do that, a median split has been performed on the movement durations for each participant and each hand, the proprioceptive weights were then computed and compared. The proprioceptive weights for slow and fast movements were significantly different for both the left (slow = .59, fast = .46 ; $t(15) = 3.5, p = .004$) and the right hand (slow = .61, fast = .42 ; $t(15) = 6.0, p < .001$). However, the left and right hand proprioceptive weights were not significantly different from each other for either slow ($t(15) = -.7, p = .48$) or fast movements ($t(15) = 1.5, p = .15$). Thus, although there were differences in visual-proprioceptive integration for fast and slow movements, the left and right hand multisensory integration weights were not different from one another for either slow or fast movements.

Sensory reliabilities of the left and right hands and vision

To obtain an independent evaluation of visual and proprioceptive variability, we next compared the sensory reliabilities of the left and right hands during the passive and active

localization tasks. If proprioceptive weights were based on actual sensory reliabilities, we should observe similar strong positive correlations between the sensory variabilities of the left and right hands. Each sensory reliability was assessed by the variability. We tested for significant correlations between left and right hand parameters in order to determine whether the same proprioceptive weights across both hands could be explained by similar sensory reliabilities between left and right hands.

Passive localization tasks. The participants were presented with visual or proprioceptive targets at different locations and were asked to respond whether they were on the left or the right relative to the body midline. Because sensory modalities were tested without movements in this particular context, we only measured variability for visual targets once, whereas we measured this twice for proprioceptive targets : once for each hand. Therefore, correlations between left and right hands were not possible for vision in the passive localization task. For proprioception, the correlation between left and right proprioceptive variabilities was non-significant ($p > .05$), as depicted in Fig. 2.6. This result indicates that unlike the weights, each participants' variabilities were not the same across the two hands. Pairwise comparisons showed that the range of proprioceptive variabilities ($Z = -1.29, p = .20$, left hand range = [.05 ; 1.28], right hand range = [.14 ; 1.08]) did not differ between left and right hands across the population. At the individual level, half of the participants showed a significant difference between the left and right proprioceptive variabilities (Fig. 2.6).

Active localization tasks. The participants were asked to point towards either visual or proprioceptive targets, with their left and right hands separately. This task was designed to measure the sensory reliabilities in a movement context similar to the one used in the reaching task (but without shifting prisms). The performance of a typical participant is depicted while using the right hand to reach towards visual (Fig. 2.7A) or proprioceptive targets (Fig. 2.7B).

Regarding reaches to proprioceptive targets (Fig. 2.8B), no significant correlation was found between left and right hand variabilities ($p > .05$). Thus, we also found differences

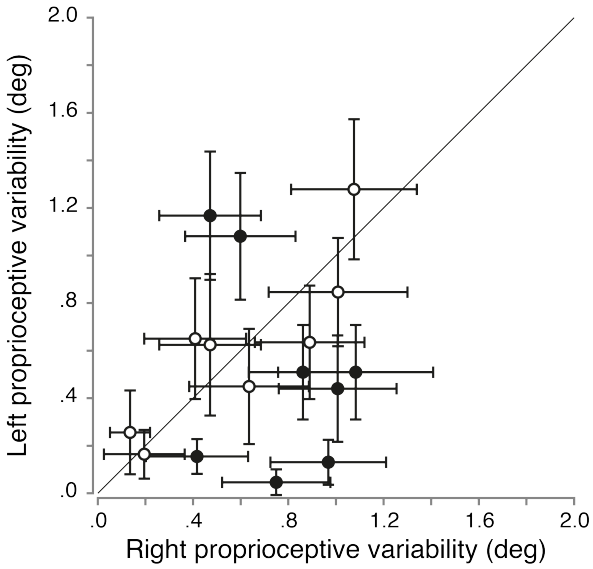

Figure 2.6 – Correlation between left and right proprioceptive variabilities in the passive localization task. The error bars are the 95% confidence intervals for the JNDs. No significant correlation between left and right hand was observed for the proprioceptive variabilities ($p > .05$). The solid black line corresponds to the line of unity, open circles represent participants who do not show left/right difference and filled circles represent participants showing a significant left/right difference.

between the proprioceptive variabilities between the left and right hands within each individual for this task. Note that proprioceptive variability of the right hand was evaluated in the condition where participants had to localize their right target hand when reaching with their opposite, left hand. Similarly, left hand proprioceptive variability was obtained when the left hand was the target hand. This is because we wish to measure the precision of proprioceptive spatial position for each hand. Pairwise comparisons did not show differences in the overall proprioceptive variabilities between the two hands (Fig. 2.8B, $Z = -.52, p = .61$, left hand range $= [11.95\,;\,26.42]$, right hand range $= [12.03\,;\,29.14]$). At the individual level, 13 participants out of 16 showed a significant difference between the left and right hand proprioceptive variabilities (Fig. 2.8B). Taken together these findings suggest an influence of the visual reach target information on reach variability rather than an influence of the hand used.

In summary, we found no correlation between the left and right hand proprioceptive variabilities for each participant in both the active and passive localization tasks. These findings demonstrate differences in left and right hand proprioceptive variability at the individual participant level that should – if combined in a statistically optimal fashion with vision – result in different proprioceptive weights for left and right hands. This is explicitly evaluated in the following section and contrasted against the proprioceptive weights found in the multi-sensory integration task (with prism shifts).

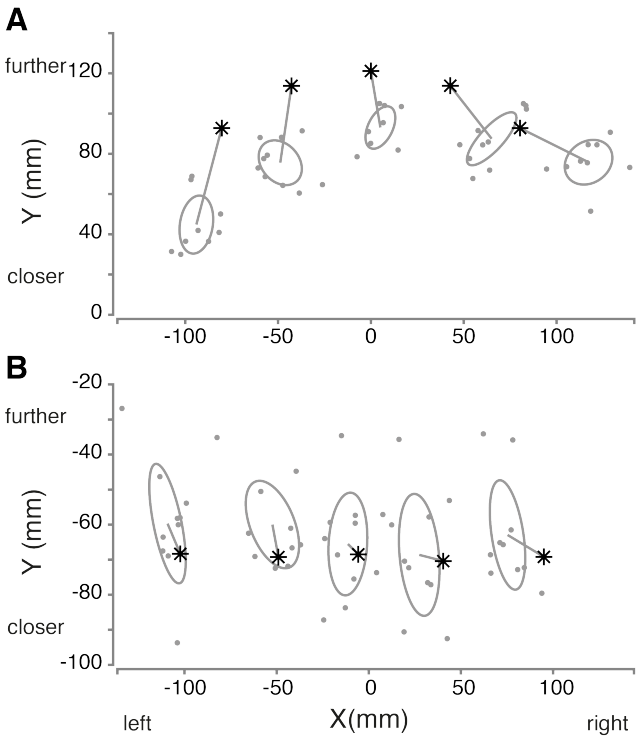

Figure 2.7 – Right-hand reach endpoints of one participant when pointing towards visual (A) and proprioceptive targets (B). Our workspace area is centered around the initial hand position whose coordinates are thus (0,0). The stars represent the targets and the one-standard-deviation ellipses were computed for each target. The center of the ellipses corresponds to the mean endpoint error.

Testing for the statistical optimality

If sensory variability is indeed used to determine multi-sensory integration weights, individual participant differences between left and right proprioceptive reliabilities should result in different proprioceptive weights between both hands. In order to determine whether the attribution of sensory weights was in line with the Bayes-optimal cue combination hypothesis, the proprioceptive weights observed during the reaching task (computed through linear regression ; see Figs. 2 and 4 and Methods) using shifting prisms were compared to those predicted from the sensory variabilities measured in the passive and active localization tasks (equation 2). The differences in proprioceptive weights between left and right hands were then calculated ($W_{left} - W_{right}$) for each participant. A difference equal to 0 means that the sensory weights are the same for left and right hands. Fig. 2.9 depicts the individual participants' observed differences in proprioceptive weights (prism shift task) plotted as a function of the differences predicted by the Bayesian cue combination model (separately for active and passive tasks, Fig. 2.9A and B respectively). In both the passive and the active localization tasks, most participants showed inter-manual differences in predicted proprioceptive weights. However, these differences

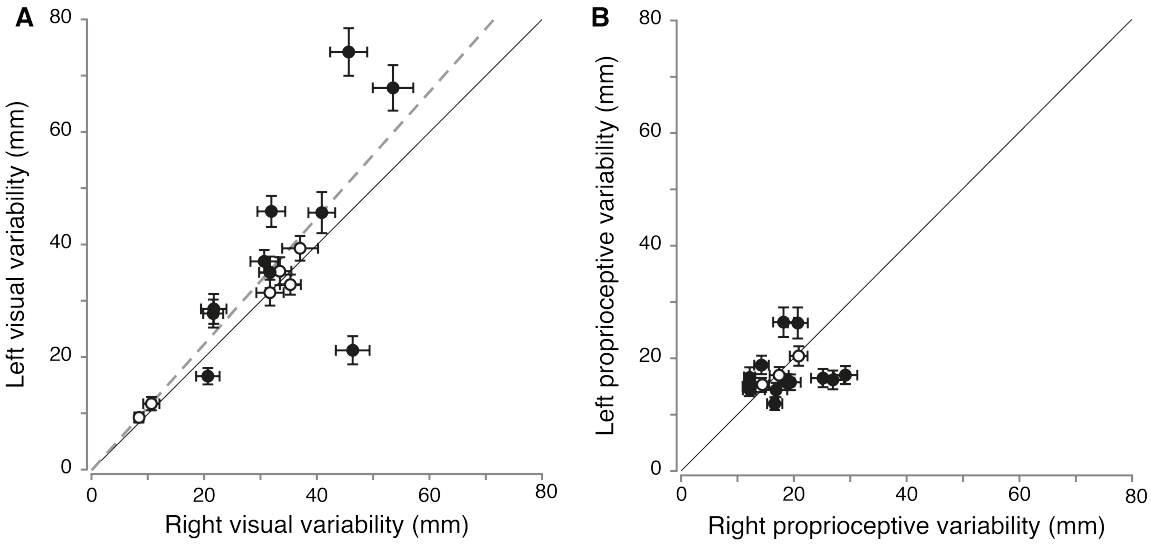

Figure 2.8 – Correlations between left and right hand variabilities for vision (A) and proprioception (B) in the active localization task. The error bars are the bootstrapped standard deviations. The dashed grey line illustrates the line of best fit for the significant correlation. The solid black line corresponds to the line of unity, open circles represent participants who do not show left/right difference and filled circles represent participants showing a significant left/-right difference. A. There was a significant correlation between left and right visual variabilities ($r = .72, p = .002; R^2 = .62, p < .001$). B. No significant correlation was observed between left and right proprioceptive variabilities ($p > .05$).

did not correlate with measured differences in proprioceptive multi-sensory integration weights (all $p > .05$), contradicting reliability-based proprioceptive weight computations. Moreover, simple linear regressions were performed to determine if there were significant relationships between observed and predicted differences in proprioceptive weights. The results showed that there was no linear relationship between the two variables, either for the passive ($R^2 = .02, p = .57$) or for the active localization task ($R^2 = .08, p = .30$).

An alternative way to evaluate whether visual and proprioceptive variability was accounted for is to look at the ratio of proprioceptive variance over visual variance. If for a given participant the ratio is high (i.e., if the proprioceptive variability is greater than the visual one), the proprioceptive weight should be low for that participant. Thus, when plotting observed proprioceptive weights against these ratios, we should observe negative correlations for both left and right hands. Correlations were computed separately for left and right hands, in both active and passive localization tasks (Fig. 2.10A and B respecti-

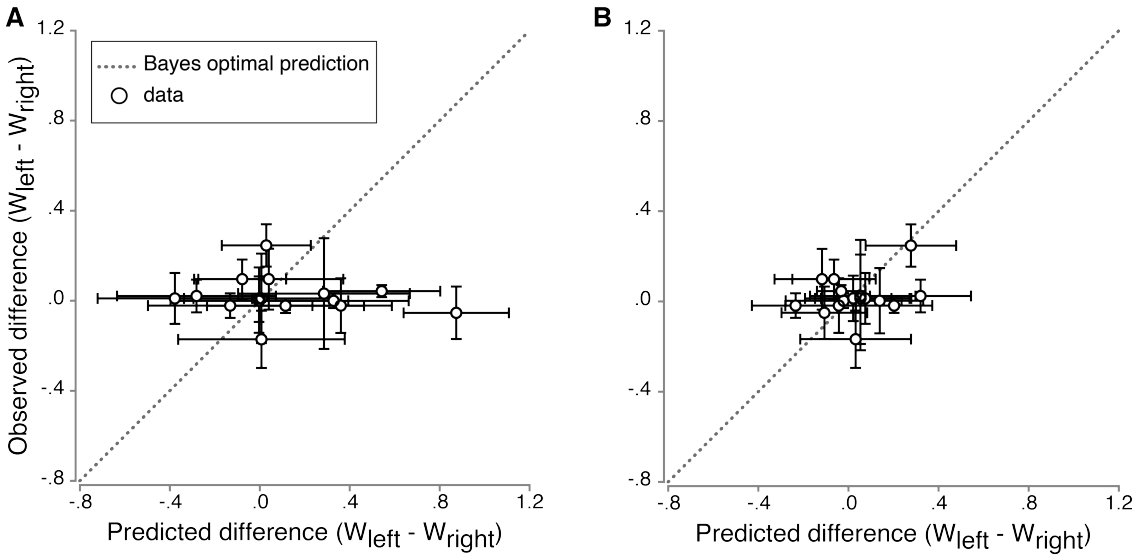

Figure 2.9 – Observed differences plotted as a function of predicted differences in proprioceptive weights ($W_{left} - W_{right}$) computed with the sensory variabilities measured in the passive (A) and the active (B) hand localization tasks. The vertical error bars are the 95% confidence intervals for the regression coefficients and the horizontal error bars are the standard deviations obtained by bootstrapping. The grey dotted line illustrates the Bayesian optimal prediction (i.e., observed and predicted sensory weights are the same). Most participants' differences in proprioceptive weights were around 0 for both localization tasks.

vely). None of the four correlations reached significance (all $p > .05$) and the four simple linear regressions showed that the ratio of sensory variances did not predict the proprioceptive weights that we observed (all $p > .05$). These results suggest that the individual sensory variabilities we measured were not taken into account to determine the sensory weights used for multi-sensory integration.

Discussion

Multi-sensory integration is conceived as an optimal combination of information from several sensory modalities to gain a more accurate representation of the environment and our body (Deneve & Pouget, 2004). Bayesian theory postulates that the weight given to each sensory modality is proportional to the reliability (i.e., the inverse variance) of each signal (Deneve & Pouget, 2004 ; Ernst & Banks, 2002 ; Ernst & Bülthoff, 2004 ; Jacobs, 2002 ; Lalanne & Lorenceau, 2004 ; O'Reilly et al., 2012). While overall, data seems to

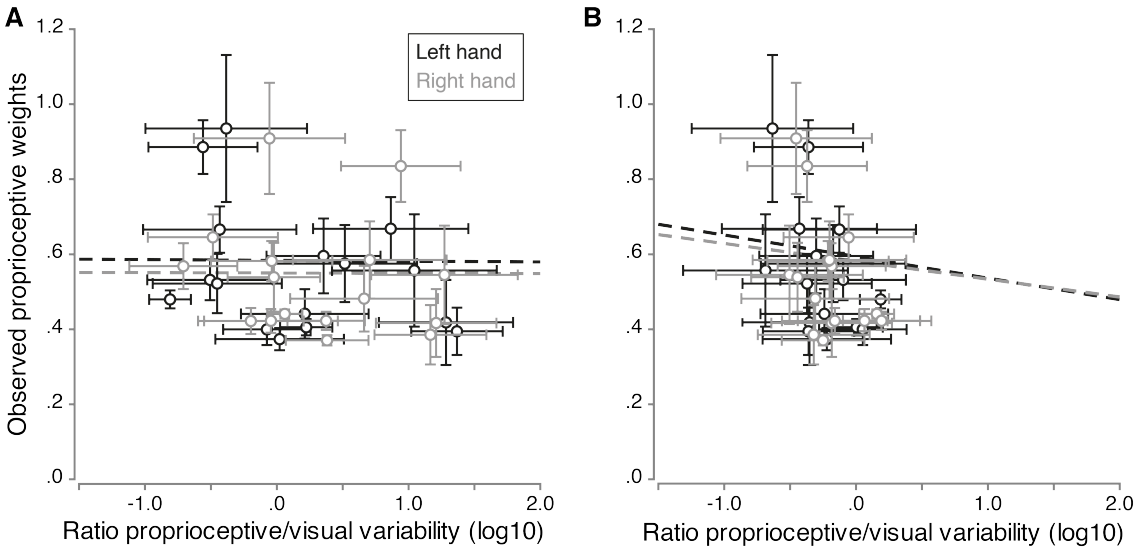

Figure 2.10 – Observed proprioceptive weights as a function of the log10 of the ratio of proprioceptive and visual variabilities measured in the passive (A) and the active (B) hand localization tasks. Data for left and right hands are represented in black and grey, respectively. The vertical error bars are the 95% confidence intervals for the regression coefficients and the horizontal error bars are the bootstrapped standard deviations. The dashed lines correspond to the correlations between the observed proprioceptive weights and the ratio of sensory variabilities ; none of them was significant (all $p > .05$).

be consistent with this prediction (e.g. Ernst & Banks, 2002 ; Körding & Wolpert, 2004 ; Sober & Sabes, 2005 ; van Beers et al., 1999a), it has to our knowledge never been critically tested. Here we devised such a test and show that differences in proprioceptive reliabilities of the left and right hand are not predictive of differences in multi-sensory weights for reaching.

Limitations

There are several important limitations to our study. One possible limitation is that the prism shift has introduced a sensory conflict between vision and proprioception. In that case, following the causal inference framework (Kayser & Shams, 2015 ; Körding et al., 2007 ; Shams & Beierholm, 2010), one would expect either that vision was not used at all (total breakdown of causality) which was not observed or that it would be weighted less (partial breakdown of causality) than predicted. The result of a partial breakdown of causality would be a reduced visual weighting that should result in a slope <1 (but >0)

in Figure 9. However, we did not find any relationship between predicted and observed weights despite that, on average both vision and proprioception were weighted about equally (no total breakdown of causality). Thus, we do not think that the introduction of prism shifts can explain our findings.

We were interested in how visual and proprioceptive information about the hand is weighted during the planning of reaching movements, that is to say at the IHP before movement initiation. One may argue that since our tasks measuring visual and proprioceptive variabilities were performed in different areas of the workspace (as indicated in Fig. 2.1C), they might therefore differ from those performed at the IHP. Both passive and active proprioceptive localization tasks were performed in the near workspace, close to the IHP area whereas passive and active visual localizations tasks were performed in the further and the middle workspace, respectively. It has been shown that hand localization is more precise for positions closer to the shoulder than further away (van Beers et al., 1998) and also that target distance did not significantly affect visual localization precision. The visual targets they used were roughly arranged between 35 and 55 cm from the cyclopean eye. Our workspace area did not exceed 63.5 cm (position of the LED bar) so distance should have no (or very little) influence on the visual reliabilities we measured. In addition, the passive visual task using the LED bar in the far workspace was a left-right discrimination and vision has been shown to be more precise in azimuth (horizontal plan) than in depth (van Beers et al., 1998). These insights suggest that our measures of visual and proprioceptive variabilities are appropriate to investigate visual-proprioceptive integration about the hand when planning a reaching movement. More importantly however, where possible we compared left and right hand variabilities as well as weights within the same task and not across tasks.

We assume that our perceptual and motor tasks are appropriate to measure proprioceptive variability of the hands. We chose these tasks because one could argue in two different ways regarding the brain's evaluation of sensory reliability : (1) the brain uses the actual sensory reliability that is inherent to performing a certain task – captured by our motor task. Therefore we measured visual and proprioceptive variabilities using a

similar reaching task to the prism task. (2) The brain uses the perceived reliabilities in a default fashion – captured by our perceptual task. This follows a prominent thesis by which perception can guide our actions (Binsted & Elliott, 1999 ; Both et al., 2003 ; Brenner & Smeets, 1996 ; D. B. Elliott et al., 2009 ; Jackson & Shaw, 2000 ; McCarley et al., 2003 ; Sheliga & Miles, 2003 ; Taghizadeh & Gail, 2014 ; van Donkelaar, 1999 ; Westwood et al., 2001). However, neither reliability measure could explain our multi-sensory integration data during action. This was less surprising for the perceptual context since previous research suggested that multi-sensory integration was different for perception and action (Blangero et al., 2007 ; Dijkerman & de Haan, 2007 ; Knill, 2005), in line with visual information processing within the ventral and the dorsal streams (Goodale & Milner, 1992). Moreover, a recent study showed that spatial priors learned in a sensorimotor task do not generalize to a computationally-equivalent perceptual task, thus suggesting that priors differ between perception and action (Chambers et al., 2017). It was much more surprising that our motor task did not predict multi-sensory weightings. As discussed below, we think that this might point towards a learned, default weighting rather than an individual trial and effector reliability-based weighting of multi-sensory information for reaching.

Several previous studies have reported effects of non-uniform priors on perception and action (Fernandes et al., 2014 ; Jacobs, 1999 ; Körding & Wolpert, 2004 ; Verstynen & Sabes, 2011). Unlike uniform priors where all prior probabilities are equal, non-uniform priors favor some particular values over others and can bias the cue combination results. It is possible that such priors also play a role in visual-proprioceptive integration tasks. For example, the sensory variability measured in the active proprioceptive localization task includes both the effector and the target variabilities. This target variability can be described as a non-uniform prior because it cannot be isolated and excluded, thus leading to an overestimation of the variance and therefore a potential bias in the multi-sensory weights. In that case, the prior would act like another cue in the multi-sensory integration. The result of that would be a reduction of the sensory weights because the denominator of the Bayesian weight term would have an additional, prior variance term (assuming Gaussian distributions) ; or in other words the sum of all weights (visual, proprioceptive,

prior) still has to be 1, thus reducing the visual and proprioceptive weights when introducing a prior. As a result, this would predict a reduced slope when comparing observed to predicted weights in Figure 9. However, the fact that we did not find any relationship whatsoever between observed and predicted weights indicates that the potential influence of priors cannot explain our results.

Interpretation of main findings

We found a strong correlation between the sensory weights of left and right hands (Fig. 2.5) but no such correlation was present between left and right proprioceptive reliabilities, either in the passive or in the active localization task (Figs. 6 and 8). Indeed, individual sensory weights were very similar between both hands despite individual differences in left and right hand proprioceptive reliabilities measured in the perceptual and the motor contexts. Jones et al. (2010) also assessed the precision of proprioception in two different contexts, using passive and active localisation tasks similar to ours : judgement of proprioceptive hand location relative to visual or proprioceptive reference for the former, and reaching with a seen hand to the proprioceptive hand location (unseen other hand) for the latter. The authors reported that the precision of proprioceptive localization did not differ significantly between left and right hands across the population ; however, they did not investigate whether there was a significant difference between left and right hands of each individual participant.

Moreover, in our present study, the relative variability of vision and proprioception, i.e. the ratio measured for each hand in the motor context, also failed to predict the sensory weights. It was not possible to know whether a similar relationship measured in the passive localization task would predict the relative sensory weights of the two hands because the visual variability was measured by a unique *verbal* judgement and thus cannot be compared between hands. These findings are not in agreement with the predictions made by the Bayesian model of multi-sensory integration. Thus, it seems that the sensory weights that are used for multi-sensory integration during reach planning are independent of left and right hand sensory reliabilities.

Our results rather suggest that the sensory weighting of hand location for reaching is task-dependent and learned. Task dependency has previously been suggested in a different context, though interpreted as an attentional effect (Sober & Sabes, 2005). The similar sensory weights we found across both hands suggest that they might be determined through learning the contingencies of the task rather than being specific to each effector. Our findings are in line with previous research showing that in certain cases the brain does not seem to compute a maximum-likelihood estimate of hand position (Jones et al., 2012). Likewise, when performing a bimanual task, proprioceptive signals from left and right arms are not assigned integration weights that are related to their respective proprioceptive reliabilities (Wong et al., 2014). This latter study showed that uni-manual proprioceptive variabilities were different between the two limbs and that the bimanual estimate of hand position did not result from an optimal combination of proprioceptive signals from left and right limbs. Instead, the nervous system seemed to ignore information from the arm with the lower reliability and to use only signals from the limb that has the best proprioceptive acuity for the bimanual task. Generalized motor programs (GMPs) have been introduced by (Schmidt, 1975) and are thought to specify generic, but not specific, instructions to execute movements. This allows for motor equivalence which is the capacity to achieve the same movement output irrespective of the effector used. The GMP comprises invariant features describing the overall movement pattern as well as parameters which are context-dependent and adjusted according to the goal of the action. Invariant components of the GMP might specify a common proprioceptive weight to both left and right hands whereas parameters induce small variations between both effectors, as observed in the present study. Invariant features of the GMP are likely to be learned early in development since children typically refine their reaching movements during the first years (Hadders-Algra, 2013). In contrast, parameters are task-dependent and might involve learning on a shorter time scale, maybe on a trial-by-trial basis, allowing for adjustments to specific situations.

One implication of Bayes-optimal integration is that the brain should have a good representation of sensorimotor variabilities. However, some studies have demonstrated

that the motor system does not always exactly estimate motor variability. It seems that, under some circumstances, human observers underestimate their own motor uncertainty (Mamassian, 2008) and do not show an accurate estimate of their motor error distributions (Zhang et al., 2013). In this last study, the authors concluded that reach planning in their specific task was based on an inaccurate internal model of motor uncertainty. Similarly, it has been found that humans have limited knowledge of their retinal sensitivity map, resulting in an inaccurate model of their own visual uncertainty during visual search (Zhang et al., 2010). In the case of multi-sensory integration and in the absence of the ability to robustly and accurately estimate sensorimotor variability, it might be advantageous for the brain to use integration weights that are learned and thus are more stable, rather than based on highly inaccurate sensory reliabilities. Thus, our study supports the notion that multi-sensory weights might be learned, which could represent an advantageous alternative for the sensorimotor system when sensory variability is difficult to reliably estimate.

Conclusions

In the present study, we investigated how visual and proprioceptive signals about hand position are weighted during multi-sensory integration for the planning of pointing movements. We found very similar proprioceptive weights for left and right hands despite differences in proprioceptive reliabilities between the two effectors, as measured in active perceptual and motor contexts. These results are in accordance with the hypothesis of modality-specific integration weights that are learned across both hands, rather than weights that are based on task- and hand-dependent sensory reliabilities.

Acknowledgements

This research did not receive any specific grant from funding agencies in the public, commercial, or not-for-profit sectors. GB and AK were supported by NSERC (Canada). AK was additionally supported by the Canada Research Chair program (Canada). LP was

supported by the CNRS and the Labex/Idex ANR-11-LABX-0042 (France). This work was performed at the “Mouvement & Handicap” platform at the Neurological Hospital Pierre Wertheimer in Bron (France). We would like to thank Claude Prablanc who designed the setup we used as well as Olivier Sillan and Roméo Salemme for programming the different tasks.

3 Étude 2 Intégration des informations proprioceptives et tactiles pour les mouvements de pointage

Vibrotactile information improves proprioceptive reaching target localization

Laura Mikula, Sofia Sahnoun, Laure Pisella, Gunnar Blohm, Aarlenne Z Khan

Article soumis pour publication dans *Plos One*

Points importants

- La mise en commun de plusieurs informations sensorielles permet une localisation plus précise d'un objet dans l'espace.
- L'objectif de cette étude est de déterminer si l'ajout d'informations tactiles permet d'améliorer la localisation proprioceptive de la main, lorsque celle-ci sert de cible à un mouvement de pointage.
- La précision de la localisation de la main est évaluée grâce à une tâche de pointage proprioceptif au cours de laquelle les participants doivent pointer avec leur main droite en direction de leur index gauche (index cible). Des stimulations vibrotactiles peuvent être délivrées sur le doigt cible avant l'initiation du mouvement.
- L'application de stimulations tactiles sur l'index cible entraîne une diminution des erreurs de pointage ainsi qu'une amélioration de la précision des mouvements.
- Ces résultats suggèrent que les informations proprioceptives et tactiles sont intégrées ensemble et permettent d'optimiser la localisation de la main en l'absence d'indices visuels.

Abstract

When pointing to parts of our own body (e.g., the opposite index finger), the position of the target is derived from proprioceptive signals. Consistent with the principles of multisensory integration, it has been found that participants better matched the position of their index finger when they also had visual cues about its location. Unlike vision, touch may not provide additional information about finger position in space, since fingertip tactile information theoretically remains the same irrespective of the postural configuration of the upper limb. However, since tactile and proprioceptive information are ultimately coded within the same population of posterior parietal neurons within high-level spatial representations, we nevertheless hypothesized that additional tactile information could benefit the processing of proprioceptive signals. To investigate the influence of tactile information on proprioceptive localization, we asked 19 participants to reach with the right hand towards the opposite unseen index finger (proprioceptive target). Vibrotactile stimuli were applied to the target index finger prior to movement execution. We found that participants made smaller errors and more consistent reaches following tactile stimulation. These results demonstrate that transient touch provided at the proprioceptive target improves subsequent reaching precision and accuracy. Such improvement was not observed when tactile stimulation was delivered to a distinct body part (the shoulder). This suggests a specific spatial integration of touch and proprioception at the level of high-level cortical body representations, resulting in touch improving position sense.

Introduction

To execute a hand reaching movement, the central nervous system needs to localize the target with respect to the hand. Its position can be derived from inputs provided by one or multiple sensory modalities such as vision, audition or somatosensation. Multisensory integration is referred to as the combination of information arising from different sensory modalities to form a unified and coherent representation of our environment and body. Accordingly, the brain combines all the relevant sensory information about the object

of interest in order to decrease the variance (the uncertainty) and build a more reliable representation of that object (Knill & Pouget, 2004 ; O'Reilly et al., 2012). Indeed, it has been shown that spatial localization was less variable for visual-auditory targets than for targets specified by vision or audition only (Godfroy-Cooper et al., 2015 ; Hairston et al., 2003). These findings suggest that the more sensory information available about the target, the more accurate its estimate.

When pointing to unseen parts of our own body (e.g. the opposite index finger), the position of the target is derived from proprioceptive signals. Proprioception corresponds to the sense of our body position in space. Consistent with the principles of multisensory integration, it has been found that participants better matched the position of their index finger when they could see their opposite arm during movement than when being blindfolded during the task (van Beers et al., 1996, 1999b). The localization of the fingertip was more precise in the presence of both vision and proprioception than when using visual or proprioceptive signals only. These results provide evidence that fingertip localization can be more precise if another sensory modality, in addition to proprioception, provides further information about the finger position.

Unlike vision, touch may not provide additional information about finger position in space, since fingertip tactile information theoretically remains the same irrespective of the postural configuration of the upper limb. However, touch can be regarded as a possible source of additional information for position sense, since touch and proprioception, although considered as separate modalities, have been shown to closely interact with each other. Behavioral studies have shown that tactile perception can be modulated by changes in proprioceptive signals, induced by active changes in hand posture (Warren et al., 2011) or tendon vibration (de Vignemont et al., 2005). Conversely, a finger-position matching task has been reported to be affected by nerve block and cutaneous anesthesia (Moberg, 1983), indicating that cutaneous afferents may provide a crude position sense for the fingers. Moreover, it has been shown that the localization of a proprioceptive target (i.e., the fingertip) was improved when participants contacted a surface with their target fingertip, which provides them with tactile feedback (Helms Tillery et al., 1994 ; Rao &

Gordon, 2001 ; Rincon-Gonzalez et al., 2012). Similarly, accuracy in pointing movements was enhanced when endpoint contact occurred with the effector fingertip (Lackner & Dizio, 1994). In contrast, digital anesthesia resulted in impaired fingertip localization (Rao & Gordon, 2001) as well as decreased movement accuracy during typing (A. M. Gordon & Soechting, 1995). This relationship between touch and proprioception is likely to be explained by the convergence of proprioceptive and tactile signals at the cortical level ; electrophysiological recordings in monkey have shown that neurons in the hand representation of the primary somatosensory cortex code both tactile and proprioceptive modalities during a reach-to-grasp task (Rincon-Gonzalez et al., 2012, 2011). It has also been established that neurons in the somatosensory cortex have both cutaneous and proprioceptive receptive fields (D. A. Cohen et al., 1994 ; Prud'homme et al., 1994). Taken together, these findings suggest that tactile afferent information may contribute to proprioception and improve the accuracy of the hand proprioceptive estimate.

The skin contains several mechanoreceptors, including Meissner and Pacinian corpuscles. Meissner corpuscles are located in the superficial layers of the skin and are sensitive to light touch while Pacinian corpuscles are found in deeper layers and respond to deep skin pressure and vibration. The properties of these two receptors suggest that they might be activated by fingertip contact ; Pacinian and Meissner corpuscles are fast-adapting receptors which are both sensitive to abrupt but not sustained stimuli (Macefield, 2005), such as when a finger makes or breaks contact with an object. Therefore, it is difficult to distinguish the relative contributions of Pacinian and Meissner corpuscules to the enhancement of proprioception following fingertip contact with a surface (Helms Tillery et al., 1994 ; Lackner & Dizio, 1994 ; Rao & Gordon, 2001 ; Rincon-Gonzalez et al., 2012). However, these two types of mechanoreceptors show different responses to cutaneous vibrations. Meissner corpuscles respond to low frequencies, 10-80 Hz, whereas Pacinian corpuscles are sensitive to vibrations at higher frequencies, 80-450 Hz (Talbot et al., 1968). Consequently, by stimulating either of these receptors, it would be possible to know which one contributes to the enhancement of proprioceptive localization.

It has been shown that the ability to detect flexion and extension movements imposed

at the interphalangeal joints of a finger was impaired when 300 Hz vibrations were applied to the adjacent or the test digit. In contrast, vibrotactile stimuli at 30 Hz did not alter proprioception in the finger (Weerakkody et al., 2007, 2009). The detection of passive finger movements at the interphalangeal joints is thus impaired by the specific activation of Pacinian, but not Meissner, afferents. These results demonstrate that vibrotactile stimulation can modulate proprioceptive acuity in a passive perceptual task, in which no action is involved. However, to our knowledge this has not been tested in a motor task, such as reaching, where the target location corresponds to the position of the fingertip.

The goal of the present study was to investigate the influence of vibrotactile information on the proprioceptive localization of the finger in a motor context. To this purpose, we asked participants to perform reaches to proprioceptively defined targets. They reached with the right index finger (reaching finger) to the unseen left index finger (target finger), which was passively displaced to different locations. Tactile vibrations at 30 or 300 Hz were delivered to the target index fingertip prior to movement onset. When vibrations are applied, the left index finger receives tactile information, in addition to existing proprioceptive information, about its location in space. In order to reach accurately, we presume that the brain constructs a reliable estimate of the target finger position using all the sensory information available. As suggested by previous studies (Talbot et al., 1968 ; Weerakkody et al., 2007, 2009), high- and low-frequency vibrations are more likely to activate Pacinian and Meissner corpuscles, respectively. We thus used 30 and 300 Hz vibrotactile stimulations to determine if one of these two mechanoreceptors contribute more than the other to touch-proprioception integration, or whether they both contribute to finger proprioceptive localization. We measured reach endpoint accuracy and precision to assess the effect of vibrations. We found that vibrotactile stimulations delivered at low and high frequencies improved both accuracy and precision of finger localization in a proprioceptive reaching task. A control condition in which the vibration was applied elsewhere on the body showed that this improvement in proprioceptive localization cannot be attributed to a global arousal enhancement induced by the tactile stimulus.

Methods

Participants

Nineteen participants took part in this study (12 females, mean ± SD age = 25.3 ± 10.7 years). They were all right-handed, as assessed by the Edinburgh Handedness Inventory and all had normal or corrected-to-normal vision. Participants were administered a questionnaire to ensure that they did not suffer from neurological, sensory or motor deficits, which may have interfered with their performance. All gave informed written consent to participate in this experiment which conformed to the Declaration of Helsinki (2008) for experiments on human subjects. All experimental procedures were approved by the health research ethics committee in France (CPP Nord-Ouest I, Lyon, 2017-A02562-51) and at the University of Montreal (17-034-CERES-D).

Apparatus

Participants sat in a dark room on a height-adjustable chair in front of a slanted table. Their head was held steady on a chin rest, aligned with their body midline. A wide-screen OLED monitor (55 inches diagonal, 1920 x 1080 pixels, LG) was placed facing downwards above the table and a half-reflecting mirror was positioned in between the screen and the table so that the screen was projected onto the tabletop surface. The half-reflecting mirror prevented participants from seeing their hands unless there was light underneath the mirror ; in that case vision of the hand was possible. Participants performed a proprioceptive pointing task. They were asked to reach with the right index finger (reaching finger) to the unseen left index finger (target finger). Participants' left forearm was resting on a platform in such a way that when the left index finger was aligned with the body midline, the elbow was located on average 17.5 cm on the left relative to the center (Fig. 3.1A). The left forearm was positioned at an angle of 47°. The forearm platform was motorized and could move laterally (left or right) to different target positions. The target locations for the left index finger were at -10, -5, 0, +5 and +10 cm

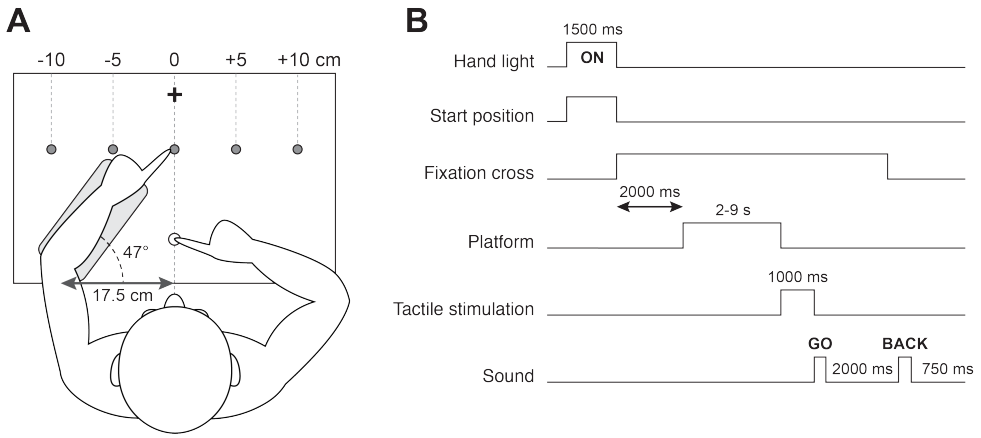

Figure 3.1 – A. Schematic of the apparatus, top view. Participants' left forearm was resting on a motorized platform that could move laterally to the five proprioceptive target positions (grey circles). The left forearm was positioned at an angle of 47° approximately. When the left index finger was aligned with the central target, the left elbow was 17.5 cm left relative to the body midline. The start position (white circle) for the right index finger was 15 cm ahead of the participants' torso. The fixation cross (black cross) was located further than the proprioceptive target positions. B. Sequence of a trial. The hang light and the start position were first turned on for 1500 ms and participants were asked to align their right index finger with the start position. Then, the fixation cross appeared and participants maintained gaze on the cross until the end of the trial. After 2000 ms, the platform started moving the left target hand for a variable amount of time (between 2 and 9 s). Afterwards, a tactile vibration was delivered to the left index finger for 1000 ms. Then a first auditory tone served as a "go" signal for participants to start reaching with their right index finger towards their left index fingertip. After 2000 ms, a second auditory tone was presented and participants put their right index finger back to the start position. The next trial started 750 ms later.

with respect to the body midline. A tactor was positioned on the left index fingertip and connected to an amplifier (TactAmp 4.2, Dancer Design, England, United Kingdom) that delivered tactile vibrations at a frequency of either 30 or 300 Hz. Eye movements were monitored using an EyeLink 1000 Plus (SR Research, Mississauga, Ontario, Canada) at a sampling rate of 1000 Hz. The positions of both left and right index fingers were measured using an Optotrak 3D Investigator recording system (NDI, Waterloo, Canada). This system recorded the position of two infrared emitting diodes, each one attached to the tip of each index finger. The movement of the infrared markers was tracked and sampled at a rate of 500 Hz.

Procedure

The sequence of a trial is depicted in Fig. 3.1B. At the beginning of each trial, a light was switched on for 1500 ms so that participants could see their hands. At the same time, a red dot aligned with the body midline and 15 cm distant from the torso was displayed also for 1500 ms. The red dot served as a start position and participants were asked to align their right index fingertip with the red dot and to keep it in this position until they began reaching. They kept their right fingertip balanced in the air above the table (no surface contact). As soon as the start position disappeared, a white fixation cross was displayed and participants were required to fixate the cross until the end of the trial. The fixation cross was aligned with the body midline above the target positions. After two seconds, the motorized platform moved the left target index finger to one of the 5 possible target locations. To prevent participants from learning proprioceptive target positions across trials, the platform made several back-and-forth movements (from 1 to 5) before stopping on a target location. Then, a vibrotactile stimulation was applied to the left target index fingertip for 1000 ms. Vibrations could be delivered at 0 (no vibration condition), 30 or 300 Hz. After the tactile stimulation, a first auditory tone signaled to the participants that they could begin reaching with their right hand. Participants had 2 s to complete their reach before a second auditory tone instructed them to return to the start position. Participants were instructed to reach to a location just above their left fingertip, pause in the air, then return to the start position. Specifically, participants were asked to reach to where they thought their left index fingertip was as accurately as possible and to avoid contacting their left target index finger with their right hand. To ensure that participants performed the task properly, they first did a practice block and were asked to report when finger-finger contact occurred during the experiment. The next trial began after 750 ms.

Each block was composed of 15 trials (3 vibration frequencies x 5 target positions). Each of the possible combinations of target and vibration frequency was presented in a random order. Each participant completed between 10 and 20 blocks to obtain at least 4 trials for each combination of target and vibration frequency.

To test for a possible effect of the fingertip vibration by arousal enhancement, participants performed 2 additional control blocks in which the location of the vibrotactile stimulus was varied. The trials were identical to those in the main experiment except that the vibration was delivered to the left shoulder. The order of the blocks (control and main experiments) was counterbalanced across participants.

Data analysis

In this proprioceptive reaching task, errors were defined as the difference between the positions of the left (target) index finger and the right (reaching) index finger at the end of the movement. Since the position of the target hand was varied in the horizontal axis, we only considered reaching errors in the x-direction. Errors in the x-direction were computed for each trial by subtracting the x-position of the target hand from the x-position of the right-hand endpoint. The constant x-error was expressed in mm and corresponded to the mean error in the x-direction for each target ; this measure provides an estimate of the accuracy of the localization of the fingertip position. We used dispersion error as a measure of reach precision (Rossetti et al., 1994). The dispersion error corresponded to the surface area of the endpoints around each corresponding target, it was expressed in mm^2 and computed with the following formula : $SD_x \times SD_y \times \pi$. With SD_x and SD_y corresponding to the standard deviations of reach endpoints in the x- and y-direction, respectively. Dispersion error provides an estimate of the precision of the localization of the fingertip position. Constant x-errors and dispersion errors were first calculated for each participant, vibration condition and target position, then averaged across target positions and participants. To test the influence of the vibration frequency on constant x-errors and dispersion errors, a one-way repeated measures ANOVA was performed for each type of error separately. Similarly, one-way repeated measures ANOVAs were performed on constant x-errors and dispersion errors for each of the two attention control experiments. Tukey HSD tests were used for post-hoc comparisons of the means. The threshold for statistical significance was set at 0.05 for all analyses.

Results

Reach endpoints relative to the five possible proprioceptive target locations are depicted in Fig. 3.2 for one participant. Endpoints are represented for all three experimental conditions : the no vibration condition, the 30 Hz and the 300 Hz vibration conditions (in red, green and blue, respectively). The one-standard-deviation ellipses correspond to the dispersion of reach endpoints and the center of ellipses represents the mean reach error. For this participant, reach endpoints were overall more scattered when no tactile stimulus was delivered to the target index fingertip (in red) compared to the 30 Hz and the 300 Hz vibration conditions (in green and blue).

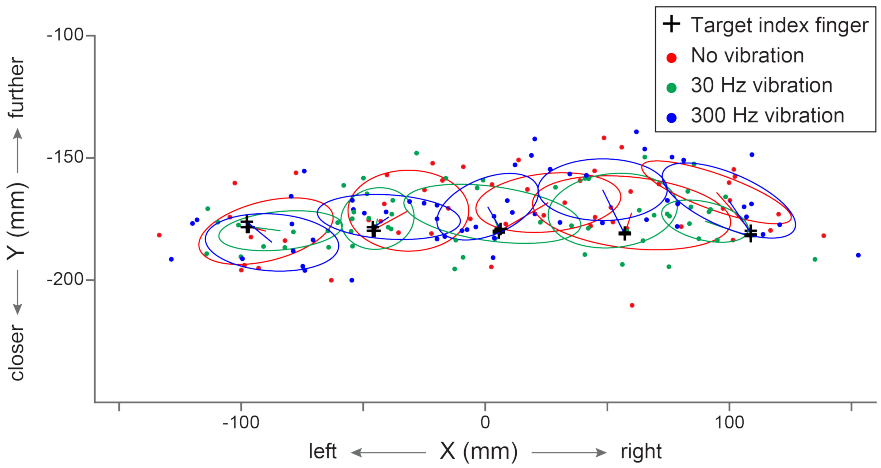

Figure 3.2 – Reach endpoints for one participant. The participant reached in the dark with his right hand towards his unseen left target index finger under three conditions. A vibrotactile stimulation could be applied to the left index fingertip prior to movement onset at either 30 Hz (in green) or 300 Hz (in blue). Alternatively, no vibration was delivered (in red). Black crosses correspond to the average position of the target index finger to reach for. One-standard-deviation ellipses were computed for each target and each vibration condition. The center of the ellipses corresponds to the mean error in each condition.

Constant x-errors

A one-way repeated measures ANOVA was performed on the reach errors in the x-direction. It revealed a significant effect of the vibration frequency ($F_{2,36} = 7.56$, $p = 0.002$, $\eta^2 = 41.30$). Constant x-errors were equal to 12.3 $\pm$ 2.5 mm (mean $\pm$ SE) when no

vibration was applied prior to the proprioceptive reach onset (Fig. 3.3). Constant x-errors in the 30 Hz and the 300 Hz vibration conditions were 8.9 ± 2.1 mm and 9.1 ± 2.2 mm, respectively. Post-hoc tests showed that, compared to the no vibration condition, constant x-errors were significantly reduced when either a 30 Hz (mean ± SE of the difference = 3.4 ± 1.2 mm, $t_{18} = 3.29$, $p = 0.004$) or a 300 Hz vibration (3.2 ± 1.0 mm, $t_{18} = 3.09$, $p = 0.006$) was delivered to the left target index finger. However, constant x-errors were not significantly different between the 30 Hz and the 300 Hz vibration conditions (-0.2 ± 0.7 mm, $t_{18} = 0.02$, $p > 0.05$).

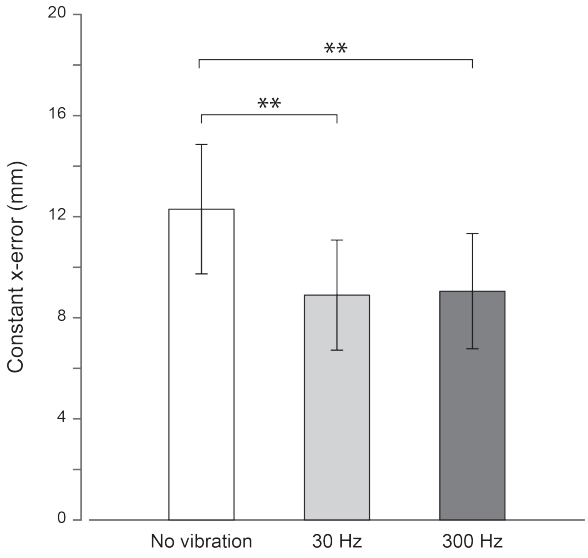

Figure 3.3 – Constant x-errors (in mm) as a function of the vibrotactile stimulation applied. Errors when no vibration is applied to the left target index finger are represented by the white bar. Errors when 30 and 300 Hz vibrations are delivered are represented in light and dark grey bars, respectively. The error bars correspond to the standard error of the mean across participants. $^{**}p < 0.01$.

Dispersion errors

The one-way repeated measures ANOVA on the dispersion errors was also significant ($F_{2,36} = 4.61$, $p = 0.017$, $\eta^2 = 46.83$). As depicted in Fig. 3.4, the greatest dispersion errors are observed in the no vibration condition (923.1 ± 91.3 mm^2), followed by dispersion errors in the 30 Hz (819.7 ± 82.3 mm^2) and then in the 300 Hz vibration condition (805.6 ± 68.8 mm^2). Post-hoc tests showed that these errors significantly decreased when vibrotactile stimuli were delivered at 30 Hz (103.3 ± 41.6 mm^2, $t_{18} = 2.10$, $p = 0.050$) and 300 Hz (117.5 ± 44.0 mm^2, $t_{18} = 2.49$, $p = 0.023$). Dispersion errors between the 30 and 300 Hz vibration conditions did not significantly differ from each other (14.2 ± 37.6 mm^2, $t_{18} = 0.08$, $p > 0.05$).

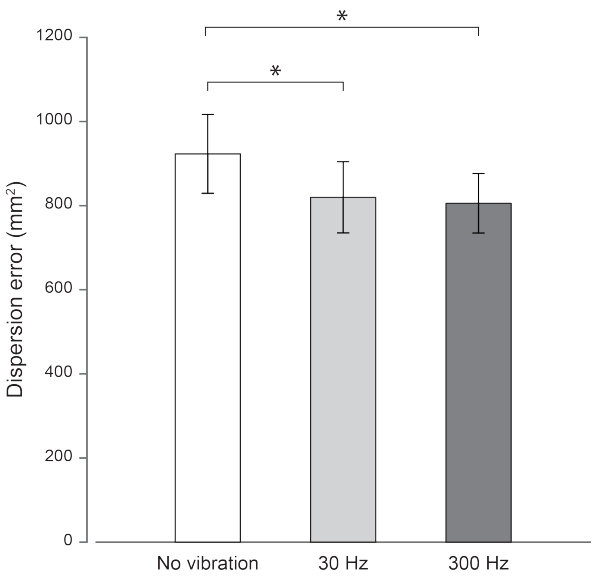

Figure 3.4 – Dispersion errors (in mm^2) as a function of the vibrotactile stimulation applied. Errors when no vibration is applied to the left target index finger are represented by the white bar. Errors when 30 and 300 Hz vibrations are delivered are represented in light and dark grey bars, respectively. The error bars correspond to the standard error of the mean across participants. $^*p < 0.05$.

Control experiment

We found that both high- and low-frequency vibrations applied to the target fingertip reduced constant x-errors and dispersion errors, suggesting that tactile information was combined with proprioception and improved spatial localization of the left target finger. It could be due to an effect of the vibration by arousal enhancement. To test for this, we investigated whether constant x-errors and dispersion errors changed when the vibration was delivered elsewhere. Thus, participants performed a control experiment where the vibrotactile stimulus was applied to the left shoulder. If reduced errors consecutive to the vibration of the left fingertip result from an effect of arousal, they should also be observed in this control condition. If they rather result from a specific spatial multisensory integration, then stimulation on the shoulder should not improve constant or dispersion errors compared to the no vibration condition.

The constant x-errors and the dispersion errors when the vibration was applied on the left shoulder are shown in Figs. 5A and B, respectively. Constant x-errors in the no, 30 Hz and 300 Hz vibration conditions were equal to 8.1 ± 3.5 mm, 13.4 ± 3.1 mm and 11.3 ± 2.8 mm, respectively (Fig. 3.5A). The one-way repeated measures ANOVA on the constant x-errors showed that the vibration frequency effect was significant ($F_{2,36} = 3.7$, $p = 0.035$, $\eta^2 = 41.30$). Post-hoc tests showed that constant x-errors were specifically increased when vibrotactile stimulation was delivered at 30 Hz (-5.2 ± 2.2 mm, $t_{18} = 2.39$, $p = 0.028$) and

not when delivered at 300 Hz (-3.2 ± 1.8 mm, $t_{18} = 1.22$, $p > 0.05$). However, constant x-errors were not different between low- and high-frequency vibrotactile stimulations (2.0 ± 1.6 mm, $t_{18} = 0.61$, $p > 0.05$). As for dispersion errors, there was no significant effect of vibration frequency when the left shoulder was stimulated ($F_{2,36} = 0.26$, $p > 0.05$; Fig. 3.5B). These findings suggest that the improved spatial localization of the left target finger following vibrotactile stimulus on the fingertip is unlikely due to global arousal effect of the vibration.

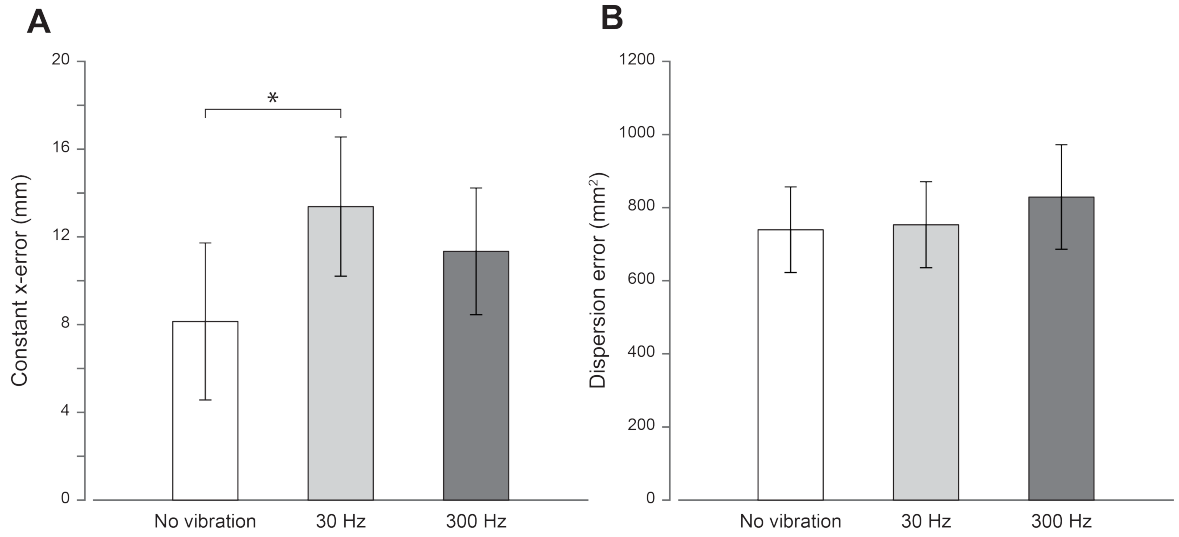

Figure 3.5 – Constant x-errors (A) and dispersion errors (B) for the control experiment. In this experiment, vibrotactile stimulations are delivered to the left shoulder. Errors when no vibration is applied are represented by the white bar. Errors when 30 and 300 Hz vibrations are delivered are represented in light and dark grey bars, respectively. The error bars correspond to the standard error of the mean. A. Constant x-errors (in mm) as a function of the vibrotactile stimulation applied to the left shoulder. B. Dispersion errors (in mm^2) as a function of the vibrotactile stimulation applied to the left shoulder. *$p < 0.05$.

Discussion

In the context of multisensory information, it is acknowledged that the brain combines all the available sensory information to build a precise and robust representation of the world (Ernst & Bülthoff, 2004; Knill & Pouget, 2004). For instance, accurate reaching movements require precise target localization prior to motor execution and several studies

have shown that this localization was better when more than one sensory modality provided information about the target position (Godfroy-Cooper et al., 2015 ; Hairston et al., 2003 ; van Beers et al., 1999a). When pointing to our body parts (e.g. the opposite index finger), the target is proprioceptively defined and reaches tend to be more variable than those directed to visual targets (Sober & Sabes, 2005). This might be related to a greater uncertainty in the localization of proprioceptive versus visual targets (van Beers et al., 1998). Hence, proprioceptive reaching might be improved if a second sensory modality provides additional information about the spatial location of the target. The interaction between touch and proprioception that has been reported in previous studies (de Vignemont et al., 2005 ; Moberg, 1983 ; Warren et al., 2011) suggests that tactile information could be used as a second source of sensory information to improve the localization of a proprioceptive target.

The goal of this study was to investigate the influence of tactile information on the proprioceptive localization of the index finger in a motor context. In order to do so, we had participants perform a position-matching task in which they were asked to make reaches with the right index finger to a proprioceptive target (i.e., the opposite left index finger). No visual feedback of the hand was provided during reach execution and 30 or 300 Hz vibrotactile stimulations were applied on the left target index fingertip prior to movement onset. Trials in which no tactile vibration was delivered to the left index finger were also included. Constant x-errors and dispersion errors were measured and compared across all three experimental conditions. Constant x-errors represent the reach accuracy, that is to say how close the right reaching finger is from the left target finger ; the smaller the constant x-error, the greater the reach accuracy. Dispersion errors refer to reach precision which reflect how consistent reach endpoints are when repeated ; the smaller the dispersion error, the greater the reach precision.

We found that reach accuracy and precision, measured as constant and dispersion errors respectively, were both affected by the application of vibrotactile stimulations on the left target index fingertip. Indeed, both the constant and the dispersion errors were reduced when 30 or 300 Hz vibrations were delivered, as compared to the no vibration

condition. Thus, it seems that cutaneous vibrations at either low or high frequencies provided the nervous system with additional (though slightly different) tactile information about the left index finger position. As a result, the spatial localization of the proprioceptive target was enhanced and both the accuracy and the precision of reaching were improved relative to the condition with no tactile stimulation. These results suggest that tactile information from the cutaneous vibrations is integrated with proprioceptive information about the position of the target index finger. In accordance with multisensory integration principles, the congruent proprioceptive and tactile information enhanced the finger proprioceptive localization, and ultimately improved proprioceptive reach performance.

The finding that both 30 and 300 Hz vibrotactile stimulations similarly improve reaching performance does not allow us to conclude about the specific contributions of Meissner and Pacinian corpuscles to touch-proprioceptive integration. According to previous studies, low- and high-frequency cutaneous vibrations appear to have distinct effects on proprioceptive acuity (Weerakkody et al., 2007, 2009). Performance in a passive finger movement detection task was impaired when stimulations at 300 Hz were delivered to the finger. In contrast, the application of 30 Hz vibrations did not alter task performance. However, in our study we found similar results when either 30 or 300 Hz vibrotactile stimulation was applied to the proprioceptive target of the reach (i.e., the left index finger). Both high- and low-frequency tactile stimulations led to an improvement in reach accuracy and precision when pointing to the left index finger. These discrepancies might be explained by the fact that the tasks used in these studies were fundamentally different. Participants in Weerakkody's studies (Weerakkody et al., 2007, 2009) performed a perceptual task in which they reported whether the movement imposed to their finger was a flexion or an extension. In contrast, in our study, participants were asked to localize a proprioceptive target and match its position by reaching with the opposite index finger. It has been proposed that somatosensory, and thus proprioceptive and tactile information is processed differently for perception and for action (Dijkerman & de Haan, 2007). Similar to the two cortical processing streams described in the visual system (Goodale & Mil-

ner, 1992), the "ventral" pathway is concerned with conscious somatosensory perception and object recognition while the "dorsal" pathway is relevant for guidance of action. The functional dissociation between the two somatosensory pathways has been established by studies in brain-damaged patients showing that they could perform motor actions towards somatosensory targets which were not consciously perceived (Aglioti et al., 1996 ; Paillard et al., 1983 ; Rossetti, Rode, & Boisson, 1995). These two separate somatosensory streams might explain why vibrotactile information is processed differently in perceptual and motor tasks. Nevertheless, it has been reported that separating the different tactile afferent fibers is challenging. It does not only depend on the stimulus frequency, but also on other parameters such as skin temperature (Bolanowski et al., 1988). Moreover, Meissner and Pacinian corpuscles are likely to have partially overlapping sensitivities, and thus detection thresholds which are relatively close to each other (Talbot et al., 1968 ; Bolanowski et al., 1988 ; Mountcastle et al., 1972). In the present study, it is therefore possible that the two vibrotactile frequencies delivered to the left target index finger might have activated both Meissner and Pacinian corpuscles. That could also explain why we did not observe difference between the 30 and 300 Hz vibration conditions.

In the present study, we found that tactile information provided on fingertip was integrated with proprioception, resulting in an improved spatial localization of the target fingertip during proprioceptive reaching. It could be that this improvement in spatial localization produced by the tactile stimuli was due to arousal enhancement related to the presence of an additional signal (i.e., the vibration). However, we found in a control experiment that putting the same vibration on the left shoulder did not improve reach precision (dispersion errors) as it did when the finger was vibrated, and while it produced changes to reach accuracy (constant x-errors), these were in the opposite manner as expected. Indeed, there was a decrease in accuracy rather than an increase as would be expected by increased arousal. Furthermore this effect was not consistent across the two vibration frequencies. Alternatively, enhanced spatial localization of the left target finger following vibrotactile stimuli could be explained by spatial attentional cueing effects. The vibration would act as a cue driving attention to the left index finger. If this was

the case, a cue from another sensory modality (e.g. audition) delivered nearby the hand should improve fingertip localization as well. We believe that this is unlikely to account for our results since it has recently been shown that auditory cueing does not modulate hand localization accuracy (Bellan et al., 2017). Thus, we can rule out arousal and spatial attentional cueing effects.

Our effect results from a specific spatial integration of tactile and proprioceptive information. However, the exact mechanisms underlying this multisensory integration remain to be determined. According to the classic view of somatosensory processing, although both ascending through the dorsal column-medial lemniscal pathway, tactile and proprioceptive inputs remain segregated and are transmitted to distinct areas of the primary somatosensory cortex (S1) (Mountcastle, 2005). Somatosensory signals are not merged together until they reach higher-order somatosensory areas, such as the posterior parietal cortex. This integration is thought to be mediated by area 5 in the intraparietal cortex, where both tactile and proprioceptive inputs converge (Rizzolatti et al., 1998). However, electrophysiological recordings (mainly in areas 3b, 1 and 2) have provided evidence that some neurons in S1 respond to both tactile and proprioceptive signals (D. A. Cohen et al., 1994 ; Prud'homme et al., 1994 ; Weber et al., 2011). These findings support an alternative but not exclusive hypothesis that multimodal interaction, and thus integration, between touch and proprioception might also occur at the level of S1, presumably in all sub-areas. Indeed, about half of S1 neurons, located in multimodal areas 1 and 2 but also in the previously thought modality-specific areas 3a (proprioception) and 3b (cutaneous), showed responses to both proprioceptive and tactile stimuli (Kim et al., 2015). Further research is needed to elucidate the mechanisms underpinning touch-proprioceptive integration and determine how tactile inputs influence the processing of proprioceptive information.

Acknowledgements

LM received support from a PhD excellence scholarship from Faculté des Etudes Supérieures et Postdoctorales and École d'Optométrie de l'Université de Montréal (FESP-ÉOUM). AZK and GB were funded by the Natural Sciences and Engineering Research

Council of Canada (NSERC). AZK was additionally supported by the Canada Research Chair program. LP was supported by the CNRS and the Labex/Idex ANR-11-LABX-0042, France. The authors would like to thank Romain Fournet for technical assistance.

4 Étude 3 Dégradation de l'estimation de la position de la main en mouvement suite à une lésion du cortex pariétal

Movement drift in optic ataxia

Laura Mikula, Laure Pisella, Gunnar Blohm, Aarlenne Z Khan

Article en préparation

Points importants

- Lors de mouvements de pointage répétés dans le noir, la main dévie progressivement des cibles à atteindre. Ce phénomène aurait pour origine une mauvaise mise à jour de la position de la main et impliquerait le CPP.
- Cette étude a pour but de déterminer les effets de lésions du CPP sur la mise à jour de la représentation interne de la main pendant le mouvement.
- Les participants doivent effectuer des pointages successifs vers deux cibles dans le noir. En plus des participants sains contrôles, deux patients avec ataxie optique présentant une lésion unilatérale ou bilatérale du CPP sont testés.
- Dans le noir, la déviation motrice est plus importante chez les patients ataxiques que chez les sujets sains, plus particulièrement lorsque la main se déplace dans le champ visuel inférieur. Cependant, les performances sont similaires entre patients et sujets contrôles lorsque la main est visible.
- L'ensemble des résultats démontre que le CPP est impliqué dans la mise à jour de l'estimation de la position de la main, sur la base des réafférences sensorielles et de la copie des commandes motrices.

Abstract

Planning and execution of reaching movements relies on accurate estimates of the arm position based on efference copy and sensory reafferences. Along with the cerebellum, the posterior parietal cortex (PPC) is thought to be involved in internal state estimation, and more specifically in the updating of the hand position estimate during movements. To test this hypothesis, we examined movement drift, a phenomenon that manifests in gradual shifts of hand position across movements in the absence of visual feedback. It is thought that this drift might related to the accuracy of the internal hand representation ; the more variable the hand position estimate, the greater the drift. Thus, if the PPC has indeed a role in the updating of the hand estimate, we should observe greater movement drift following lesions involving the parietal cortex. We tested fourteen healthy control participants as well as two patients with optic ataxia (OA), following either unilateral or bilateral damage to the PPC. We found that both OA patients were not impaired when provided with visual feedback of the hand during repetitive movements ; they showed performances similar to controls. However, in the absence of hand vision, patients showed substantially greater movement drift than control participants, especially when moving within the lower peripheral visual field. These findings indicate that the PPC might be involved in the updating of the internal representation of the hand based on both visual and proprioceptive reafferences. As a consequence of PPC damage and in the absence of visual feedback, the hand position estimate is not properly updated, thus causing errors to accumulate over successive trials.

Introduction

The central nervous system must generate estimates of the state of the world and the body to plan movements and monitor them during execution. The state estimate of a motor effector, such as the arm, is generated by combining a copy of the ongoing motor command, known as the efference copy, with the latest afferent sensory information, referred to as sensory feedback or reafference (Wolpert et al., 1995 ; Wolpert & Ghahramani,

2000). The optimal integration of both motor and sensory signals reduces the overall uncertainty of the arm state estimate (Abidi & Gonzalez, 1992 ; Vaziri et al., 2006). In order to update the state of the arm across movements (Wolpert & Miall, 1996), the brain continually combines reafferent sensory information and copies of descending motor commands as the movement unfolds (Wolpert & Ghahramani, 2000). State estimates can be inaccurate but optimal state estimation postulates that these inaccuracies are reverberated when computing updated estimates of the state of the arm. Thus, recursive state estimation assumes that the internal representation of the arm must be stored and then updated as a function of the incoming sensory and motor signals (Wolpert, Goodbody, & Husain, 1998). The cerebellum is a key structure for state estimation (Blakemore et al., 2001 ; Miall et al., 2007 ; Wolpert, Miall, & Kawato, 1998) and previous studies have suggested that the posterior parietal cortex (PPC) might also contribute to the internal state estimate during goal-directed movements (Buneo & Andersen, 2006 ; Desmurget & Grafton, 2000 ; Mulliken et al., 2008).

The PPC is a sensorimotor interface particularly important for visually-guided hand movements as well as multisensory integration (Andersen et al., 1997 ; Y. E. Cohen, 2009). The PPC is a good candidate to build an internal state estimate of the hand for reaching movements (Buneo & Andersen, 2006 ; Desmurget & Grafton, 2000 ; Mulliken et al., 2008). First, the PPC is reciprocally connected to the cerebellum (Amino et al., 2001 ; Clower et al., 2001 ; Glickstein, 2000). Moreover, resting state fMRI revealed functional connectivity between these two regions (Buckner et al., 2011). These findings suggest that the PPC might work in conjunction with the cerebellum, which has been shown to be causally involved in state estimation (Miall et al., 2007). Second, the PPC has numerous reciprocal connections with the frontal motor areas, particularly the premotor and the primary motor cortex (Gharbawie et al., 2011 ; P. B. Johnson et al., 1996 ; Wise et al., 1997). Thus, the efference copy from the primary motor cortex can reach the PPC through these projections (Kalaska et al., 1983 ; Mountcastle et al., 1975). Reciprocally, the parieto-frontal connections allow the PPC to influence the ongoing motor commands. Finally, electrophysiological recordings in monkeys showed that the PPC combines both visual

and proprioceptive signals to encode the position of the arm (Graziano et al., 2000).

Previous studies showed that hand position drift is observed when participants are asked to perform repetitive movements between two stationary targets without visual feedback of the hand (Brown et al., 2003 ; Cameron et al., 2015 ; Smeets et al., 2006). Reaches gradually drift away from the intended targets and errors accumulate while remaining undetected by participants. It has been proposed that movement drift is a passive mechanism of error accumulation (Cameron et al., 2015). In the absence of visual feedback, the predicted hand position estimate has higher uncertainty and deteriorates over time as it is too coarsely updated (Wolpert & Ghahramani, 2000). As a consequence, participants fail to compensate for motor execution errors and movements drift (Cameron et al., 2015). Thus, the limb position drift might be attributable to an inaccurate storage and/or updating of the arm state estimate involving the superior parietal lobule (SPL) of the PPC. This has been suggested by the observation of a patient with a unilateral lesion centered on the SPL, affecting mainly area 5. In the absence of vision, she experienced a drift of the perceived location of her contralesional arm that could only be prevented by looking at it. During hand matching tasks, participants had to match the location of their unseen stationary hand by using the opposite hand. In this paradigm, the patient's perception of her static limb position started to drift after about 18 seconds without visual feedback and gradually drifted by 30 cm 20 seconds later (Wolpert, Goodbody, & Husain, 1998). In contrast, previous studies have shown that neurologically intact participants drifted by only a few centimeters over the course of 120 seconds in the dark (Paillard & Brouchon, 1968 ; Wann & Ibrahim, 1992). The authors concluded that the patient was unable to store her own body state estimate and the internal representation of her contralesional limbs decayed over time (Wolpert, Goodbody, & Husain, 1998). This finding underlines the importance of the PPC in maintaining the internal representation of the body (Sirigu et al., 1996 ; Wolpert, Miall, & Kawato, 1998) which is updated during movement. If this was the case, damage to the PPC would be expected to substantially impact movement drift following repeated reaches in the dark.

The aim of this study is to examine whether the PPC is involved in the updating of

the hand position estimate and the error accumulation underlying movement drift. To do so, we tested two patients with optic ataxia (OA). Optic ataxia is a consequence of brain damage to the superior parieto-occipital cortex (Karnath & Perenin, 2005). OA is a visuomotor deficit that is not attributable to primary visual, proprioceptive or motor deficits (Garcin et al., 1967 ; Vighetto, 1980). Patients with OA have difficulty making accurate visually-guided movements, especially when targets are located in peripheral vision, within the visual field opposite to the damage (Buxbaum & Coslett, 1998 ; Milner et al., 1999 ; Perenin & Vighetto, 1988 ; Rossetti et al., 2003). They exhibit inaccuracies in central vision and in the ipsilesional visual field only when using the hand opposite to the damage (Perenin & Vighetto, 1988 ; Vighetto, 1980). Errors made when using the contralesional/ataxic hand are referred to as the "hand effect" whereas the "field effect" describes errors when reaching to targets presented in the contralesional/ataxic visual field. The hand and field effects are additive and OA patients show greatest errors when reaching with the ataxic hand to targets located in the ataxic visual field.

Here, we asked participants to make repetitive movements between two targets without visual feedback about hand position. We tested two OA patients, one with unilateral and one with bilateral PPC damage, as well as 14 neurologically intact control participants. The spatial and temporal patterns of movement drift in patients were compared to those observed in control participants. In control participants, we expect to find hand position drifts similar to what has been reported in anterior studies (Brown et al., 2003 ; Cameron et al., 2015 ; Patterson et al., 2017 ; Smeets et al., 2006). If the PPC is causally involved in the internal representation of the hand, we should observe substantial differences between movement drift in OA patients and controls. More specifically, we predict greater, faster and/or more variable hand position drift in patients compared to the control group as a result of inaccurate hand state estimation.

Methods

Participants

Two patients with OA took part in the present study. Patient CF is a right-handed male, who was 40 years old at the time of testing. In 2003, he suffered from a posterior watershed infarct resulting in distributed and asymmetrical bilateral lesions of Brodmann's areas BA 18, 19, 7, 5 and 2 with a minute extension to the centrum semiovale. Chronically, he exhibited isolated unilateral OA predominantly in his left visual field, thought to be the consequence of larger damage in the right hemisphere of both BA 7 and the intrahemispheric parieto-frontal fibers (Fig. 4.1A). Patient IG was a right-handed 48-year-old woman who, in 1998, suffered from an ischemic stroke related to acute vasospastic angiopathy in the posterior cerebral arteries. The lesion involved mainly BA 19, 18, 7, a limited part of area 39 as well as the intraparietal sulcus of both hemispheres (Fig. 4.1B). Examinations after the stroke demonstrated a chronic bilateral optic ataxia. Neither patient show any purely motor, somatosensory, visual deficits or signs of neglect.

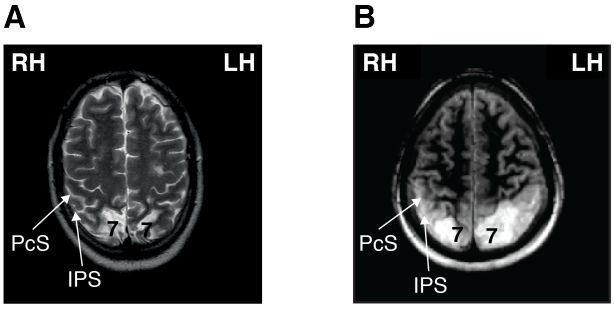

Figure 4.1 – A. Magnetic resonance imaging scan of patient CF. The white areas at the bottom of the scan show asymmetrical lesions to the occipito-parietal region, especially around Brodmann's area 7. The damage is larger in the right than in the left hemisphere. B. Magnetic resonance imaging scan of patient IG. The lesion is fairly symmetrically located in the posterior parietal and upper and lateral occipital cortico-subcortical regions. LH : left hemisphere, RH : right hemisphere, PcS : postcentral sulcus, IPS : intraparietal sulcus.

In addition, we tested fourteen neurologically intact control participants (8 females, mean age = 21.3 ± 2.8 years). They were all right-handed, as assessed by the Edinburgh Handedness Inventory and all had normal or corrected-to-normal vision. All participants

(including patients) were administered a questionnaire to ensure that they did not suffer from neurological, sensory or motor deficits during the 6 months prior to the experiment, which may have interfered with their performance. Participants gave informed written consent to participate in this experiment which conformed to the Declaration of Helsinki for experiments on human subjects. All experimental procedures were approved by the health research ethics committee (CPP Nord-Ouest I, Lyon, 2017-A02562-51) in France and at the University of Montreal in Canada.

Apparatus

Participants sat in a dark room on a height-adjustable chair in front of a slanted table. Their head was held steady on a chin rest, aligned with their body midline. An array of light emitting diodes (LEDs) and a half-reflecting mirror were positioned above the table so that the LEDs were projected onto the tabletop surface. The half-reflecting mirror allowed participants to see the LEDs while preventing the vision of their hand in the dark. Sight of the hand was possible only when a light source was illuminated underneath the mirror. Participants were required to reach with the index finger towards two targets aligned with the body midline. The distance between the near target (NT) and the far target (FT) was 12.5 cm. The NT was located 40 cm away from the table's edge and approximately 47 cm in front of the participants' torso. The position of the index finger was measured using an Optotrak motion-analysis system (NDI, Waterloo, Canada) ; the 3D position (in mm) of an infrared emitting diode attached to the index fingertip was recorded and data were sampled at 1000 Hz. Eye movements were recorded binocularly through an electrooculogram (EOG) using a DC electrooculograph system (50 Hz, model BM623, Biomedica Mangoni, Pisa, Italy). Two electrodes were placed outside the left and right eyes and a third one was positioned on the first thoracic vertebra and served as the reference electrode.

Experimental task

Participants were asked to reach back and forth between the FT and the NT, in time with auditory cues. The sequence of events during the task is depicted in Figure 4.2. At the beginning of the block, participants aligned their index fingertip with the illuminated NT, which served as a start location. After 500 ms, an auditory tone was presented and the NT was extinguished while the FT was illuminated. Participants were instructed to move quickly and accurately to the illuminated target upon hearing the tone. The NT and the FT were presented successively and the time between two consecutive targets was randomly selected in 100-ms intervals between 800 and 1200 ms. Each block was composed of 50 back-and-forth movements and lasted approximately 3 minutes. One trial comprised a movement to the FT and one toward the NT, thus corresponding to one back-and-forth movement. During the first 5 trials, participants could see the targets as well as their hand moving in between. Then, visual information about the hand position was removed for the remaining 45 trials. Participants were informed in advance that vision of the hand would be occluded after the fifth trial.

Participants were asked to make reaches under four different experimental conditions. In the 'free gaze' condition, eye movements were unconstrained. In contrast, participants were required to maintain gaze on the NT and the FT in the 'NT fixation' and 'FT fixation' conditions, respectively. The constraints on fixation were applied to address field effects, specifically for the unilateral patient. The 'hand vision' condition served as a control and was similar to the 'free gaze' condition, except that the hand was always visible so that participants could see their hand during the entire 50-trial block. Eye positions were monitored to ensure that participants maintained fixation on the required target during the fixation conditions.

Experimental design

Each control participant completed a total of 13 blocks : 1 block in the 'hand vision' condition and 4 blocks for each of the three other experimental conditions ('free gaze',

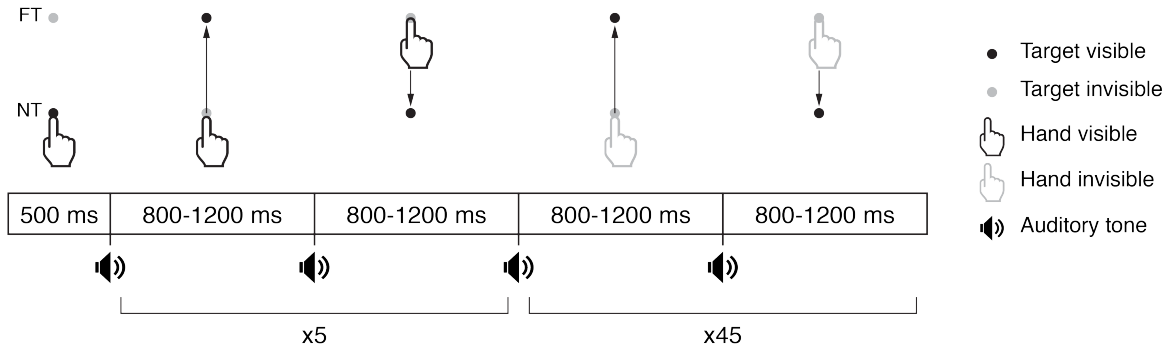

Figure 4.2 – Sequence of events during the experimental block. The near target (NT) and the far target (FT) were aligned with participants' body midline and were separated by 12.5 cm. Targets and hand depicted in black are visible whereas those in gray are not. Participants were instructed to reach toward the illuminated target when hearing tone. Targets were presented for 800 to 1200 ms. One trial consists of a reach to the FT, followed by another one to the NT. Participants had hull vision of their hand throughout the 5 first trials, whereas it was occluded during the 45 remaining trials. In the 'hand vision' condition, however, participants performed 50 trials with their hand visible.

'NT fixation' and 'FT fixation'). For all control participants, movements were made with the right hand. Similar to controls, bilateral patient IG performed 13 blocks using her right (most affected) hand. In addition, she performed 5 blocks with her left hand : 4 in the 'free gaze' condition as well as 1 in the 'hand vision' condition. Unilateral patient CF completed the same 13 blocks as control participants but with his left (contralesional) hand as well as 11 blocks with the right (ipsilesional) hand : 4 in 'free gaze', 3 in 'NT fixation', 3 in 'FT fixation' and 1 in 'hand vision' condition. We tested patients with both hands to address hand effects, as mentioned in the introduction.

Data analysis

Data were analyzed off-line using custom-written Matlab software (The MathWorks, Natick, MA, USA) and the CircStat toolbox for circular statistics (Berens, 2009). The 3D start and end positions of the index fingertip were calculated for each trial using velocity criteria (80 mm/s). Hand drift over time was characterized by the cumulative and the instantaneous drift, as defined by Brown et al. (2003). Accordingly, cumulative drift is the Euclidean distance between the start location during trial 1 and each successive

start location ($location_i - location_1$ with $i = [1; 50]$). The drift direction and distance correspond, respectively, to the angle (in degrees) and the magnitude (in mm) of the vector joining the initial position in the first trial without visual feedback (trial #6) and the final position in the last trial (trial #50). For every participant, the drift direction and distance were first computed for each block and then averaged within experimental conditions (except for the 'hand vision' condition which had only one block). The mean drift directions and distances were calculated using circular statistics. The instantaneous drift corresponds to the Euclidean distance between start locations on two successive trials ($location_i - location_{i-1}$ with $i = [2; 50]$). The instantaneous drift variability was computed by the standard deviation of the instantaneous drift over trial #6 and #50. For every participant, the standard deviation was first computed for each block and then averaged within experimental conditions (except for the 'hand vision' condition which had only one block).

To assess whether the performance of OA patients was significantly different from that of healthy participants, we used Crawford's modified two-tailed t-tests which are specifically designed to compare a single case to a control group (Crawford & Garthwaite, 2002 ; Crawford & Howell, 1998). The threshold for statistical significance was set to 0.05.

Results

The vectors between movement endpoints made by a typical control participant are shown in Figure 4.3. Movements during the first block for each of the 4 experimental conditions are depicted. Only endpoints from trial 6 to 50 are represented since they correspond to movements performed without visual feedback of the hand in the free gaze, NT fixation and FT fixation conditions. When visual feedback of the hand was provided in the hand vision condition, reaches made by control participants remained accurate throughout the block and did not deviate from the targets. Reaches performed by control participants in free gaze were slightly deviated from the targets when vision of the hand was removed but nevertheless remained quite accurate. The magnitude and the direction of reaching movements were relatively preserved over time despite the absence of visual

feedback of the hand. A similar observation was made for the NT fixation and the FT fixation conditions.

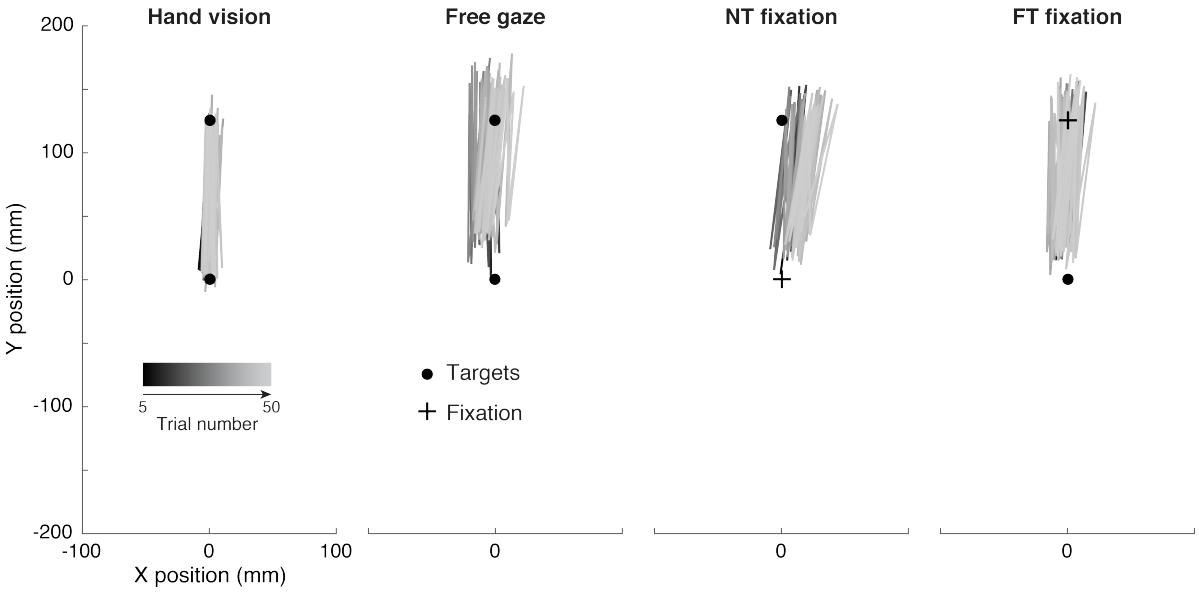

Figure 4.3 – Vectors between movement endpoints for a typical control participant, separated by experimental conditions (free gaze, NT fixation, FT fixation and hand vision). The cross indicates where participants are asked to maintain fixation throughout the block. Movements during the first block of each of the 4 experimental conditions are depicted. Only end positions from trial 5 to 50 are represented since they correspond to movements performed without visual feedback of the hand in the free gaze, NT fixation and FT fixation conditions. The color shade of the vectors represents the progression of trials throughout the block, with early trials being darker than late trials.

Vectors between reach end positions are represented in Figure 4.4 for both patients IG (top row) and CF (bottom row), in all experimental conditions. Both patients IG and CF exhibited accurate reaching movements with no drift when their moving hand was visible during the block (Figure 4.4, hand vision). In contrast, OA patients showed a substantial drift of hand movements in all three conditions in which visual feedback of the hand was not available (i.e. free gaze, NT fixation and FT fixation). The hand position progressively drifted during the task ; the first movements were close to the targets and then reaches moved away from targets' locations throughout the block. In the OA patients, both hands drifted in opposite directions. The right hand drifted to the left of the targets whereas left hand moved to the right. Bilateral patient IG seemed to be particularly impaired when

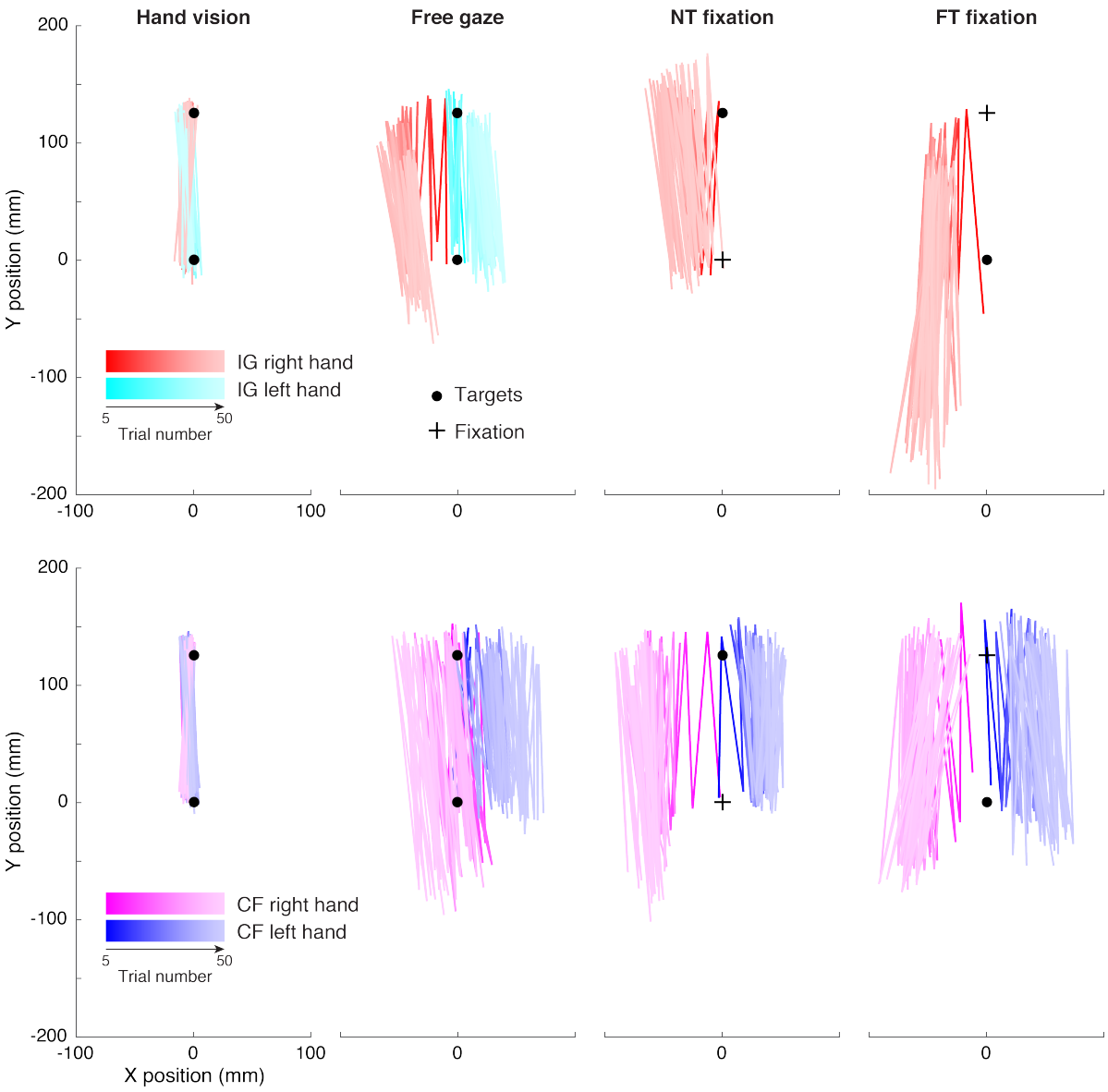

Figure 4.4 – Vectors between movement endpoints for patients IG (top row) and CF (bottom row), separated by experimental conditions (free gaze, NT fixation, FT fixation and hand vision). The cross indicates where participants are asked to maintain fixation throughout the block. Movements during the first block of each of the 4 experimental conditions are depicted. Only end positions from trial 5 to 50 are represented since they correspond to movements performed without visual feedback of the hand in the free gaze, NT fixation and FT fixation conditions. The color shade of the vectors represents the progression of trials throughout the block, with early trials being darker than late trials. Note that patient IG's left hand was only tested in the free gaze and hand vision conditions.

required to reach while maintaining fixation on the FT (Figure 4.4, top row). In addition to the movement drift observed in the free gaze and NT fixation conditions, the magnitude of the reach in the FT fixation condition was extensively increased over time. At the end of the block, patient IG undershot the NT by almost 200 mm. However, movement direction was relatively preserved.

In order to characterize the hand deviation over time, the cumulative drift was calculated for each trial. The cumulative drift across all control participants is represented in Figure 4.5 as well as the mean cumulative drift of patients IG and CF (left and right columns, respectively). In the hand vision condition, patients IG and CF showed very small and overall constant cumulative drift throughout the block, similar to control participants, when using either left or right hand. In the free gaze condition, IG showed a pattern of cumulative drift that was comparable to controls, for both her left and right hand. During the five first trials with hand visual feedback, cumulative drift was negligible, it increased gradually when vision of the hand was removed and reached a plateau around trial 30. CF's cumulative drift for both hands was very similar to that of control participants when hand visual feedback was provided. In the dark, however, his left and right hands progressively deviated from targets and differed from controls' drift around trial 10 after which the drift continued to accumulate but at a slower rate.

In the NT fixation condition, drift for IG's right hand and CF's left hand was similar to the cumulative drift observed in controls. In contrast, CF's right hand showed greater cumulative drift when vision of the hand was absent. The drift rapidly increased during the first trials in the dark, then errors continued to accumulate, albeit more slowly.

In the FT fixation condition, IG showed a drastic increase in cumulative drift when using the right hand. The hand started to deviate from targets during the first five trials in which the moving hand was visible. When vision of the hand was removed, cumulative drift continued to rapidly increase and reached 150 mm around trial 20 while control participants' drift was less than 50 mm. Patient IG's cumulative drift did not seem to plateau although it slowed down around trial 30. IG exhibited a cumulative drift close to

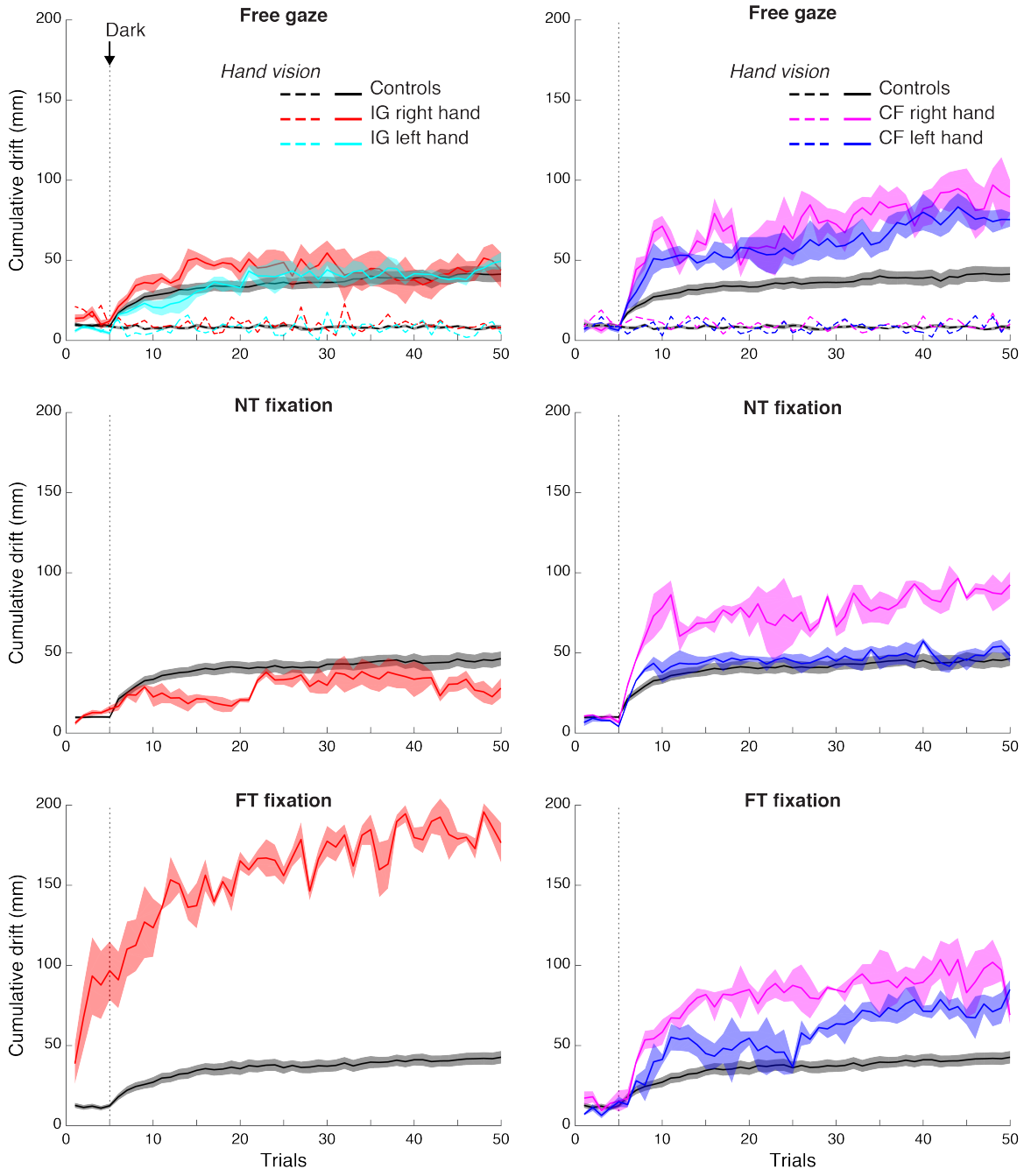

Figure 4.5 – Cumulative drift (in mm) as a function of trials for control participants and patients IG (left column) and CF (right column). Control participants' data are represented in black (right hand). Data from patient IG are depicted in red and cyan whereas those from patient CF are depicted in magenta and blue, for right and left hands respectively. The shaded area represents the standard error of the mean across participants for controls and across blocks for individual patient IG and CF. Dashed lines in the topmost subplots represent the cumulative drift measured in the hand vision condition. Note that patient IG's left hand was only tested in the free gaze and hand vision conditions.

200 mm by the end of the block. As for patient CF, when maintaining fixation on the FT, both hands drifted more compared to control participants. By the end of the block, CF showed cumulative drifts that were almost twice as much as controls.

The drift direction and distance for each participant, in all four experimental conditions are depicted in Figure 4.6. The drift direction and distance correspond, respectively, to the angle and the magnitude of the vector joining the initial hand position on the 6^{th} trial and the final hand position on the 50^{th} trial. In all four experimental conditions, there was no consistent drift direction across control participants since they each exhibited deviation in different directions. For both OA patients, consistent with what has already been described in Figure 4.4, the right hand moved toward the left of the targets while the left hand deviated to the right. Overall, patients tended to drift toward their body (Figure 4.6). However, due to the large variability between control participants, it was not possible to assess whether drift directions in patients were significantly different compared to controls (Crawford's tests, all $p > 0.05$).

In contrast, OA patients and control participants did not exhibit the same range of drift distance. In the hand vision condition, controls showed very little drift distance (9.6 $\pm$ 4.2 mm) as well as OA patients who did not exhibit significantly greater drift distances (Crawford's tests, all $p < 0.05$). In the free gaze condition, control participants drifted on average by 37.7 $\pm$ 14.7 mm from the NT. Unilateral patient CF showed significantly greater drift distance for both left (75.3 mm ; Crawford's test, $p = 0.029$) and right hands (88.1 mm ; Crawford's test, $p = 0.006$). However, bilateral patient IG did not drift significantly more than controls when using either the left (48.2 mm ; Crawford's test, $p > 0.05$) or right hand (34.0 mm ; Crawford's test, $p > 0.05$). In the NT fixation condition, the drift extent for controls was on average 43.2 $\pm$ 14.8 mm. Patient CF showed larger drift distance than control participants, specifically when using the right (93.6 mm ; Crawford's test, $p = 0.006$) but not the left hand (51.6 mm ; Crawford's test, $p > 0.05$). Drift distance observed for patient IG's right hand was not significantly different from controls (20.6 mm ; Crawford's test, $p > 0.05$). Finally, in the FT fixation condition, the

average drift distance for control participants was 37.8 ± 13.4 mm. When fixating on the FT, drift distance was significantly greater for both CF's hands (95.5 mm for left hand and 73.5 mm for right hand ; Crawford's tests, both $p < 0.05$) and IG's right hand (88.7 mm ; Crawford's test, $p = 0.003$).

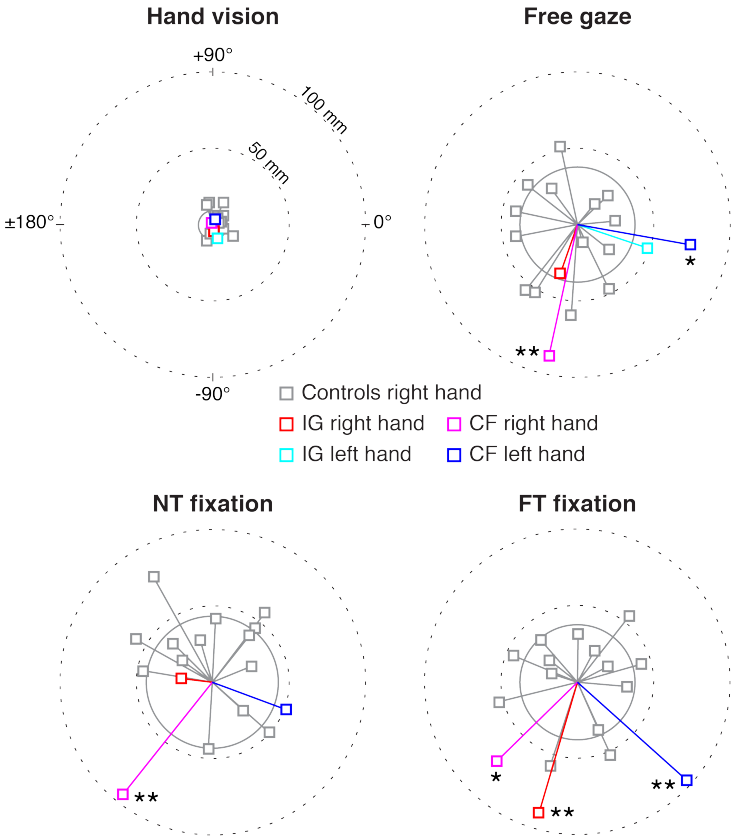

Figure 4.6 – Average drift distance (in mm) and direction (in degrees) for each participant, originating from the NT. Drift distance corresponds to the magnitude of the vector and drift direction to the vector angle. Negative and positive directions correspond to drifts toward and away from the body, respectively. Data from control participants are represented in gray while data from OA patients are depicted in different colors. The gray circle represents the mean drift distance averaged across all control participants. Note that patient IG's left hand was only tested in the free gaze and hand vision conditions. $*p < 0.05$, $**p < 0.01$.

In summary, both OA patients had similar performances to controls when visual feedback of the hand was available. Bilateral patient IG was not impaired in the free gaze and the NT fixation conditions but she showed greater movement drift compared to control participants when fixating on the NT. In the NT fixation condition, movements were predominantly performed in the lower visual field. In contrast, patient CF's drift distance was greater compared to controls when reaching with the right hand in the dark (free gaze, NT fixation and FT fixation conditions). Moreover, he also exhibited substantial drift with his left hand when moving in the free gaze and FT fixation, but not in the NT fixation condition.

The mean instantaneous drift is represented in Figure 4.7. In control participants,

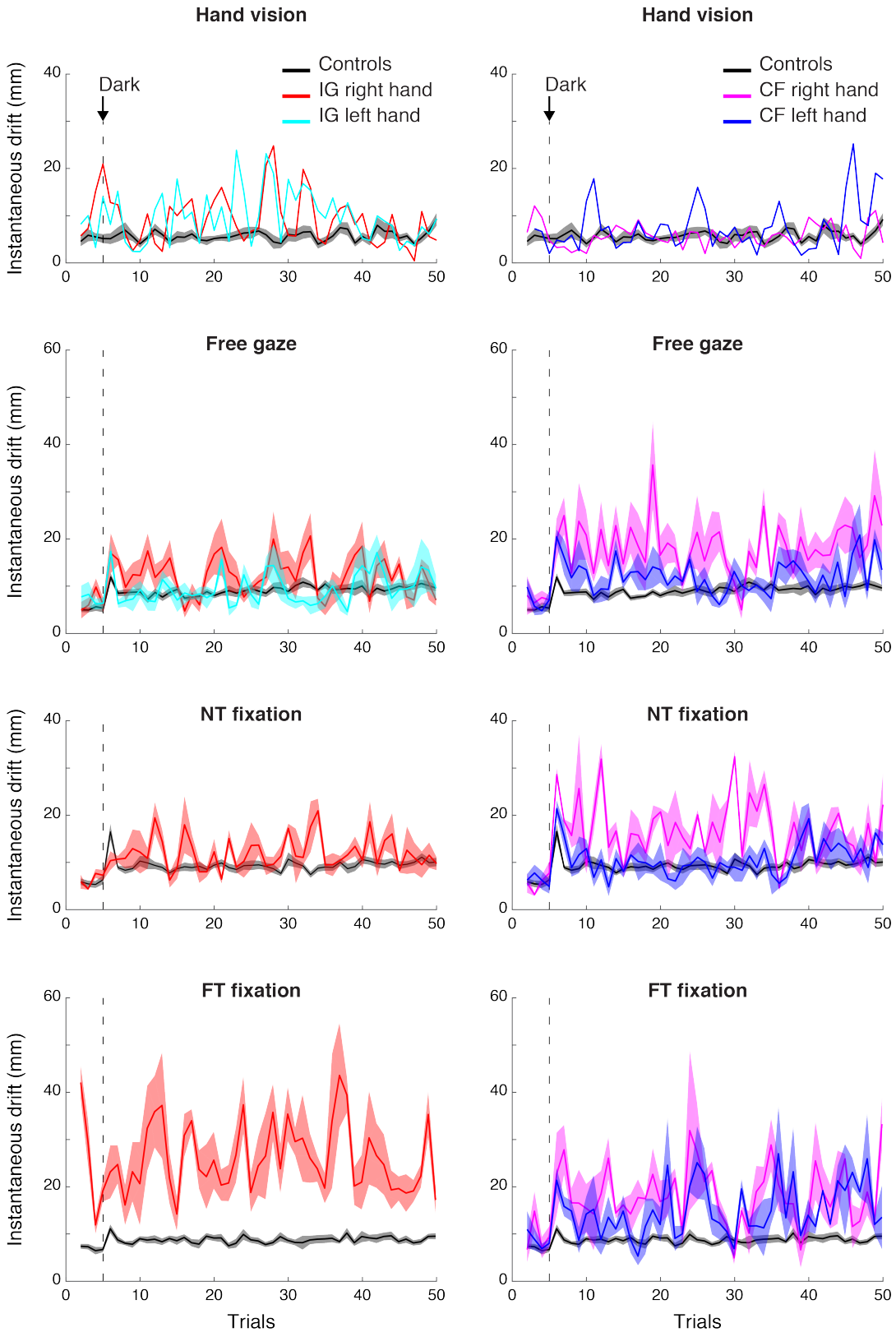

Figure 4.7 – Instantaneous drift (in mm) as a function of trials for patients IG, CF and control participants. The color code is the same as in previous figures. The shaded area represents the standard error of the mean across participants for controls and across blocks for individual patient IG and CF. Note that patient IG's left hand was only tested in the free gaze and hand vision conditions.

the instantaneous drift remained relatively constant around 5 mm in the hand vision condition. In the three other conditions where visual feedback of the hand was removed, the instantaneous drift slightly increased during the first trials in the dark and then stabilized at about 10 mm for the remaining trials of the blocks. Compared to controls, both OA patients showed larger instantaneous drifts in all four experimental conditions. This was especially true for patient IG in the NT fixation condition. In unilateral patient CF, the instantaneous drift appeared to be overall larger when using his ipsilesional (right) hand.

Figure 4.8 depicts the standard deviation of the instantaneous drift for patients compared to control participants in all four experimental conditions. In the hand vision condition, control participants showed small instantaneous drift variability (3.5 ± 1.3 mm) as did IG (5.5 mm for left hand and 5.2 mm for right hand) and CF (5.2 mm for left hand and 2.3 mm for right hand) ; patients were not significantly different from controls (Crawford's tests, all $p > 0.05$). In free gaze, the standard deviation of the instantaneous drift was slightly increased in controls (5.5 ± 1.2 mm). Variabilities in instantaneous drift also increased for IG's right hand (7.4 mm ; Crawford's test, $p > 0.05$) and CF's left hand (6.8 mm ; Crawford's test, $p > 0.05$) but only CF's right hand exhibited significantly greater instantaneous drift standard deviation compared to controls (10.8 mm ; Crawford's test, $p = 0.002$). In the NT fixation condition, control participants' variability in instantaneous drift was equal to 5.7 ± 1.0 mm. Similar to the free gaze condition, the standard deviation of the instantaneous drift did not differ from controls for IG's right hand and CF's left hand (6.6 and 6.3 mm, respectively ; Crawford's test, both $p > 0.05$) and CF showed greater variability when using his right hand (9.2 mm ; Crawford's test, $p = 0.005$). In the FT fixation condition, control participants had a variability in instantaneous drift of 5.2 ± 1.0 mm and both patients IG (14.1 mm for right hand) and CF (10.5 and 10.8 mm for left and right hands, respectively) showed greater standard deviations of the instantaneous drift compared to controls (Crawford's test, all $p < 0.001$).

In summary, both OA patients showed greater variability in their movements from trial to trial compared to controls. Instantaneous drift fluctuated to a greater degree from

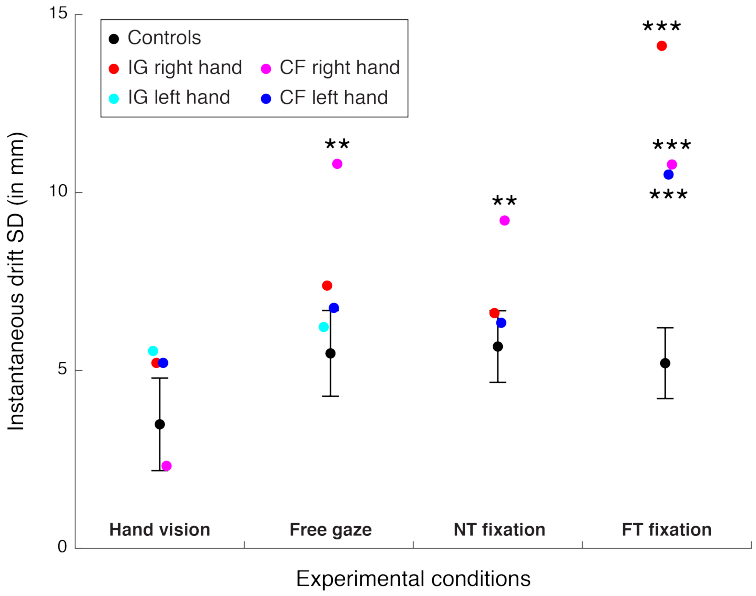

Figure 4.8 – Instantaneous drift standard deviation (in mm) as a function of experimental conditions for patients IG, CF and control participants. The color code is the same as in previous figures. The error bars represent the standard deviation across participants control participants. Note that patient IG's left hand was only tested in the free gaze and hand vision conditions.

trial to trial for the patients compared to the controls, especially when fixating on the FT (Figure 4.7). This was confirmed by the analysis of the standard deviation of the instantaneous drift. Both OA patients were most impaired in the FT fixation condition. Moreover, unilateral patient CF showed higher variability when reaching with the right hand in free gaze, NT fixation and FT fixation conditions (Figure 4.8).

Discussion

The brain needs to compute accurate estimates of the arm position in order to plan and execute reaching movements. In the absence of vision, the hand position progressively drifts away from the intended targets as reaching movements are repeated over time. This drift is thought to result from inaccuracies in the hand state estimate induced by a lack of visual reafferences. The goal of this study was to investigate the involvement of the PPC in the estimation of hand position during movement control. To this aim, we asked two OA patients with PPC damage as well as neurologically intact control participants to perform back-and-forth movements between two targets without visual feedback of their moving hand. If the integrity of the PPC is necessary for the estimation of hand position during movements, we expect differences in movement drift between OA patients compared to controls. Specifically, we predict hand position drift to be larger, faster and more variable

in patients compared to controls, as a result of inaccurate hand state estimate following PPC damage.

The results we found in control participants confirmed that repetitive movements in the absence of visual feedback induce hand position drift. The cumulative drift was progressively increased after the removal of hand vision and a plateau was observed after approximately 30 trials while instantaneous drift remained fairly constant throughout the blocks. These findings are in accordance with previous reports (Brown et al., 2003 ; Cameron et al., 2015 ; Patterson et al., 2017). The magnitude and the direction of individual reach movements were relatively preserved, in line with the observation that the shape of the hand path is maintained when doing continuous back-and-forth (Brown et al., 2003) or circular motions (Zelaznik & Lantero, 1996) while hand position drifts. We found no consistent drift direction across control participants, which has also been previously reported (Brown et al., 2003).

When the hand was always visible, OA patients were not impaired and exhibited a cumulative drift similar to control participants. In the dark, bilateral patient IG was specifically impaired in the FT fixation condition, but not in the free gaze and NT fixation conditions. She showed a very large hand position cumulative drift compared to controls, even before the visual feedback of the hand has been removed and errors continued to accumulate throughout the block. In the FT fixation condition, participants moved their hand in the lower visual field. It has been shown that the PPC over-represents the lower visual field and the periphery (Pitzalis et al., 2013 ; Previc, 1990 ; Rossit et al., 2013). Consistent with these findings, patient IG exhibited specific perceptual and motor impairments in processing hand-to-target distances within the lower visual field, in the absence of visual feedback of the hand (Bartolo et al., 2018). That would explain why IG is specifically impaired when fixating on the FT in the present experiment but is able to compensate for these deficits when eye movements are not restricted (free gaze) or when reaching in the upper visual field (NT fixation condition).

Similarly, unilateral patient CF was impaired when performing repetitive reaching movements within the lower visual field (FT fixation condition), using either left or right

hand. However, in contrast to IG, patient CF showed a systematic cumulative drift greater than controls in the dark when using the right hand, which corresponds to his ipsilesional/healthy hand. This may be surprising at first, but in this study we showed that CF's right hand drifted to the left, that is, toward his contralesional visual field. One possible explanation is that the OA field effect (i.e., errors made specifically in the contralesional visual field) is not specific to visual targets. Accordingly, large mislocalisation errors are observed in unilateral OA when proprioceptive targets are presented in the contralesional visual field (Blangero et al., 2007). This idea is reinforced by the finding that modalities other than visual can also be represented in eye-centered coordinates (Pouget et al., 2002). Thus, the cumulative drift observed in CF when moving with the right hand would correspond to a mislocalisation of the healthy hand from proprioceptive information within the contralesional visual field. To further support this hypothesis, it would be of interest to have OA patients perform repetitive movements toward targets located in either visual field, instead of aligned with the midline. In these conditions, we would expect no or very little cumulative drift when moving in the ipsilesional field with the healthy hand and the greatest deficits while using the ataxic hand to reach within the contralesional field.

In addition to the cumulative drift, we also measured the instantaneous drift which corresponds to changes in hand location between each successive movement. We found that OA patients had a greater instantaneous drift, and thus higher trial-to-trial variability in drift. More specifically, compared to control participants, patient IG exhibited larger trial-to-trial variability in instantaneous drift when reaching while maintaining fixation on the FT. Patient CF showed greater instantaneous drift standard deviation than controls when using his right hand in both the free gaze and the NT fixation conditions. In the FT fixation condition, he was impaired when using either hand and showed higher trial-to-trial variability in instantaneous drift compared to control participants.

Altogether, these findings suggest that state estimation is impaired in both bilateral patient IG and unilateral patient CF, following lesions to the PPC. The PPC is a cortical region involved in various higher-order cognitive functions including both multisensory and sensorimotor integration. The PPC receives extensive projections from several sen-

sory cortices (Andersen et al., 1997 ; Y. E. Cohen, 2009), the surrounding somatosensory and visual areas in particular. Hence, it combines visual and proprioceptive information together to produce a unified coherent percept of the hand. Furthermore, a copy of the motor commands is sent to the PPC through its reciprocal connections with the frontal motor regions, such as the dorsal premotor and the primary motor cortex (Kalaska et al., 1983 ; Mountcastle et al., 1975). Therefore, the impairment in hand state estimation observed in OA patients subsequent to PPC lesions can be explained by either a deficit in the actual internal hand representation (i.e., the combination of the efference copy and sensory feedbacks) or a more basic deficit of visuo-proprioceptive integration about the hand position. The present experimental design did not allow us to differentiate between these two possibilities and further research should be conducted to distinguish between both hypotheses.

In order to reach accurately, the central nervous system predicts the upcoming hand position estimate based on the efference copy and available sensory feedback. If a discrepancy is detected between the predicted and the actual hand position, the ongoing movement is corrected (Desmurget & Grafton, 2000). Both the cerebellum and the PPC have been shown to be implicated in limb state estimation (Miall et al., 2007 ; Mulliken et al., 2008). It has been proposed that the PPC is specifically involved in the storage of the internal hand position estimate over time (Wolpert, Miall, & Kawato, 1998). In this case study, a patient with a PPC lesion showed fading of somatosensory sensation and grip force over time, when using the contralesional limb in the absence of visual feedback. This patient also experienced drift in the perceived position of her contralesional hand while it remained static but out of her sight. As a consequence, she exhibited inaccuracies when pointing to peripheral targets during slow (more than 17 s) but not self-paced movements (around 2 s). Conversely, reach errors are typically reduced in OA patients when a delay is introduced between target presentation and movement onset (Milner et al., 1999 ; Revol et al., 2003).

The results of our present study suggest that, in addition to state estimate storage (Wolpert, Goodbody, & Husain, 1998), the PPC might also be involved in the updating

of the hand position estimate by means of visual and proprioceptive reafferences. The apparent discrepancy between the two studies might be explained by slightly different lesion sites in the PPC. Although patients all had damage to the SPL, the one presented in Wolpert's study exhibited extensive damage of BA 5 whereas in our study patients IG and CF both showed more posterior lesions around BA 7 with no signs of somatosensory fading or sensation of drift when the limb is static. It is possible that different parts of the PPC may subserve different functions in internal state estimation. Considering previous findings, BA 5 might be more implicated in the storage of the internal hand representation while BA 7, along with the cerebellum, might be involved in its updating based on both visual and proprioceptive reafferences. Following PPC damage and in the absence of visual feedback, the hand position estimate is not properly updated and becomes less reliable. As a consequence, motor errors are not detected nor corrected, they therefore accumulate over successive trials and the hand moves away from the intended targets and endpoints become more variable as reaches are repeated in the dark (Cameron et al., 2015).

Acknowledgements

The authors thank patients IG, CF and controls for their participation in this experiment as well as Éric Koun and Olivier Sillan for their technical assistance. LM received support from a PhD excellence scholarship from Faculté des Etudes Supérieures et Postdoctorales and École d'Optométrie de l'Université de Montréal (FESP-ÉOUM). AZK and GB were funded by the Natural Sciences and Engineering Research Council of Canada (NSERC). AZK was additionally supported by the Canada Research Chair program. LP was supported by the CNRS and the Labex/Idex ANR-11-LABX-0042, France. This work was performed at the "Mouvement & Handicap" platform at the Neurological Hospital Pierre Wertheimer in Bron (France).

5 Étude 4 Conséquences d'une lésion du cortex pariétal sur la représentation interne de la main pour le contrôle en ligne du mouvement

Parietal cortex damage reveals deficit in hand state estimation during online motor control

Laura Mikula, Aarlenne Z Khan, Gunnar Blohm, Laure Pisella

Article soumis pour publication dans *Cortex*

Points importants

- Suite à une atteinte du CPP, les patients avec ataxie optique sont incapables de corriger les mouvements pendant leur exécution. Ces corrections motrices en ligne seraient dépendantes de l'estimation de la position de la main.
- Cette étude s'intéresse au rôle du CPP dans la représentation interne de la main utilisée pour le contrôle en ligne des mouvements de pointage.
- Les participants doivent pointer vers la position mémorisée de cibles dans trois conditions : sans vision de la main, avec vision de la main avant l'initiation du mouvement et vision de la main avant et pendant le mouvement. Un patient atteint d'ataxie optique unilatérale gauche est testé.
- Le patient ataxique présente des erreurs de pointage plus importantes lorsque la main n'est pas visible pendant le mouvement. Par ailleurs, la vision de la main avant l'initiation du mouvement ne permet pas de réduire ces erreurs.
- Ces résultats indiquent que le CPP serait impliqué dans l'intégration des réafférences sensorielles pour construire une représentation interne de la main qui est nécessaire pour l'ajustement et le contrôle en ligne des mouvements.

Abstract

Optic ataxia (OA) is a consequence of brain damage to the posterior parietal cortex (PPC) resulting in errors during visually-guided movements. Patients exhibit difficulties to plan and correct hand movements in-flight. To make online corrections, the brain needs to compute an estimate of the hand position, based on sensory reafferences and efference copy of the motor commands. The PPC encodes both target and hand positions by integrating visual and proprioceptive information as well as efference copy signals from frontal motor areas. The present work seeks to investigate the role of the PPC in the visual-proprioceptive integration underlying the estimate of the hand position during online motor control. To this aim, we asked a patient with left unilateral OA to reach with his right/healthy hand toward remembered peripheral visual targets while maintaining fixation under three different conditions : without vision of the hand (noV), with vision of the hand only before the movement (startV) or during the entire reach (fullV). In addition, six neurologically intact control participants took part in the same experiment. We found that the OA patient was impaired, particularly in his left/ataxic visual field, when reaching in complete darkness (noV) and visual feedback of the hand provided before movement onset (startV) did not reduce reach errors. However, vision of the moving hand (fullV) improved his performance. These results show a role of the PPC in the position estimate of the moving hand derived from proprioceptive reafferences and/or efference copy, especially in the contralateral eye-centered space.

Introduction

Dexterous manipulation is a dominant form of human interaction with the environment and requires moving the hand toward objects in visual space. During these goal-directed movements, information about target position is derived from visual signals whereas hand location, when visible, is inferred from both vision and proprioception. It is believed that during planning, the target and the hand locations are coded and compared in a common eye-centered reference frame (Buneo et al., 2002). Comparisons between hand

and target locations are also required during motor execution in order to update ongoing reaching movements. To do so, the central nervous system needs to build an estimate of the hand position using visual and proprioceptive feedbacks as well as efference copies of the motor command (Wolpert et al., 1995 ; Wolpert & Ghahramani, 2000). In case of discrepancy between the predicted and the observed hand position estimate, an error signal is computed and corrections are implemented. Hence, movement accuracy is related to the precision of the hand position estimate. Indeed, motor accuracy has been shown to decrease when visual feedback about the hand was not available (Spijkers & Lochner, 1994 ; Spijkers & Spellerberg, 1995) as well as when proprioception was experimentally disturbed (Redon et al., 1991 ; Steyvers et al., 2001) during movement execution. These findings suggest that online motor corrections are based on visual and proprioceptive reafferences about hand location.

The posterior parietal cortex (PPC) is known to be involved in the eye-centered sensorimotor transformations underlying reach movement planning (Andersen et al., 1997, 2004 ; Buneo & Andersen, 2006 ; Dijkerman et al., 2006 ; Khan, Pisella, Rossetti, et al., 2005) and in the internal hand state estimate (Desmurget & Grafton, 2000 ; Mulliken et al., 2008 ; Wolpert, Goodbody, & Husain, 1998) allowing online control of reaching movements. For example, Desmurget et al. (1999) used a double-step reaching paradigm, in which participants reached to a target that jumped to a new location at movement onset, thus requiring online adjustments of the hand trajectory during motor execution. Transcranial magnetic stimulation applied over the PPC at movement onset disrupted these corrections of ongoing movements in response to the target jump. Moreover, a positron emission tomography study revealed that the PPC was involved in both the online adjustments during goal-directed movements and the computation of motor errors (Desmurget et al., 2001). Further evidence for the involvement of the PPC in online motor control comes from studies in patients with optic ataxia (OA). OA is a consequence of brain damage to the PPC resulting in an impairment of visually guided arm movements (Perenin & Vighetto, 1988). It is a higher-level visuomotor deficit that is not attributable to a primary visual, proprioceptive or motor disorder. In double-step reaching paradigms,

patients with OA have difficulty producing fast online corrections during ongoing movements. They show delayed corrections and tend to complete the movement to the initial target position before making a second one to the final target jump position (Gréa et al., 2002 ; Pisella et al., 2000 ; Prablanc et al., 2003). In contrast, neurologically intact participants smoothly correct their ongoing hand movement in response to the target jump. Consequently, the PPC has been proposed to act as an automatic pilot for the hand since its integrity is crucial for automatic but not intentional motor corrections (Pisella et al., 2000). These results underline the role of the PPC in fast, online control of reaching.

Evidence from patients with unilateral PPC lesions demonstrates that this region is involved in integrating visual information about the target and proprioceptive information about the hand during online control of reaching. Using a double-step reaching paradigm in OA patient CF, fewer online corrections were observed when the target jumped toward the contralesional/ataxic visual field, known as the "field" effect, and when he used his contralesional/ataxic hand, the "hand" effect (Blangero et al., 2008). These two effects have been shown to be additive and independent, as they can appear in isolation from each other (Blangero et al., 2007, 2008). The field effect has been well characterized in luminous conditions as a systematic bias of target encoding toward ocular fixation in the ataxic visual field (Blangero et al., 2010 ; Vindras et al., 2016). Deficits related to the field effect have been shown to depend on the target location in eye-centered rather than in head- or body-centered reference frames (Dijkerman et al., 2006 ; Khan, Pisella, Rossetti, et al., 2005). Besides, the hand effect seems to be linked to a poorer localization of the ataxic compared to the healthy hand. Specific hand effect errors observed in Blangero et al. (2008) could not be attributed to the field effect since movements of both hands began from a central position and were aimed toward a foveated target (before it jumped). Thus, visual feedback was identical for left and right hands regardless of whether the central target jumped leftward or rightward. This suggests that the deficit of online correction for the ataxic hand is a result of faulty proprioceptive-motor integration, and presumably inaccurate hand state estimation, during motor execution.

To specifically investigate the spatial integration of proprioceptive information for

pointing movements in OA, patients have been tested in a proprioceptive pointing task in the dark while fixating a visible location (Blangero et al., 2007). The ipsilesional hand was mislocalized only in the contralesional eye-centered space while the ataxic hand was mislocalized in the entire visual space with nevertheless more errors in the contralesional eye-centered space. These results imply that the PPC transforms proprioceptive information about the hand in both eye-related and hand-related representations (Bosco et al., 2015) : in a given hemisphere there is a representation of controlateral eye-centered space in which proprioceptive information about both hands may be represented when they lie in the same space and a representation of the eye-centered contralateral hand location across both hemifields.

The interpretation of faulty proprioceptive-motor integration during motor execution is consistent with the finding that the hand effect errors (i.e., errors made specifically with the ataxic hand when pointing toward visual targets) were greatly reduced in both visual fields when visual feedback of the hand was provided (Blangero et al., 2007). It also signifies that the field effect (i.e., errors made with the healthy hand specifically in the ataxic visual field) may not be exclusively due to the now well-characterized mislocalization of visual targets in the contralesional visual field (Blangero et al., 2010 ; Vindras et al., 2016). Consistent with eye-centered visual but also proprioceptive contralateral sensory representations within the PPC (Buneo et al., 2002), there might be additional errors consecutive to PPC lesions related to the proprioceptive localization of the healthy hand in the ataxic visual field. These errors are likely specific to online control, arising from the update of the hand position estimate as it approaches the target in the contralesional visual field.

This study investigates the role of the PPC in the dynamic visual-proprioceptive integration underlying the state estimate of the ipsilesional hand position in the contralateral visual space (i.e., field effect). We asked a patient with unilateral left OA to reach with his healthy hand to remembered target locations while maintaining fixation. Targets were presented in the left (ataxic) or the right (healthy) peripheral visual field. Movements were performed under three different conditions : without vision of the hand (noV) or

with vision of the hand only before movement onset (startV) or during the entire reach (fullV). These lighting conditions allowed us to control the availability of the visual feedback of the hand during movement planning and execution. In OA patients we predict that, particularly when the hand moves into the ataxic visual field, there might be erroneous corrections implemented after peak velocity due to an incorrect updating of the hand position estimate in the dark based on proprioceptive feedbacks and/or efference copy during online motor control. These errors would be additive to errors arising before peak velocity, when present, which are related to motor planning before reach onset. Since providing visual feedback to OA patients has been shown to reduce the hand effect proprioceptive-motor errors, we expect that visual reafference should also improve accuracy of the internal representation, and thus the movement, of the healthy hand within the contralesional eye-centered space.

Methods

Participants

Patient CF was a right-handed male patient who, in 2003, suffered from a cerebral angeitis, initially presenting with headache without fever. One week later, the patient was moderately confused with signs of Balint's syndrome. Cerebral angiography then showed vasospasm in the left middle cerebral artery territory and in the right posterior cerebral artery territory. MRI scans showed a posterior watershed infarct (ischemic lesion of junctional territories) resulting in distributed and asymmetrical bilateral lesions of the occipito-parietal region (Brodmann's areas BA 18, 19, 7, 5 and 2) with a minute extension to the centrum semiovale. None of the laboratory studies provided a clear aetiology either in terms of inflammatory or autoimmune disease. During the following months, simultanagnosia and neglect rapidly disappeared leaving the patient with a stable and isolated unilateral optic ataxia predominantly in his left visual field, thought to be the consequence of larger damage in the right hemisphere from both BA 7 lesions and a parieto-frontal disconnection from intra-hemispheric fibers lesions (Figure 5.1A, see also

Khan et al., 2007). He did not exhibit any purely motor, somatosensory or visual deficits. Visual fields and visual perception were preserved as well as pattern recognition and color perception.

In addition, six neurologically intact control participants (age range : 23-31, 4 female) also took part in this study. All participants, including the patient, gave informed written consent to participate in the experiment which conformed to the Declaration of Helsinki for experiments on human subjects. All experimental procedures were approved by the health research ethics committee in France (CPP Nord-Ouest I, Lyon, 2017-A02562-51) and at the University of Montreal in Canada (17-034-CERES-D).

Apparatus

Figure 5.1B depicts the setup of the experimental device. Participants were seated in front of a horizontal table on which they performed their reaching movements using their right hand. A light-emitting diode (LED) target array was located above the table and was projected onto it using a half-reflecting mirror. The mirror allowed participants to see their hand if a light was illuminated under the mirror, in addition to the LEDs (closed loop reaching condition). If the light remained extinguished, they were only able to see the LED targets (open loop reaching). The target array consisted of three fixation LEDs located at 24° left, 0° center and 24° right relative to the cyclopean eye position located midway between the two eyes (shown in Figure 5.1B as white circles). The fixation LEDs were at a distance of 58.5 cm from the participants' eyes and were all aligned horizontally. Two reach LEDs were located at 12° left and 12° right, slightly below the fixation targets that were also aligned horizontally (shown as grey circles) at a distance of 57.5 cm from the participants' eyes. Participants began their reaching movements from one of the two start positions located 44.5 cm from the participants' eyes. The start position LEDs were located at 12° left and 12° right of the participants' torso aligned to the midsagittal plane (shown as black circles). All LEDs were projected onto the same plane. Participants' head was fixed using a chin rest and a forehead support vertically aligned with both the 0° fixation and reach targets.

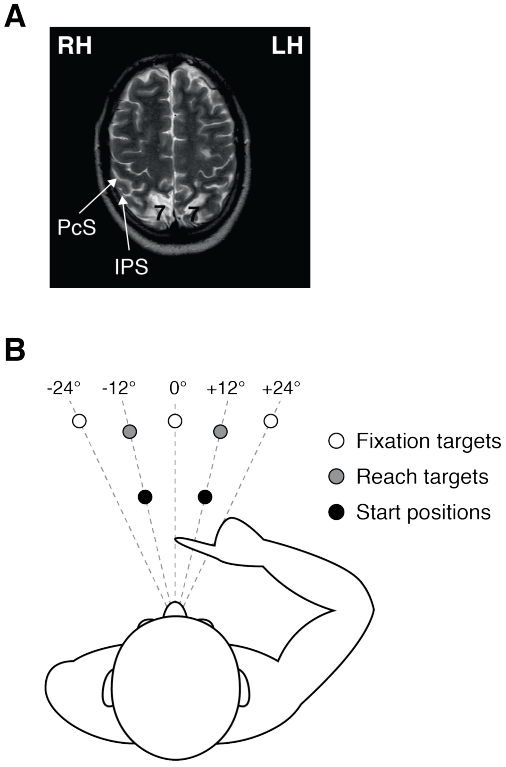

Figure 5.1 – A. Magnetic resonance imaging scan of patient CF. The white areas at the bottom of the scan show asymmetrical lesions to the occipito-parietal region, especially around Brodmann's area 7. The damage is larger in the right than in the left hemisphere. B. Experimental setup. Participants fixated on one of three fixation targets (white circles) while reaching to one of the reach targets (gray circles). Reach movements were initiated from one of both start positions (black circles). The angular distance of all targets relative to the cyclopean eye position is shown. LED targets located above the participants were reflected to appear on the tabletop using a half-reflecting mirror. The mirror was used to control for participants' visual feedback since the hand was only visible when a light was illuminated under the mirror. In the fullV condition, participants could see their hand during the entire movement. In the startV condition, the hand was visible only at the beginning of the trial (on the start position) but not during movement execution. In the noV condition, the hand was never visible and reaches were performed in complete darkness.

Participants used their right hand for reaching and movements of the index finger were recorded using the Optotrak 3020 motion-analysis system (NDI, Waterloo, Canada). Data were sampled at 1000 Hz and finger movements were measured in 3D space (in mm) relative to the central position between both start positions, aligned with participants' midline. Projected LED positions for all fixation, reach targets and start positions as well as the 3D position of the cyclopean eye (participants placed their finger between their left and right eyes) were measured for each participant. Horizontal eye positions were recorded binocularly through an electrooculogram (EOG) using a DC electrooculograph system (50 Hz, model BM623, Biomedica Mangoni, Pisa, Italy) by placing electrodes outside the left and right eyes.

Procedure

Participants performed reaches to the reaching targets in one of three conditions. In the "full vision" condition (fullV), participants had vision of their hand during the entire trial. In the "no vision" condition (noV), participants had no vision of their hand at all and reached in complete darkness. A plastic washer was placed at the start position to provide haptic information about the correct hand starting position. In the "start vision" condition (startV), participants were provided with visual feedback at the beginning of each trial while the start position LED was illuminated, but not during the reaching movement.

For all conditions, each trial began with the illumination (2 s) of an LED signaling the start position (see Figure 5.1B, black circles). Participants placed their finger at the location of the LED. In the fullV and startV conditions, they were able to see their finger through the half-reflecting mirror and so used visual information to align their finger with the LED location. In the noV condition, they used the haptic information provided by plastic washers to align their finger with the start position LED. Next, one of the three fixation LEDs (white circles in Figure 5.1B) was illuminated for 2 s and participants were required to fixate on it. After 1 s, a reaching target (gray circles) was illuminated for 1 s. Both fixation and reach targets were then extinguished and participants were asked to reach to the remembered reach target location while maintaining fixation on the remembered location of the fixation target. Participants performed two blocks of 163 trials each, one block with the left start position and the second with the right start position. The order of the start position was randomized across participants. Within each block, fixation targets, reach targets and lighting conditions were randomly interleaved.

At the end of each session, we performed a set of calibration trials, where we illuminated all targets (as well as the room) and asked participants to fixate and point to each fixation, reach and start position LEDs in sequence while maintaining the same head position. Because of the room illumination, they were able to use visual feedback through the mirror to accurately reach to each target. We also asked participants to place their finger at the point between their eyes, which we considered as the cyclopean eye position.

Data analysis

During the task, participants' eye movements were monitored to confirm that they were performing the task correctly. Immediately following the completion of each trial, we confirmed that after the appropriate eye movement, fixation was held at the correct location during the reach movement. If any eye movement occurred or if the trial was performed incorrectly for any reason, the trial was repeated.

Data were analyzed using custom-written Matlab software (MathWorks, Natick, MA, USA). The 3D start and end positions for the right index fingertip were calculated for each trial using velocity criteria (80 mm/s). The velocity criteria were also used to calculate reach latency and movement duration. Reach movements were considered anticipatory if they occurred less than 100 ms after target offset, and the maximum time allowed for the hand movement to begin was 1000 ms after target offset.

Several parameters were computed to quantify reach performance in the OA patient and control participants. Maximum reach curvatures were calculated for each trial as the largest deviation (in mm) from the straight line between start and end movement positions. 3D finger positions in Cartesian coordinates were converted into polar coordinates relative to the cyclopean eye (as determined by the calibration trials). Angular and amplitude errors were computed as the difference between the finger and the target position and were expressed in degrees and mm, respectively. Variable error was calculated as the surface area of a 1 SD ellipse around reach endpoints and was expressed in mm^2 (Rossetti et al., 1994) ; it was first computed for left and right targets separately and then averaged both targets. Movement duration corresponded to the time between movement start and movement. Acceleration duration was the time between movement start and peak velocity whereas deceleration duration was defined as the time between peak velocity and movement end.

There were two possible start positions (left or right) for the hand as well as two reach targets (left or right) so participants performed reaches in all four possible combinations of start position and reach target. While reaching, participants were required to fixate on three possible locations (left, center or right). Reaches in the left visual field (LVF)

comprised movements from the left start position to the left target in central fixation as well as all possible reaches when fixation was on the right fixation target. Similarly, reaches in the right visual field (RVF) grouped together movements from the right start position to the right target in central fixation and all reaches made while fixating the left fixation target (Figure 5.1B).

All incorrect trials were removed from the analysis (3.1% for CF and 4.9% for controls). Trials were considered incorrect when movement endpoints fell outside the range of 3 standard deviations from the individual mean endpoint position, when peak velocity was greater than 2000 mm/s or when participants went to the incorrect reach target. Data in control participants and in the individual patient were analyzed in similar ways. For patient CF, two-way ANOVAs were performed with lighting condition (fullV, startV and noV) and visual field (left, right) as factors. For control participants, we used repeated measures ANOVAs with the same factors. When the interaction effect of two-way or repeated measures ANOVAs was significant, Tukey HSD tests were used for post-hoc comparisons of the means. When one or both main effects were significant but not the interaction, we used Holm-Bonferroni corrections which control the familywise error rate for multiple comparisons. Since data sets for variable errors in patient CF were very small (2 observations in each condition), pairwise permutation tests were used instead of a two-way ANOVA. Permutations tests are non-parametric tests that work by resampling and permuting the observed data in accordance with the null hypothesis being true. In our analysis, each dataset was resampled 1000 times and p-values were adjusted for multiple testing using the Holm-Bonferroni method. To assess whether the OA patient's performance was significantly different from that of healthy participants, we used Crawford's modified two-tailed t-tests which are specifically designed to compare a single case to a control group (Crawford & Garthwaite, 2002 ; Crawford & Howell, 1998). The threshold for statistical significance was set at 0.05 for all analyses, except for the Holm-Bonferroni method in which the thresholds were corrected accordingly (Holm, 1979).

Results

Movement trajectories

Raw traces of movement trajectories are depicted in Figure 5.2 for CF (A & B) and a typical control (C & D) for the reaches within the LVF (left two panels) and the RVF (right two panels). The start position and reach target were the same, however fixation position changed. The traces are colour-coded for the three different lighting conditions. A number of observations can be made from these movement trajectories. First, CF performed reaches with greater errors and variability compared to the control, for example, in the left visual field the patient exhibited curved trajectories with a movement initially biased toward ocular fixation (undershoot toward the right) but final errors tended to be target overshoots in X and Y axes. Second, for both CF and the control there were differences in reaching in the three different lighting conditions ; final errors appeared to be larger when reaching in the noV (green traces) and the startV (yellow traces) conditions compared to the fullV (blue traces), though this was exaggerated in CF compared to the control participant. These observations are explored in more detail within the next sections.

Constant angular errors

We first investigated angular errors at the end of the movement as a function of lighting condition and visual field for both CF (Figure 5.3A) and controls participants (Figure 5.3B). Negative values indicate errors directed away from fixation whereas positive values correspond to errors directed toward fixation. For CF (Figure 5.3A), a two-way ANOVA revealed significant main effects of both lighting condition ($F_{2,252} = 10.8$, $p < 0.001$) and visual field ($F_{1,252} = 104.1$, $p < 0.001$) as well as a significant interaction effect ($F_{2,252} = 28.6, p < 0.001$). Post-hoc analyses revealed that angular errors were significantly different for the fullV (1.25°) compared to the noV (-3.44°, $p < 0.001$) and startV (-2.97°, $p < 0.001$) conditions in the LVF whereas they did not differ between the three

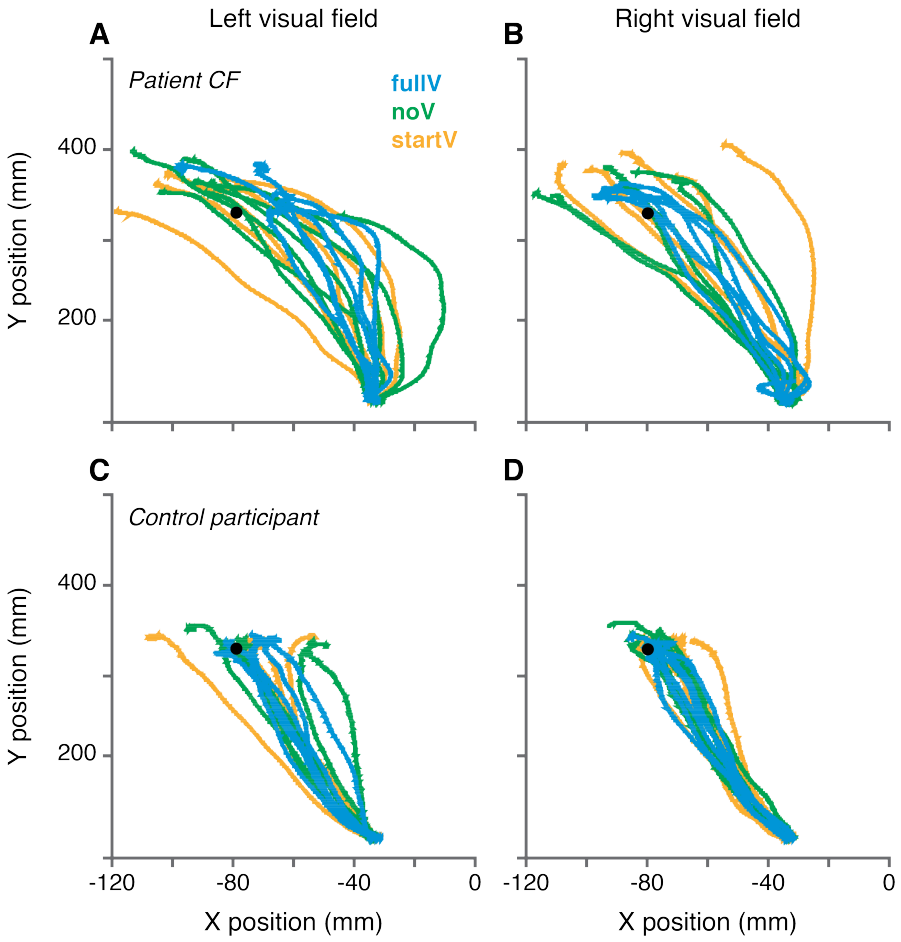

Figure 5.2 – Raw traces for movements. Movement trajectories are depicted in the fullV (blue), the noV (green) and the startV (yellow) light conditions. For the four panels, all reaches were made from the leftward start position to the leftward reach target. The reach target is represented by the black circle. X and Y positions are shown in mm. The traces are represented for 6 randomly chosen trials in each condition. A. Movement traces for CF when reaching within the left visual field, while fixating on either the central or rightward fixation target. B. Movement traces for CF when reaching within the right visual field while maintaining fixation on the leftward fixation target. C. Movement traces for a typical control when reaching in the left visual field. D. Movement traces for a typical control when reaching in the right visual field.

lighting conditions in the RVF (all $p > 0.05$). Moreover, we found that angular errors were significantly different between LVF and RVF, for both the noV (2.29°, $p < 0.001$) and the startV (2.05°, $p < 0.001$) conditions whereas for fullV, angular errors were similar across both visual fields. Indeed, in the LVF, final angular errors in the noV and startV conditions landed away from fixation while in the fullV condition, they landed slightly toward fixation and were not different from the angular errors in the RVF.

For control participants (Figure 5.3B), a repeated measures two-way ANOVA using the same factors revealed no differences across all lighting conditions and visual fields (all $p > 0.05$). Compared to controls, CF did not show significant differences in angular errors at the end of the movement in any lighting condition or visual field (Crawford's modified t-tests, all $p > 0.05$). This lack of statistical significance is likely due to the high variability across control participants ; as can be seen in Figure 5.3A, the errors made by CF in the LVF were substantially higher for the noV and startV conditions, when compared to controls (Figure 5.3B).

We also looked at angular errors at movement peak and compared errors with those at movement end, to determine whether errors changed as a function of movement execution. Figure 5.3C & 3D depicts the mean angular errors relative to targets at the point of movement peak velocity for CF and the controls, respectively. For CF, the two-way ANOVA revealed no main effects of lighting condition or visual field and no interaction effect (all $p > 0.05$). Figure 5.3C shows that on average, movements were directed toward fixation at peak velocity in all experimental conditions.

In the controls (Figure 5.3D), a repeated measures ANOVA showed a significant main effect of visual field ($F_{1,5} = 7.8, p = 0.039$) but no main effect of lighting condition and no interaction (both $p > 0.05$). Post-hoc comparisons revealed that overall, angular errors at peak velocity were directed away from fixation in the LVF (-1.14°) but toward fixation in the RVF (1.66°, $p = 0.039$), consistent with a biomechanical bias with the trajectories always curved leftward with the right hand (Figure 5.2C & 5.2D and Figure 5.3B).

For the patient, when comparing angular errors at movement peak, one can observe that errors at movement end (Figure 5.3A) increased for the startV and noV conditions

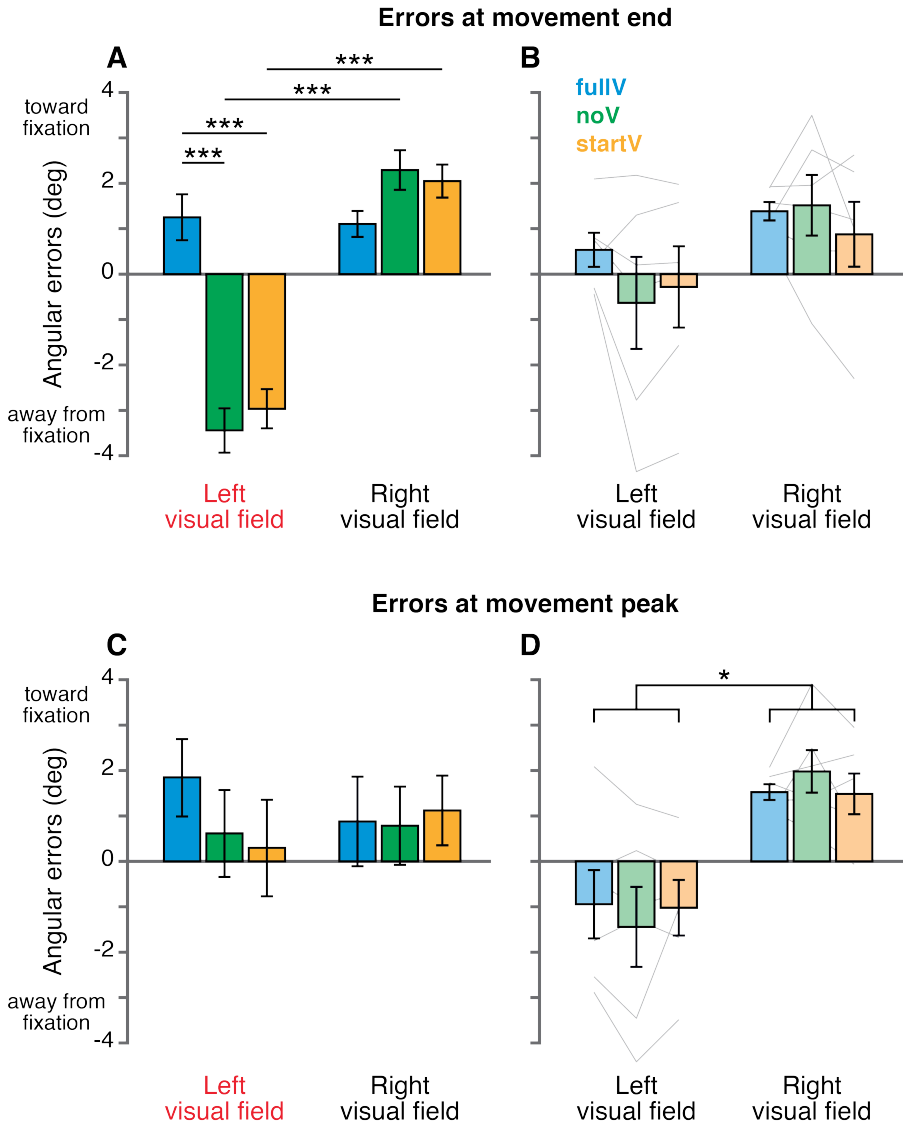

Figure 5.3 – Angular errors. Angular errors in degrees at the end of the movement are shown for CF (A) and controls (B). Negative values indicate errors directed away from the fixation point. The three bars on the left of each panel are for the left visual field (impaired in CF – red) whereas the three bars on the right are for the right visual field. Each of the three conditions are shown separately ; fullV (blue bars), noV (green) and startV (yellow). Error bars are s.e.m across all trials for CF and s.e.m across participant means for controls. For controls, light grey lines correspond to individual participant data. Angular error at the time of peak velocity of the movement for CF (C) and controls (D) are shown in the same manner as above. * $p < 0.05$, *** $p < 0.001$.

in the left (impaired) visual field and changed direction with respect to angular errors at peak velocity (Figure 5.3C) so that reaches ended away from gaze location. In contrast, errors remained similar in the fullV condition as well as in the RVF. We performed an additional two-way ANOVA on the difference between the angular error at peak velocity and at movement end. The difference was computed so that positive values correspond to reaches going toward fixation point. For CF, the ANOVA revealed no significant main effect of lighting condition ($F_{2,252} = 0.92$, $p = 0.401$) but a significant main effect of visual field ($F_{1,252} = 23.5$, $p < 0.001$) as well as an interaction effect ($F_{1,252} = 3.8$, $p = 0.025$). Post-hoc analyses showed that, after the peak velocity, errors made in the noV condition were shifted away from the fixation point (-4.06°) in the LVF whereas they were driven even more toward fixation in the RVF (1.50°, $p < 0.001$). We found the same results for the startV condition (LVF : -3.26° vs. RVF : 0.93°, $p = 0.010$). No other comparison was found to be significant ($p > 0.05$).

In contrast, controls showed an overall decrease in error at movement end compared to movement peak (Figure 5.3B vs. 5.3D), although this was not significant. Analyses on the difference between the error at peak velocity and movement end revealed significant main effects of lighting condition ($F_{2,10} = 4.8$, $p = 0.035$) and visual field ($F_{2,10} = 13.0$, $p = 0.015$) but no significant interaction ($p > 0.05$). However, post-hoc analyses did not show any difference between the three lighting conditions (all $p > 0.05$, Holm-Bonferroni corrected). In contrast, overall errors in the RVF have been found to be directed slightly away from fixation (-0.40°) after peak velocity while errors in the LVF went toward fixation (1.01°, $p = 0.015$). Given that these changes in reach directions were opposite to the angular errors measured at the peak velocity, these results show that control participants reduced their angular errors during the deceleration phase (i.e., the time between peak velocity and movement end).

In summary, CF's errors increased between movement peak and movement end in the noV and startV conditions, specifically when reaching within the LVF. In the fullV condition, errors did not change greatly from movement peak to movement end in either visual field and were similar to controls. These results point toward erroneous proprioceptive

integration during movement execution during the deceleration phase that is believed to reflect online feedback corrections. We confirmed these findings through an analysis of reach curvature below.

Reach curvatures

We calculated maximum reach curvatures as well as the time of maximum reach curvature relative to the time of peak velocity. The mean maximum reach curvatures are depicted in Figure 5.4A & 4B for patient CF and control participants, respectively. As depicted in Figure 5.4A, CF's reaches consistently curved to the right, but less so in the RVF than in the LVF. To put it in another way, reaches tended to curve away from fixation in the LVF (as can be seen in Figure 5.2A) whereas they tended to curve toward fixation in the RVF (Figure 5.2B). A two-way ANOVA revealed a significant main effect of visual field ($F_{1,252} = 54$, $p < 0.001$) but no main effect of lighting condition and no interaction effect (both $p > 0.05$). Post-hoc tests showed that reaches were overall more curved to the right in the LVF (17.2 mm) compared to the RVF (5.7 mm ; $p < 0.001$). Controls' maximum reach curvatures (Figure 5.4B) were not modulated by lighting condition or visual field (repeated measures two-way ANOVA, all $p > 0.05$). In all combinations of lighting condition and visual field, patient CF showed movement trajectories curved to the right (Crawford's modified t-tests, all $p < 0.05$) compared to control participants who exhibited overall smaller curvatures directed toward the left.

Next, the time of the maximum reach curvature was compared to the time of peak velocity. For CF, the two-way ANOVA again revealed a main effect of visual field ($F_{1,252} = 15.8$, $p < 0.001$) but no main effect of lighting condition and no interaction effect (both $p > 0.05$). Post-hoc tests showed that the maximum curvature occurred later relative to peak velocity in the LVF (76 ms) compared to the RVF (33 ms, $p < 0.001$). In control participants, a repeated measures two-way ANOVA revealed that the time of maximum reach curvature was not affected by lighting condition or visual field (all $p > 0.05$). On average, the maximum reach curvature occurred slightly but not significantly later in patient CF (55 ms after peak velocity) than in control participants (41 ms after peak

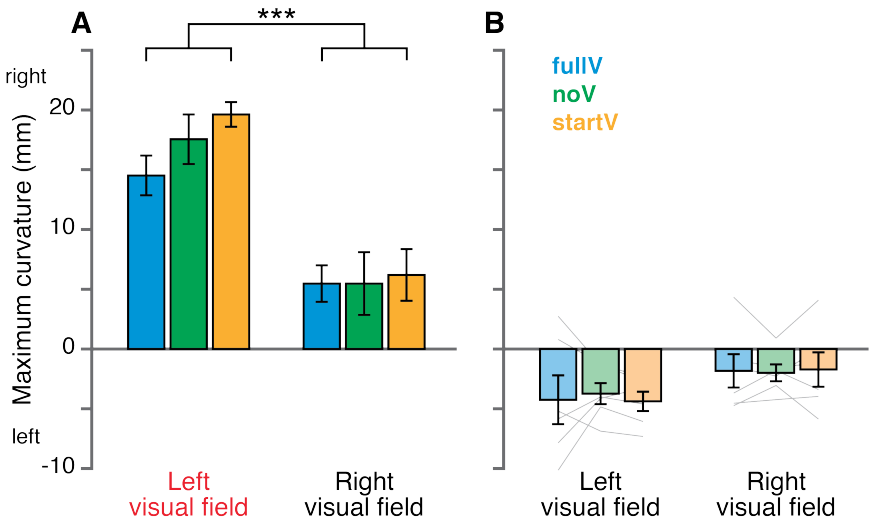

Figure 5.4 – Maximum reach curvatures. Maximum reach curvatures in mm are shown for CF (A) and controls (B). The three bars on the left of each panel are for the left visual field (impaired in CF – red) whereas the three bars on the right are for the right visual field. Each of the three conditions are shown separately ; fullV (blue bars), noV (green) and startV (yellow). Error bars are s.e.m across all trials for CF and s.e.m across participant means for controls. For controls, light grey lines correspond to individual participant data. *** $p < 0.001$.

velocity, $p > 0.05$, Crawford's modified t-test). Thus, the reason for not observing greater angular errors at peak velocity (Figure 5.3C) for CF in the LVF, as would be expected given the large maximum curvature might be due to the later time of maximum curvature relative to peak velocity ; his reaching movements tended to deviate after the acceleration phase, well into the deceleration phase.

Constant amplitude errors

We also investigated whether there were differences in amplitude errors across the different visual conditions, to determine whether reach errors were limited to the angular direction. Figure 5.5A & 5B depicts the mean amplitude errors at movement end for CF and the controls, respectively. Negative and positive values indicate undershoots and overshoots relative to the target, respectively. Overall, CF tended to overshoot the target and thus reach too far (Figure 5.5A). A two-way ANOVA showed significant main effects of visual field ($F_{1,252} = 10.5$, $p = 0.001$) and lighting condition ($F_{2,252} = 34.9$, $p < 0.001$) as well as a significant interaction effect ($F_{2,252} = 5.2$, $p = 0.006$). Post-hoc comparisons

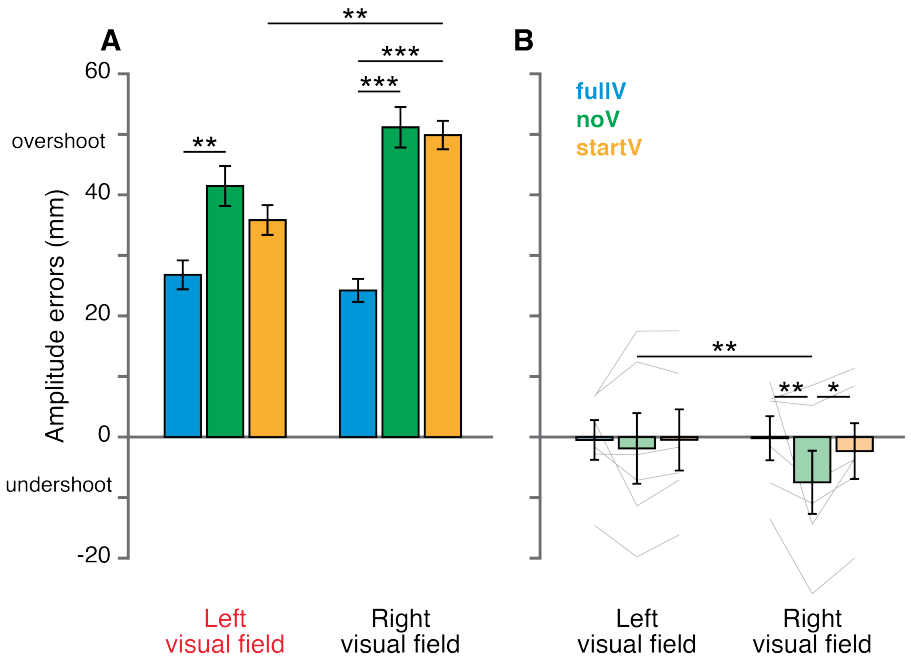

Figure 5.5 – Amplitude errors. Amplitude errors in mm at the end of the movement are shown for CF (A) and controls (B). Negative values indicate undershoots relative to the target. The three bars on the left of each panel are for the left visual field (impaired in CF – red) whereas the three bars on the right are for the right visual field. Each of the three conditions are shown separately ; fullV (blue bars), noV (green) and startV (yellow). Error bars are s.e.m across all trials for CF and s.e.m across participant means for controls. For controls, light grey lines correspond to individual participant data. * $p < 0.05$, ** $p < 0.01$, *** $p < 0.001$.

showed that, within the LVF, amplitude errors in the noV condition (41.5 mm) were significantly larger than in the fullV (26.8 mm, $p = 0.001$) condition. However, errors in the startV condition (35.8 mm) were not significantly different from errors both in the fullV and in the noV conditions (both $p > 0.05$). In the RVF, errors in fullV (24.2 mm) were significantly smaller compared to errors in noV (51.2 mm, $p < 0.001$) and startV (49.9 mm, $p < 0.001$). Post-hoc analyses revealed no significant difference between these two latter conditions ($p > 0.05$). Finally, amplitude errors were larger in the RVF compared to the LVF, but this was true for the startV condition ($p = 0.003$) and not for the fullV or the noV condition (both $p > 0.05$).

Control participants showed small amplitude errors meaning that they tended to reach to the correct target distance (Figure 5.5B). Within controls, a repeated measures ANOVA revealed no significant main effects (both $p > 0.05$) but a significant interaction effect

($F_{2,10} = 6.4$, $p = 0.016$). Post-hoc analyses showed that, in the RVF, participants reached significantly closer to themselves in the noV (-7.5 mm) compared to the fullV (-0.2 mm, $p = 0.001$) and the startV (-2.3 mm, $p = 0.012$) conditions. In contrast, amplitude errors in the LVF were not significantly modulated by the lighting conditions (all $p > 0.05$). Post-hoc comparisons also revealed that undershoot in the noV condition was bigger in the RVF than in the LVF (-1.9 mm, $p = 0.007$). Patient CF exhibited significantly greater amplitude errors compared to controls in all possible combinations of visual field and lighting condition (Crawford's modified t-tests, $p < 0.05$), except for the fullV condition in the RVF ($t_5 = 2.53, p > 0.05$).

In summary, CF showed larger overshoots compared to controls in both visual fields but these amplitude errors were significantly reduced in fullV compared to the two other lighting conditions.

Variable errors

We investigated variable errors for reach endpoints to determine whether precision was also different, in addition to accuracy, across the different lighting conditions. Figure 5.6A & Figure 5.B depicts the variable error of the reach endpoints for CF and the controls, respectively. Variable errors correspond to the surface area (in mm^2) of a 1 SD ellipse around reach endpoints. For CF, as can be seen in Figure 5.6A, the greatest variable errors were found in the noV condition, in both visual fields (1232.7 mm^2 and 1157.1 mm^2 for LVF and RVF, respectively). These errors decreased in the startV condition, in both the LVF (823.3 mm^2) and the RVF (818.5 mm^2), suggesting an improvement of reach planning precision with visual feedback prior to movement onset, although this did not reach significance (both $p > 0.05$, Holm-Bonferroni corrected). Additional visual feedback throughout motor execution further decreased the variable error of patient CF with respect to startV in both the LVF (911.6 mm^2, $p = 0.009$, Holm-Bonferroni corrected) and the RVF (429.3 mm^2, $p = 0.009$, Holm-Bonferroni corrected). Additionally, variable error in fullV was significantly smaller than in the startV condition, when reaches were made in the RVF ($p = 0.009$, Holm-Bonferroni corrected) but not in the LVF ($p > 0.05$,

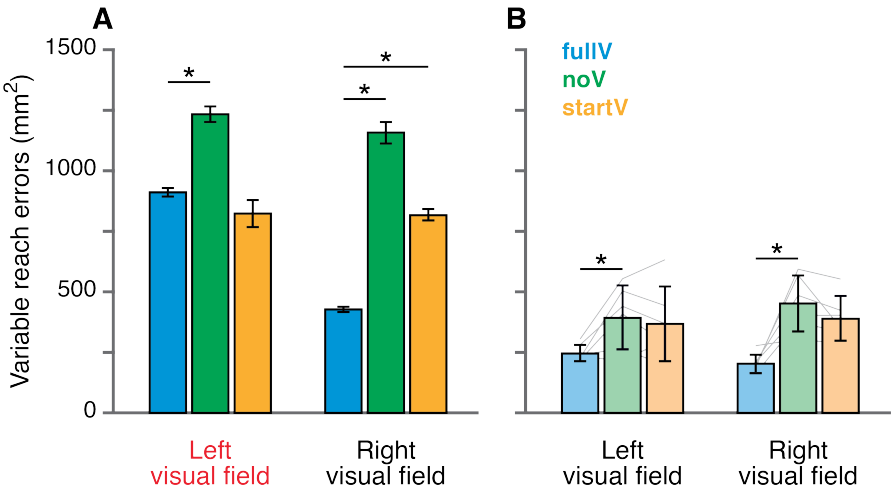

Figure 5.6 – Variable errors. Variable errors in mm^2 are shown for CF (A) and controls (B). The three bars on the left of each panel are for the left visual field (impaired in CF – red) whereas the three bars on the right are for the right visual field. Each of the three conditions are shown separately ; fullV (blue bars), noV (green) and startV (yellow). Error bars are bootstrapped standard deviations for CF and s.e.m across participant means for controls. For controls, light grey lines correspond to individual participant data. * $p < 0.05$.

Holm-Bonferroni corrected), as if dynamic visual information about hand location could not reduce the variable errors in the ataxic visual space.

For control participants (Figure 5.6B), we were able to perform a repeated measures two-way ANOVA which revealed a significant effect of lighting condition ($F_{2,10} = 15.2$, $p = 0.001$) but no other significant effects ($p > 0.05$). Post-hoc tests showed that the endpoint surface area was significantly smaller for the fullV (225.6 mm^2) compared to the noV condition (424.4 mm^2, $p = 0.013$, Holm-Bonferroni corrected). The difference in variable error between fullV and startV (379.2 mm2) conditions showed a trend toward significance ($p = 0.052$, Holm-Bonferroni corrected). In addition, there was no significant difference in variable errors between noV and startV conditions ($p > 0.05$, Holm-Bonferroni corrected). Compared to controls, CF had significantly greater variable errors for all three lighting conditions, in both visual fields (Crawford's modified t-tests, $p < 0.05$ for all comparisons).

To summarize, both CF and controls showed similar patterns of behaviour. Their reaching movements were overall more precise in the fullV condition, followed by the startV condition and then the noV condition. Control participants thus showed benefits on the precision of their movements of seeing their moving hand before and during movement

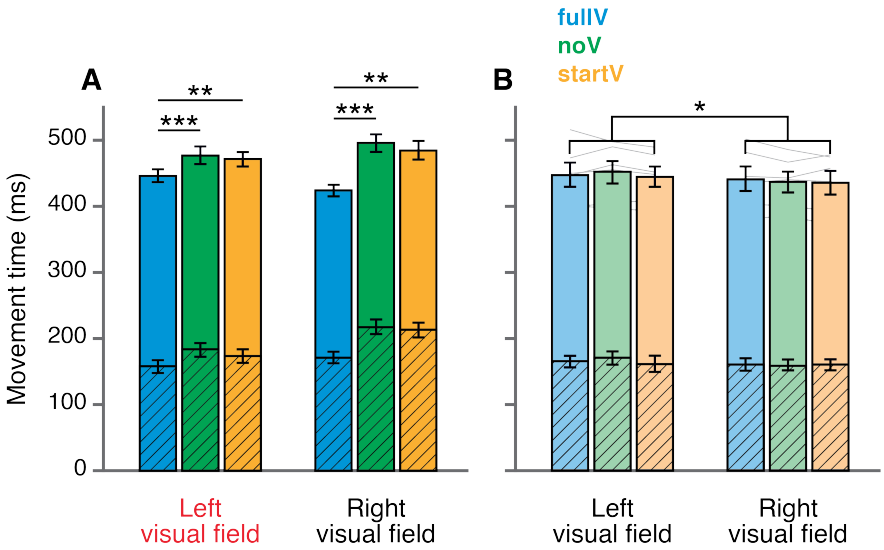

Figure 5.7 – Movement and acceleration time. Movement and acceleration durations in ms are shown for CF (A) and controls (B). The three bars on the left of each panel are for the left visual field (impaired in CF – red) whereas the three bars on the right are for the right visual field. Each of the three conditions are shown separately ; fullV (blue bars), noV (green) and startV (yellow). The entire stacked bar depicts total movement time whereas the bottom part of the bar (hatched) represents the acceleration phase (time from movement onset to peak velocity). Error bars are s.e.m across all trials for CF and s.e.m across participant means for controls. The statistics reported in the figure are those for the total movement durations. For controls, light grey lines correspond to individual participant data. * $p < 0.05$, ** $p < 0.01$, *** $p < 0.001$.

execution.

Movement, acceleration and deceleration durations

We compared movement, acceleration and deceleration phase durations for CF and controls to determine whether there was an increase in durations for CF in the noV and startV conditions, in which he demonstrated greater reaching errors. Figure 5.7 represents the total movement duration as well as acceleration and deceleration phases for patient CF (Figure 5.7A) and control participants (Figure 5.7B) in each lighting condition and visual field. The bottom section of the stacked bars (hatched) corresponds to the acceleration phase (time from movement onset to peak velocity) whereas the upper part represents the deceleration phase (time from peak velocity to the end of movement). Thus, the height of the two stacked bars corresponds to the total movement duration.

For movement duration, CF exhibited a main effect of lighting condition ($F_{2,252} = 10.1$, $p < 0.001$), but no main effect of visual field and no interaction effect (both $p > 0.05$). Overall, post-hoc tests showed significantly shorter movement durations for the fullV condition (435 ms) compared to both the noV (487 ms, $p < 0.001$, Holm-Bonferroni corrected) and the startV conditions (478 ms, $p = 0.003$, Holm-Bonferroni corrected). There was no difference between the latter two conditions ($p > 0.05$, Holm-Bonferroni corrected). Control participants showed only a main effect of visual field ($F_{1,5} = 13.9$, $p = 0.014$) with longer movement durations in the LVF (448 ms) compared to the RVF (438 ms, $p = 0.014$). There were no differences in overall movement duration between CF (467 ms) and the controls (441 ms, Crawford's modified t-test, $p > 0.05$).

For acceleration duration, CF showed a main effect of lighting ($F_{2,252} = 6.8$, $p = 0.001$) and a main effect of visual field ($F_{1,252} = 12.6$, $p < 0.001$) but no interaction effect ($p > 0.05$). Post-hoc tests revealed that acceleration durations were overall shorter in the LVF (171 ms) than in the RVF (201 ms, $p < 0.001$). Moreover, acceleration durations were shorter for the fullV condition (165 ms) compared to the noV (200 ms, $p = 0.005$, Holm-Bonferroni corrected) and the startV conditions (193 ms, $p = 0.028$, Holm-Bonferroni corrected). There was no difference between the noV and startV conditions ($p > 0.05$, Holm-Bonferroni corrected). Acceleration durations in control participants were not modulated by the lighting condition or the visual field (all $p > 0.05$). There were no overall differences in acceleration times between patient CF (186 ms) and controls (164 ms, Crawford's modified t-test, $p > 0.05$).

For deceleration duration, CF showed only a main visual field effect ($F_{2,252} = 19.0$, $p < 0.001$) with longer deceleration durations in the LVF (294 ms) compared to the RVF (267 ms, $p < 0.001$). Controls themselves showed no significant differences between any of the experimental conditions (all $p > 0.05$). On average, there were no differences between CF (280 ms) and control participants (277 ms, Crawford's modified t-test, $p > 0.05$).

In summary, CF had shorter total movement and acceleration durations for the fullV condition compared to the other two lighting conditions. Thus, CF's greater reach errors observed in the noV and startV were associated with longer total movement and accele-

ration phase durations. Overall, he also demonstrated shorter acceleration durations and longer deceleration durations when reaching in the LVF compared to the RVF.

Latency

For patient CF, movement latencies did not significantly vary across any of the experimental conditions (all $p > 0.05$). Similarly, control participants showed no differences for any condition (all $p > 0.05$). Overall, CF was slightly faster to initiate movement (265 ms) than controls (316 ms), however this difference was not significant (Crawford's modified t-test, $p > 0.05$).

Peak velocity

Patient CF did not show any modulation of the peak velocity amplitude as a function of experimental conditions (all $p > 0.05$). For controls, we found a significant main effect of lighting condition ($F_{2,10} = 4.3$, $p = 0.046$), but no main effect of visual field nor an interaction effect (both $p > 0.05$). However, post-hoc tests revealed no significant differences between the three lighting conditions (all $p > 0.05$, Holm-Bonferroni corrected). CF's mean peak velocity was 988°/s, which was slightly but not significantly higher than the control participants' mean peak velocity (849°/s, Crawford's modified t-test, $p > 0.05$).

Discussion

In this study, we asked a patient with left OA as well as six neurologically intact control participants to reach with their right hand to remembered target locations in the left or the right visual field, under three different lighting conditions. Participants either performed reaches in complete darkness without vision of the hand (noV), when they could see their right hand only before the movement (startV) or both before and during the entire movement (fullV).

Control participants showed relatively straight movements with a slight leftward curvature. At movement peak velocity, this curvature corresponded to directional errors toward

fixation in the RVF and away from fixation in the LVF. In contrast, patient CF exhibited rightward deviations from the straight-line path markedly in the LVF. This deviation toward ocular fixation is known as an attraction of the hand toward where the eyes look in OA patients, called "magnetic misreaching" (Carey et al., 1997 ; Jackson et al., 2005), which translates into a systematic under-estimation of target visual eccentricity in the contralesional visual field (Blangero et al., 2010 ; Vindras et al., 2016). In addition to this rightward planning error, in the absence of visual feedback of the hand after peak velocity (in noV and startV conditions), patient CF overcompensated and moved away from fixation in the LVF and ended up overshooting the target location both in angular direction and in amplitude. However, the overshoots tended to be smaller when reaching in the fullV condition. These findings show that when no visual feedback of the moving hand is available after peak velocity, the OA patient is less accurate, both in direction and amplitude.

In healthy participants, angular errors were reduced between movement peak velocity and movement end for all lighting conditions, reflecting online motor corrections implemented after peak velocity based on efficient visual and/or proprioceptive updating of hand location. In contrast, CF's angular errors increased during the deceleration phase in the noV and startV conditions when visual updating of hand location was prevented. Our interpretation is that this suggests a role of the PPC in integrating proprioceptive reafference in the contralateral space for on-line motor control.

The errors found in control participants at the different phases of the movement and their modulation by lighting conditions are also noteworthy. First, they showed relatively small angular, amplitude and variable errors at the end of the movement. Variable errors computed in control participants as a measure of reach precision were found to decrease only in the fullV condition (i.e., specifically when visual feedback of the hand was available throughout motor execution). The addition of visual feedback during motor planning (startV condition) did not improve reach precision significantly with respect to the noV condition. This is inconsistent with a previous study in which healthy participants were asked to reach in the dark toward targets with or without vision of the hand prior to

movement onset. The authors found that variable errors were decreased when visual feedback of the hand was provided during motor planning (Rossetti et al., 1994). This may be due to a ceiling effect ; visual planning errors may be negligible for healthy controls in our study. One possible explanation could be that participants' reaches were restricted to 4 different movements (2 start positions x 2 targets) in our experiment compared to 7 in Rossetti's study (1 start position x 7 targets), thus reducing overall reach imprecision. Alternatively, smaller variable errors in our study could be related to shorter reach distances ; our reach targets were approximately 130 mm closer to start positions than targets in Rossetti's setup (Rossetti et al., 1994). Probably for similar reasons, we did not observe any modulation of final angular errors by the different lighting conditions and amplitude errors were only slightly increased in the noV condition, within the RVF. These results suggest that controls remain quite accurate in direction but are mildly impaired in amplitude when vision of their moving hand is prevented during reaching.

Other studies have shown that pointing errors are decreased when visual information about the hand is provided before or during movement execution and that this reduction of errors is coupled with a longer deceleration phase (Desmurget et al., 1995 ; Rossetti et al., 1994 ; van der Meulen et al., 1990). Deceleration time is thought to be associated with control and feedback processes. For control participants, the total movement time and the deceleration time were quite similar for the three lighting conditions. This additional discrepancy might be explained by a major difference in the experimental conditions : in our study, participants aimed toward a remembered target. During the deceleration phase, the reaching is guided through feedback processes allowing for a comparison between the visual target position and the position of the hand (Desmurget et al., 1995). In our study, this direct hand-target comparison was not possible since the target was extinguished just before the movement began and participants reached to its remembered location. However, we observed a reduction in angular errors during the deceleration phase of movement. Collectively, these findings suggest that only fast online correction mechanisms that do not extend the deceleration time, might be recruited when reaching to remembered target locations. These fast corrective processes are likely based on visual

and proprioceptive updating of hand location that can be compared to the predicted location through efference copy. It may be that a comparison of ongoing visual information about the target and visual/proprioceptive information about the hand takes more time to process compared to a predicted location.

The OA patient's reach latencies, total movement and deceleration durations did not differ from controls, thus suggesting that the deficits observed in CF are unlikely to be due to general slowing of visual or motor processing. Nevertheless, we observed faster movements in fullV compared to the noV and startV conditions. In addition, CF exhibited longer deceleration durations in the ataxic compared to the healthy visual field. This is consistent with the field effect found in patient CF. In addition, this finding combined with the observation of a lengthened deceleration phase in the ataxic visual field reflects impairments in fast feedback processes. We surmise that in the absence of PPC, other structures with slower processing might be recruited for online guidance of the hand (Gréa et al., 2002 ; Pisella et al., 2000) when the target is located in the contralesional visual field.

Our results agree with previous studies in OA patients showing that the PPC is necessary to perform online adjustments of reach movements (Blangero et al., 2008 ; Gréa et al., 2002 ; Pisella et al., 2000). Indeed, the PPC has some features that are useful for online correction mechanisms. Firstly, the PPC is reciprocally connected to motor areas in charge of movement execution (Archambault et al., 2015 ; Battaglia Mayer et al., 1998 ; Wise et al., 1997). Secondly, this region can encode both target and hand positions by integrating visual and proprioceptive information (Medendorp et al., 2005 ; Rossetti, Desmurget, & Prablanc, 1995) as well as efference copy signals from frontal motor areas (Andersen et al., 1997 ; Kalaska et al., 1983). Therefore, the PPC appears to be a good candidate to elicit fast modifications of the ongoing motor commands (Archambault et al., 2015).

It is important to underline that in the present study, patient CF showed no differences between the two conditions in which only proprioceptive information about the hand position was available during reaching (i.e., noV and startV conditions), even though in the startV condition visual feedback of the hand was provided during motor planning.

We therefore propose that CF presents problem integrating dynamic rather than static proprioceptive information about the starting hand position. An alternative interpretation could be that the visual information of hand location at start was too far away from ocular fixation to be useful. Indeed, in the contralesional visual field of OA patients, visual spatial coding errors are known to increase drastically with eccentricity (i.e., polar distance from ocular fixation) (Blangero et al., 2010 ; Rossetti et al., 2005). Moreover, patients with OA might exhibit a shrinkage of their attentional visual field toward where they look (Khan et al., 2016). When the hand enters in the patient's contralesional attentional field, visual information about both the remembered target and the hand is similarly biased toward gaze location. As a consequence, improvement in accuracy when visual feedback of the hand is provided in the late phase of the movement may be related to a correct visuo-visual comparison of target and hand positions. In contrast, when hand position is specified through dynamic proprioception, it is degraded but probably not shifted toward fixation as the position of the remembered target is. This may explain the overestimation of the hand-target distance. The incorrect visuo-proprioceptive comparison between target and hand locations may therefore lead to erroneous movement corrections and overshoots.

Hand state estimation results from the integration of proprioceptive and visual reafferences, when available, as well as efference copy signals of the moving hand (Desmurget & Grafton, 2000 ; Wolpert et al., 1995). Once computed, the hand estimate can be compared to the target location and in case of a discrepancy, corrections are generated. The PPC receives visual, proprioceptive and efference copy signals and plays a key role in multisensory integration (Andersen et al., 1997 ; Andersen & Cui, 2009) ; it is thus likely to be involved in state estimation (Mulliken et al., 2008). Damage to the PPC, the superior parietal lobule (SPL) in particular, has been associated with inabilities to maintain internal representation of the contralesional hand (Wolpert, Goodbody, & Husain, 1998). Their patient explicitly reported drift in the perceived position of the contralesional hand which was abolished by visual feedback. In the present study, we tested the ipsilesional hand in patient CF who never reported an explicit drift for neither hand. We showed that SPL lesion disrupted the processes underlying the hand position estimation derived

from proprioception within the contralesional eye-centered space. In the absence of visual information during movement execution (noV and startV conditions), hand estimate is derived from proprioceptive reafferences and efference copy. In healthy participants, the resulting state estimation seems to be quite accurate as demonstrated by the relatively small reach errors. For patient CF, greater errors were observed suggesting impairments in hand state estimate. However, errors were reduced when providing additional visual reafferences about the moving hand (fullV condition), presumably related to a more accurate hand estimate. These findings reveal that lesions to the SPL affect the computation of the internal representation of not only the hand-related but also the eye-related proprioceptive reafferences and/or efference copy about the moving hand. When no visual information is available, patients with a PPC damage might exhibit difficulty computing an accurate hand state estimation during online motor control thus resulting in erroneous corrections.

Acknowledgements

We thank CF for his participation in this experiment. LM received support from a PhD excellence scholarship from Faculté des Etudes Supérieures et Postdoctorales and École d'Optométrie de l'Université de Montréal (FESP-ÉOUM). AZK and GB were funded by the Natural Sciences and Engineering Research Council of Canada (NSERC). AZK was additionally supported by the Canada Research Chair program. LP was supported by the CNRS and the Labex/Idex ANR-11-LABX-0042, France.

6 Discussion

Mon travail de thèse s'organise autour de deux grands objectifs. Le premier consiste à déterminer, chez les sujets sains, comment les informations visuelles et somatosensorielles sont combinées pendant la programmation de mouvements de pointage (études 1 et 2). En effet, malgré de nombreuses investigations, les mécanismes sous-tendant l'intégration multi-sensorielle pour l'action ne sont pas encore tout à fait connus et font débat. Le deuxième objectif est de préciser les fonctions du CPP dans l'intégration multisensorielle pour l'action (études 3 et 4). Les patients avec ataxie optique présentent une lésion du CPP et l'étude fine de leurs troubles sensorimoteurs permet de préciser les fonctions du CPP dans les processus d'intégration multimodale impliqués dans l'action.

6.1 Étude 1 - Pondération de la vision et de la proprioception

Dans l'**étude n°1**, nous avons exploré l'intégration visuo-proprioceptive concernant la position de la main, lors de la phase de programmation d'un mouvement de pointage. Le but était de déterminer si les poids attribués à la vision et la proprioception étaient inversement proportionnels à leur variabilités sensorielles respectives, tels que prédits par le modèle **bayésien** (Deneve & Pouget, 2004 ; Ernst, 2006 ; Ernst & Bülthoff, 2004 ; Knill & Pouget, 2004 ; O'Reilly et al., 2012), ou si d'autres paramètres pouvaient rentrer en compte dans la répartition des poids. Les résultats que nous avons obtenus contrastent avec l'intégration bayésienne, pourtant largement décrite dans la littérature (Braem et al., 2014 ; Burns & Blohm, 2010 ; Butler et al., 2010 ; Ernst & Banks, 2002 ; Körding & Wolpert, 2004 ; van Beers et al., 1999a). Chez la majorité des participants, les variabilités sensorielles étaient relativement différentes entre main droite et main gauche alors que les

poids attribués à la vision et la proprioception étaient très similaires entre les deux mains. Sur la base des variabilités sensorielles observées, la théorie bayésienne aurait prédit des poids visuels et proprioceptifs différents entre main droite et gauche. À la place, on observe plutôt un **même** poids sensoriel qui semble être attribué « par défaut » aux deux mains, indépendamment des fiabilités des modalités visuelle et proprioceptive.

Ces observations suggèrent que les poids assignés à chaque modalité sensorielle ne sont pas totalement dépendants de la précision relative du signal (Ernst et al., 2000 ; Jacobs & Fine, 1999 ; van Beers et al., 2011). Ces résultats font écho à une récente étude ayant montré que, lors de mouvements bimanuels, l'intégration n'est pas optimale car seules les informations provenant du bras avec la meilleure acuité proprioceptive sont prises en compte (Wong et al., 2014), ce qui pourrait également expliquer pourquoi on retrouve des poids sensoriels **communs** aux deux mains. Nous faisons l'hypothèse que les pondérations sensorielles rapportées dans notre tâche ne sont pas déterminées par les fiabilités visuelle et proprioceptive mais seraient **acquises** par expérience motrice. Dans le cas où les variabilités sensorielles sont importantes ou difficiles à estimer, il serait plus avantageux d'utiliser des poids qui sont indépendants de l'incertitude sensorielle et donc plus stables. En outre, il a été décrit que l'intégration multisensorielle était contexte-dépendante et que les poids sensoriels pouvaient par conséquent différer selon la tâche à effectuer (Sober & Sabes, 2005). À notre connaissance, cette étude est la première à examiner et comparer l'intégration visuo-proprioceptive entre main droite et main gauche. Il est donc nécessaire de poursuivre les recherches afin d'étayer nos conclusions.

6.2 Étude 2 - Intégration des informations proprioceptives et tactiles

On sait que l'intégration des informations visuelles et proprioceptives permet d'obtenir une estimation de la position de la main plus précise que lorsque seule la vision ou la proprioception est disponible (van Beers et al., 1996, 1999b). Dans l'**étude n°2**, nous avons voulu déterminer si les signaux tactiles pouvaient, comme la vision, constituer une

source supplémentaire d'informations pour améliorer l'estimation de la position proprioceptive de la main. La précision de la localisation de la main fut évaluée en demandant aux participants d'indiquer avec leur main droite la position de leur index gauche (index cible), qui était caché de leur vue. Nous avons observé une réduction **spécifique** des erreurs et de la dispersion des mouvements en direction de l'index cible suivant l'application de stimulations vibrotactiles sur le doigt cible. Ces données mettent en évidence que les informations tactiles des vibrations cutanées sont intégrées avec les informations proprioceptives renseignant sur la position de l'index cible, ce qui permet d'améliorer la localisation spatiale du doigt.

Les résultats de notre étude confirment le principe selon lequel l'intégration de plusieurs modalités sensorielles redondantes permettrait de **maximiser** la fiabilité l'estimation multimodale (Ernst & Bülthoff, 2004 ; B. E. Stein & Meredith, 1993). L'intégration des informations tactiles et proprioceptives de la main est en lien les interactions entre les deux modalités qui ont été décrites précédemment (de Vignemont et al., 2005 ; Moberg, 1983 ; Warren et al., 2011). Lors de la présente étude, les stimulations vibrotactiles délivrées activent les **corpuscules de Pacini** et de **Meissner** (Talbot et al., 1968) ce qui laisse penser que ces deux types de récepteurs cutanés contribuent à l'intégration des informations vibrotactiles et proprioceptifs. Il existe cependant d'autres méchanorécepteurs tels que les corpuscules de Ruffini et les disques de Merkel qui sont sensibles, respectivement, à l'étirement de la peau et aux vibrations entre 5 et 15 Hz (Gilman, 2002). À l'aide de stimuli somatosensoriels adaptés, il serait intéressant de voir si ces récepteurs peuvent également être impliqués dans l'intégration des stimuli tactiles et proprioceptifs pour la position de la main. Il est probable que le cortex pariétal soit recruté dans ces processus d'intégration, en particulier l'**aire 5** où convergent les signaux proprioceptifs et tactiles (Rizzolatti et al., 1998). Il est également possible que le **cortex somatosensoriel primaire** soit impliqué, comme le suggère une récente étude décrivant des interactions entre toucher et proprioception au sein de cette région (Kim et al., 2015). Cette dernière hypothèse est cohérente avec l'existence de neurones dans les cortex sensoriels primaires capables de répondre à plusieurs modalités sensorielles (Watkins et al., 2006 ; Zhou &

Fuster, 2004).

6.3 Résultats des études 1 et 2

Au travers des deux premières études chez les sujets sains, nous avons voulu tester les prédictions du modèle bayésien de l'intégration multisensorielle, dans le contexte des mouvements de pointage. Nous nous sommes focalisés sur deux aspects en particulier, à savoir i) la **pondération** des signaux visuels et proprioceptifs et ii) la **précision** de l'estimation bimodale de la position de la main. Tout d'abord, nous avons pu mettre en évidence que l'intégration multisensorielle pour la programmation des mouvements de pointage n'est pas entièrement dépendante des variabilités sensorielles, contrairement à ce qui est suggéré par la théorie bayésienne (Battaglia et al., 2003 ; Ernst, 2006 ; O'Reilly et al., 2012). Ces résultats suggèrent l'implication d'autres paramètres, autres que les variabilités intrinsèques des modalités sensorielles, dans l'intégration des signaux sensoriels. D'autre part, il est probable que les poids sensoriels soient spécifiques du contexte de la tâche et de l'action à réaliser. Dans un deuxième temps, nous avons pu confirmer que l'utilisation de plusieurs modalités sensorielles permet d'améliorer l'estimation de la position de la main. En effet, l'ajout d'informations tactiles à la position proprioceptive de la main donne lieu à une localisation **plus précise** de la main. Ces résultats sont en lien avec les études rapportant que la localisation d'une cible est **moins variable** lorsque sa position dans l'espace est renseignée par plusieurs modalités sensorielles (Godfroy-Cooper et al., 2015 ; Hairston et al., 2003 ; van Beers et al., 1999b). Cette expérience apporte une preuve supplémentaire que le cerveau utilise toutes les informations sensorielles dont il dispose afin de construire une estimation de l'environnement et du corps la plus fiable et par conséquent la plus stable possible (Knill & Pouget, 2004 ; O'Reilly et al., 2012).

6.4 Étude 3 - CPP et estimation de la position de la main

Le CPP est une aire **associative** où convergent les informations issues de plusieurs modalités sensorielles tels que les signaux visuels, auditifs, somatosensoriels ou encore vestibulaires (Andersen et al., 1997 ; Y. E. Cohen, 2009). En outre, le CPP possède des connexions réciproques avec les régions motrices frontales (Gharbawie et al., 2011 ; Marconi et al., 2001 ; Wise et al., 1997) lui permettant de recevoir la copie des commandes motrices mais également de communiquer avec les régions motrices et prémotrices afin de modifier le programme moteur en cours (Andersen et al., 1997 ; Kalaska et al., 1983). Dans le cas des mouvements d'atteinte visuellement guidés, il a été montré que le CPP intègre les informations relatives à la position de la **cible** et la position de la **main** (Beurze et al., 2007 ; Medendorp et al., 2005). Par ailleurs, l'inactivation transitoire du CPP par SMT perturbe l'intégration des signaux visuels et proprioceptifs renseignant la position de la main et nécessaires au calcul du vecteur de mouvement (Vesia et al., 2008). Cette observation souligne le rôle primordial du CPP dans l'**intégration sensorimotrice**.

Au cours de mouvement répétés dans le noir, un phénomène de déviation motrice est observé : la main des participants s'éloigne progressivement des cibles, sans qu'ils en soient conscients (Brown et al., 2003 ; Smeets et al., 2006). Du fait de ses fonctions sensorimotrices, il a été proposé que le CPP soit impliqué dans l'accumulation des erreurs qui sous-tendent la déviation motrice de la main dans le noir (Cameron et al., 2015). L'**étude n°3** avait pour objectif de déterminer si le CPP joue effectivement un rôle dans la déviation motrice. Deux patients atteints d'ataxie optique, présentant une lésion unilatérale ou bilatérale du CPP, ont été testés ainsi que des participants contrôles. Les patients ataxiques présentaient une déviation plus importante que les sujets contrôles mais uniquement dans le cas où ils ne pouvaient pas voir leur main. Les deux patients étaient particulièrement atteints dans le champ visuel inférieur, avec une accumulation des erreurs plus importante que les contrôles. De façon générale, la main gauche des patients ataxiques dérivait dans le champ visuel droit alors que la main droite déviait en direction

du champ droit.

L'accumulation exagérée des erreurs dans le champ visuel inférieur des patients ataxiques confirment le rôle du CPP dans la sur-représentation de la partie périphérique du champ visuel inférieur (Pitzalis et al., 2013 ; Previc, 1990 ; Rossit et al., 2013). En effet, il semblerait que le système visuomoteur ait un meilleur contrôle sur les actions exécutées dans la portion inférieure du champ visuel (Brown et al., 2005 ; Danckert & Goodale, 2001). Par ailleurs il a été montré que la région V6A, localisée dans la partie caudale du LPS, représente préférentiellement le quadrant inférieur controlatéral qui correspond précisément à l'espace que le bras opposé traverse pour atteindre une cible présentée en vision centrale (Fattori et al., 02 01, 2017). L'ataxie optique est typiquement associée à des lésions centrées sur le précunéus, à proximité de la JPO (Karnath & Perenin, 2005) ; or cette zone correspond à la localisation de l'aire V6A chez l'Homme (Pitzalis et al., 2013 ; Tosoni et al., 2015). C'est pourquoi on observe chez les patients ataxiques des déficits lorsqu'ils doivent exécuter des mouvements de pointage dans leur **champ visuel inférieur**. Toujours chez les patients, la déviation systématique de la main vers le côté opposé pourrait être due à un biais de perception. En effet, dans le noir, la main droite est perçue plus à droite et la main gauche plus à gauche chez les sujets sains (Wilson et al., 2010). Chez les patients ataxiques, ce biais serait plus important que chez les sujets sains et ils le compenseraient en faisant des mouvements vers le côté opposé à la main (main droite bouge vers la gauche, par exemple). Lors des mouvements, le SNC utilise un **modèle direct** permettant de prédire la future position du bras (Wolpert & Ghahramani, 2000). Le CPP, avec le cervelet, participerait à l'estimation interne de la position de la main (Desmurget & Grafton, 2000 ; Mulliken et al., 2008) qui doit constamment être mise à jour. La déviation motrice observée chez les patients ataxiques laisse penser que le CPP serait impliqué dans la mise à jour de la représentation interne du la main sur la base de réafférences **visuelles** et **proprioceptives**. En cas de lésion du CPP, l'intégration des retours visuels et proprioceptifs serait altérée et rendrait l'estimation de la position de la main **incertaine**. Par conséquent, la représentation interne de la main se **dégraderait** au fur et à mesure des mises à jour et les erreurs s'accumuleraient sans être corrigées car

elles ne sont pas détectées par le SNC. À l'avenir, il serait intéressant de tester si l'accumulation des erreurs change si, au lieu d'être alignées avec la ligne médiane, les cibles sont présentées dans le champ visuel périphérique gauche ou droit. De cette façon, les conditions seraient similaires à celles classiquement utilisées pour révéler les effets champ et main de l'ataxie optique (Blangero et al., 2007 ; Perenin & Vighetto, 1988 ; Vighetto, 1980).

6.5 Étude 4 - CPP et contrôle en ligne du mouvement

Le CPP joue un rôle prépondérant dans le contrôle des mouvements visuellement guidés permettant d'ajuster les commandes motrices en cours d'exécution (Battaglia et al., 2003 ; Desmurget et al., 1999, 2001). Par conséquent, les patients avec ataxie optique présentant une lésion du CPP éprouvent des difficultés à effectuer des corrections motrices **rapides** (Gréa et al., 2002 ; Pisella et al., 2000). L'ajustement en temps réel de la trajectoire motrice reposerait sur une représentation interne de la main fiable, et donc sur l'intégrité du CPP. L'objectif de l'**étude n°4** était d'examiner les conséquences de dommages du CPP sur la représentation interne de la main pendant le contrôle en ligne des mouvements de pointage. Pour ce faire, nous avons demandé à des participants contrôles et un patient ataxique avec lésion unilatérale du CPP d'effectuer des pointages en direction de cibles mémorisées. La vision de la main était modulée de sorte qu'elle soit visible avant et pendant le mouvement (fullV), juste avant le mouvement (startV) ou jamais visible (noV). Comparé aux participants contrôles, le patient ataxique faisait relativement peu d'erreurs quand il voyait sa main pendant le mouvement (fullV). En revanche, il était particulièrement atteint lorsque sa main n'était pas visible (noV) ; les positions finales des pointages étaient globalement situées plus loin et à gauche des cibles, comme si le patient localisait sa main plus en bas et à droite qu'elle ne l'était en réalité. Ces déficits n'étaient pas diminués dans la condition où il pouvait voir sa main avant l'initiation du mouvement (startV). Les erreurs de pointage étaient plus conséquentes dans son champ visuel contralésionnel, conformément à l'**effet champ** déjà diagnostiqué chez le patient.

L'ensemble de ces résultats suggère l'implication du CPP dans la représentation interne

de la main, sur la base des réafférences proprioceptives et/ou des copies d'efférence pendant le mouvement. Le patient ne réduit ses erreurs que lorsque la main est vue pendant la **phase terminale** du mouvement. La vision de la main au départ ne permet pas d'améliorer les prédictions de la position de la main pendant le mouvement. Ceci peut être expliqué par le fait que l'information visuelle disponible se trouve dans le champ périphérique inférieur, qui est affecté chez les patients ataxiques à cause de leur lésion du CPP (Bartolo et al., 2018 ; Vindras et al., 2016). Ces données démontrent également que le patient est capable de faire des comparaisons visuo-visuelles entre la position de la cible et la position de la main afin de corriger sa trajectoire en fin de mouvement. En revanche, les comparaisons visuo-proprioceptives (quand la vision de la main n'est pas disponible) sont altérées après lésion du CPP. Par ailleurs il a été montré, à la fois chez l'Homme et le singe, que les ajustements du programme moteur pendant l'action sont perturbés lorsque la **partie caudale du LPS** (à proximité du sillon pariéto-occipital) subit une lésion « virtuelle » induite par SMT répétée ou une lésion chirurgicale (Battaglini et al., 2002 ; Ciavarro et al., 2013 ; Desmurget et al., 1999). Ces observations démontrent l'implication du LPS dans le contrôle en ligne des mouvements d'atteinte. Lors d'une tâche de double saut de cible réalisée par des singes macaques, l'enregistrement de neurones localisés au niveau du LPS a permis de montrer que les cellules de cette région véhiculent des **signaux relatifs à la correction** des mouvements de la main (Archambault et al., 2009). L'une des fonctions du LPS consisterait à **comparer** la position prédite et la position réelle de la main pendant le mouvement. La position prédite de la main est calculée sur la base d'un modèle interne direct, qui utilise les copies d'efférence, tandis que sa position réelle est renseignée par les réafférences visuelles et somatosensorielles générées pendant le mouvement (Desmurget & Grafton, 2000 ; Kalaska et al., 2003 ; Kawato, 1999 ; Shadmehr et al., 2010). Si le LPS détecte une **disparité** entre la position prédite et réelle de la main, un signal d'erreur est généré puis transmis aux régions motrices afin d'ajuster la commande motrice (Bosco et al., 2010). Ainsi, les déficits de contrôle en ligne du mouvement observés chez les patients avec ataxie optique sont bien cohérents avec une atteinte du LPS.

6.6 Résultats des études 3 et 4

Les deux dernières études, incluant des patients avec une lésion du LPS, ont permis de confirmer le rôle de cette région dans l'intégration multisensorielle pour le **contrôle en ligne du mouvement**. Plus particulièrement, les déficits sensorimoteurs qui se manifestent chez les patients avec ataxie optique suggèrent que le LPS serait impliqué dans la **représentation interne de la main** utilisée pour effectuer des mouvements de pointage. Ce processus nécessite la mise en commun des informations visuelles, proprioceptives et de la copie de la commande motrice. En cas de dommage du LPS, la représentation interne de la main ne serait pas estimée correctement. En effet, chez le patient ataxique unilatéral gauche ayant participé aux deux expériences, il semblerait que l'estimation de la position de sa main ipsilésionnelle soit **biaisée** en direction de son champ visuel ipsilésionnel. De plus, chez les patients avec une lésion du LPS, on observe une accumulation anormale d'erreurs lors de la mise à jour de la représentation interne de la main. Ces erreurs reflètent potentiellement la dégradation de l'estimation de la position proprioceptive de la main au cours du temps. En intégrant les informations sensorielles à disposition dans un **modèle interne direct**, le LPS participerait à la construction et la mise à jour de l'estimation interne de la main nécessaire à l'ajustement des mouvements de pointage en cours d'exécution.

De manière générale, le cortex pariétal est organisé selon un **gradient** antéro-postérieur en fonction de la nature des informations traitées. Les régions les plus **rostrales** (antérieures) codent préférentiellement les informations **somatosensorielles/motrices** tandis que les régions les plus **caudales** (postérieures) sont davantage spécialisées dans le traitement des informations **visuelles** (Burnod et al., 1999 ; Filimon, 2010 ; Filimon et al., 2009 ; Stark & Zohary, 2008 ; Vesia & Crawford, 2012). En effet, il a été montré que les régions postérieures du CPP répondent préférentiellement à la présentation de **stimuli visuels** dans le champ controlatéral alors que les régions les plus antérieures répondent de manière prépondérante aux signaux de la **main** controlatérale (Beurze et al., 2009 ; Blangero et al., 2009 ; Stark & Zohary, 2008 ; Vesia et al., 2010). L'ensemble de ces études

suggère l'existence, au sein du CPP, de plusieurs modules d'intégration de la position de la cible et de la main répartis le long d'un axe antéro-postérieur selon un gradient allant de la proprioception à la vision. Une étude en IRMf a mis en évidence un **chevauchement** entre les lésions associées à l'ataxie optique et les régions pariétales les plus postérieures actives lors des mouvements d'atteinte à savoir mIPS, la partie postérieure du sillon intra-pariétal (pIPS) et la JPO (Blangero et al., 2009). Ces résultats suggèrent que les déficits observés chez les patients ataxiques lors de mouvements visuellement guidés résultent de l'atteinte de plusieurs régions pariétales impliquées dans l'intégration de la position de la cible et de la main. Plus précisément, les lésions de mIPS sont majoritairement responsables de l'**effet main** de l'ataxie optique alors que les lésions plus postérieures, au niveau de SPOC, sont davantage susceptibles de provoquer un **effet champ** (Blangero et al., 2009 ; Pisella et al., 2009).

6.7 Conclusions

L'objectif de ce travail de thèse était double et consistait à i) éclaircir certains mécanismes de l'intégration multisensorielle pour la programmation de mouvements de pointage chez les sujets sains et ii) préciser les fonctions du CPP dans l'intégration multisensorielles pour l'action avec l'étude de patients ataxiques, présentant une lésion du CPP.

Les études chez les sujets sains ont révélé que la pondération des informations visuelles et proprioceptives pour la programmation des mouvements de pointage ne dépend pas exclusivement de leurs fiabilités sensorielles. Il semblerait que les poids attribués à la vision et la proprioception puissent être **acquis** par expérience motrice. Par ailleurs, il a été confirmé que le système nerveux utilise et intègre l'ensemble des informations sensorielles qu'il a à sa disposition afin d'**améliorer** l'estimation de la position de la main.

Les études chez les patients atteints d'ataxie optique ont permis de confirmer le rôle du cortex pariétal postérieur dans l'intégration multisensorielle pour le **contrôle en ligne** du mouvement. Plus spécifiquement, le lobule pariétal supérieur serait impliqué dans l'intégration des signaux sensoriels et de la copie d'efférence pour la construction de la

représentation interne de la main. Cette dernière est nécessaire à l'ajustement des mouvements de pointage en cours d'exécution.

Bibliographie

Abidi, M. A., & Gonzalez, R. C. (1992). *Data fusion in robotics and machine intelligence*. San Diego, CA : Academic Press.

Aglioti, S., Beltramello, A., Bonazzi, A., & Corbetta, M. (1996). Thumb-pointing is humans after damage to somatic sensory cortex. *Experimental Brain Research*, *109*(1), 92-100.

Alais, D., & Burr, D. (2004). The ventriloquist effect results from near-optimal bimodal integration. *Current biology : CB*, *14*(3), 257-262. doi: 10.1016/j.cub.2004.01.029

Allison, T., McCarthy, G., Wood, C. C., & Jones, S. J. (1991). Potentials evoked in human and monkey cerebral cortex by stimulation of the median nerve. A review of scalp and intracranial recordings. *Brain : A Journal of Neurology*, *114 (Pt 6)*, 2465-2503.

Amino, Y., Kyuhou, S., Matsuzaki, R., & Gemba, H. (2001). Cerebello-thalamo-cortical projections to the posterior parietal cortex in the macaque monkey. *Neuroscience Letters*, *309*(1), 29-32.

Andersen, R. A., Andersen, K. N., Hwang, E. J., & Hauschild, M. (2014). Optic ataxia : From Balint's syndrome to the parietal reach region. *Neuron*, *81*(5), 967-983. doi: 10.1016/j.neuron.2014.02.025

Andersen, R. A., & Buneo, C. A. (2002). Intentional maps in posterior parietal cortex. *Annual Review of Neuroscience*, *25*, 189-220. doi: 10.1146/annurev.neuro.25.112701.142922

Andersen, R. A., & Cui, H. (2009). Intention, action planning, and decision making in parietal-frontal circuits. *Neuron*, *63*(5), 568-583. doi: 10.1016/j.neuron.2009.08.028

Andersen, R. A., Meeker, D., Pesaran, B., Breznen, B., Buneo, C., & Scherberger, H. (2004). Sensorimotor Transformations in the Posterior Parietal Cortex. In M. S. Gazzaniga (Ed.), *The cognitive neurosciences* (p. 463-474). Cambridge, MA : MIT Press.

Andersen, R. A., Snyder, L. H., Bradley, D. C., & Xing, J. (1997). Multimodal representation of space in the posterior parietal cortex and its use in planning movements. *Annual Review of Neuroscience*, *20*, 303-330. doi: 10.1146/annurev.neuro.20.1.303

Archambault, P. S., Caminiti, R., & Battaglia-Mayer, A. (2009). Cortical mechanisms for online control of hand movement trajectory : The role of the posterior parietal cortex. *Cerebral Cortex (New York, N.Y. : 1991)*, *19*(12), 2848-2864. doi: 10.1093/cercor/bhp058

Archambault, P. S., Ferrari-Toniolo, S., Caminiti, R., & Battaglia-Mayer, A. (2015). Visually-guided correction of hand reaching movements : The neurophysiological bases in the cerebral cortex. *Vision Research*, *110*(Pt B), 244-256. doi: 10.1016/j.visres.2014.09.009

Atkeson, C. G. (1989). Learning arm kinematics and dynamics. *Annual Review of Neuroscience*, *12*, 157-183. doi: 10.1146/annurev.ne.12.030189.001105

Baizer, J. S., Desimone, R., & Ungerleider, L. G. (1993). Comparison of subcortical connections of inferior temporal and posterior parietal cortex in monkeys. *Visual Neuroscience*, *10*(1), 59-72.

Bálint, R. (1909). Seelenlähmung des "Schauens", optische Ataxie, räumliche Störung der Aufmerksamkeit. pp. 51–66. *European Neurology*, *25*(1), 51-66. doi: 10.1159/000210464

Bard, C., Turrell, Y., Fleury, M., Teasdale, N., Lamarre, Y., & Martin, O. (1999). Deafferentation and pointing with visual double-step perturbations. *Experimental Brain Research*, *125*(4), 410-416.

Bartolo, A., Rossetti, Y., Revol, P., Urquizar, C., Pisella, L., & Coello, Y. (2018). Reachability judgement in optic ataxia : Effect of peripheral vision on hand and target perception in depth. *Cortex ; a Journal Devoted to the Study of the Nervous System and Behavior*, *98*, 102-113. doi: 10.1016/j.cortex.2017.05.013

Bastian, A. J., Zackowski, K. M., & Thach, W. T. (2000). Cerebellar ataxia : Torque deficiency or torque mismatch between joints ? *Journal of Neurophysiology*, *83*(5), 3019-3030. doi: 10.1152/jn.2000.83.5.3019

Batista, A. P., Buneo, C. A., Snyder, L. H., & Andersen, R. A. (1999). Reach plans in eye-centered coordinates. *Science (New York, N.Y.)*, *285*(5425), 257-260.

Battaglia, P. W., Jacobs, R. A., & Aslin, R. N. (2003). Bayesian integration of visual and auditory signals for spatial localization. *Journal of the Optical Society of America. A, Optics, Image Science, and Vision*, *20*(7), 1391-1397.

Battaglia-Mayer, A., Ferrari-Toniolo, S., Visco-Comandini, F., Archambault, P. S., Saberi-Moghadam, S., & Caminiti, R. (2013). Impairment of online control of hand and eye movements in a monkey model of optic ataxia. *Cerebral Cortex (New York, N.Y. : 1991)*, *23*(11), 2644-2656. doi: 10.1093/cercor/bhs250

Battaglia Mayer, A., Ferraina, S., Marconi, B., Bullis, J. B., Lacquaniti, F., Burnod, Y., ... Caminiti, R. (1998). Early motor influences on visuomotor transformations for reaching : A positive image of optic ataxia. *Experimental Brain Research*, *123*(1-2), 172-189.

Battaglini, P. P., Muzur, A., Galletti, C., Skrap, M., Brovelli, A., & Fattori, P. (2002). Effects of lesions to area V6A in monkeys. *Experimental Brain Research*, *144*(3), 419-422. doi: 10.1007/s00221-002-1099-4

Bell, A. H., Meredith, M. A., Van Opstal, A. J., & Munoz, D. P. (2005). Crossmodal integration in the primate superior colliculus underlying the preparation and initiation of saccadic eye movements. *Journal of Neurophysiology*, *93*(6), 3659-3673. doi: 10.1152/jn.01214.2004

Bellan, V., Gilpin, H. R., Stanton, T. R., Dagsdóttir, L. K., Gallace, A., & Lorimer Moseley, G. (2017). Relative contributions of spatial weighting, explicit knowledge and proprioception to hand localisation during positional ambiguity. *Experimental Brain Research*, *235*(2), 447-455. doi: 10.1007/s00221-016-4782-6

Berens, P. (2009). CircStat : A Matlab Toolbox for Circular Statistics. *Journal of Statistical Software*, *31*(10), 1–21.

Bernier, P.-M., & Grafton, S. T. (2010). Human posterior parietal cortex flexibly determines reference frames for reaching based on sensory context. *Neuron*, *68*(4), 776-788. doi: 10.1016/j.neuron.2010.11.002

Bertelson, P., & Aschersleben, G. (1998). Automatic visual bias of perceived auditory location. *Psychonomic Bulletin & Review*, *5*(3), 482-489. doi: 10.3758/BF03208826

Beurze, S. M., de Lange, F. P., Toni, I., & Medendorp, W. P. (2007). Integration of target and effector information in the human brain during reach planning. *Journal of Neurophysiology*, *97*(1), 188-199. doi: 10.1152/jn.00456.2006

Beurze, S. M., de Lange, F. P., Toni, I., & Medendorp, W. P. (2009). Spatial and effector processing in the human parietofrontal network for reaches and saccades. *Journal of Neurophysiology*, *101*(6), 3053-3062. doi: 10.1152/jn.91194.2008

Beurze, S. M., Van Pelt, S., & Medendorp, W. P. (2006). Behavioral reference frames for planning human reaching movements. *Journal of Neurophysiology*, *96*(1), 352-362. doi: 10.1152/jn.01362.2005

Binkofski, F., Dohle, C., Posse, S., Stephan, K. M., Hefter, H., Seitz, R. J., & Freund, H. J. (1998). Human anterior intraparietal area subserves prehension : A combined lesion and functional MRI activation study. *Neurology*, *50*(5), 1253-1259.

Binsted, G., & Elliott, D. (1999). Ocular perturbations and retinal/extraretinal information : The coordination of saccadic and manual movements. *Experimental Brain Research*, *127*(2), 193-206.

Blakemore, S. J., Frith, C. D., & Wolpert, D. M. (2001). The cerebellum is involved in predicting the sensory consequences of action. *Neuroreport*, *12*(9), 1879-1884.

Blangero, A., Gaveau, V., Luauté, J., Rode, G., Salemme, R., Guinard, M., ... Pisella, L. (2008). A hand and a field effect in on-line motor control in unilateral optic ataxia. *Cortex ; a*

Journal Devoted to the Study of the Nervous System and Behavior, *44*(5), 560-568. doi: 10.1016/j.cortex.2007.09.004

Blangero, A., Menz, M. M., McNamara, A., & Binkofski, F. (2009). Parietal modules for reaching. *Neuropsychologia*, *47*(6), 1500-1507. doi: 10.1016/j.neuropsychologia.2008.11.030

Blangero, A., Ota, H., Delporte, L., Revol, P., Vindras, P., Rode, G., ... Pisella, L. (2007). Optic ataxia is not only 'optic' : Impaired spatial integration of proprioceptive information. *NeuroImage*, *36 Suppl 2*, T61-68. doi: 10.1016/j.neuroimage.2007.03.039

Blangero, A., Ota, H., Rossetti, Y., Fujii, T., Ohtake, H., Tabuchi, M., ... Pisella, L. (2010). Systematic retinotopic reaching error vectors in unilateral optic ataxia. *Cortex ; a journal devoted to the study of the nervous system and behavior*, *46*(1), 77-93. doi: 10.1016/j.cortex.2009.02.015

Bolanowski, S. J., Gescheider, G. A., Verrillo, R. T., & Checkosky, C. M. (1988). Four channels mediate the mechanical aspects of touch. *The Journal of the Acoustical Society of America*, *84*(5), 1680-1694.

Borra, E., Ichinohe, N., Sato, T., Tanifuji, M., & Rockland, K. S. (2010). Cortical connections to area TE in monkey : Hybrid modular and distributed organization. *Cerebral Cortex (New York, N.Y. : 1991)*, *20*(2), 257-270. doi: 10.1093/cercor/bhp096

Bosco, A., Breveglieri, R., Chinellato, E., Galletti, C., & Fattori, P. (2010). Reaching activity in the medial posterior parietal cortex of monkeys is modulated by visual feedback. *The Journal of Neuroscience : The Official Journal of the Society for Neuroscience*, *30*(44), 14773-14785. doi: 10.1523/JNEUROSCI.2313-10.2010

Bosco, A., Breveglieri, R., Reser, D., Galletti, C., & Fattori, P. (2015). Multiple representation of reaching space in the medial posterior parietal area V6A. *Cerebral Cortex (New York, N.Y. : 1991)*, *25*(6), 1654-1667. doi: 10.1093/cercor/bht420

Both, M. H., van Ee, R., & Erkelens, C. J. (2003). Perceived slant from Werner's illusion affects binocular saccadic eye movements. *Journal of Vision*, *3*(11), 685-697. doi: 10.1167/3.11.4

Braem, B., Honoré, J., Rousseaux, M., Saj, A., & Coello, Y. (2014). Integration of visual and haptic informations in the perception of the vertical in young and old healthy adults and right brain-damaged patients. *Neurophysiologie Clinique = Clinical Neurophysiology*, *44*(1), 41-48. doi: 10.1016/j.neucli.2013.10.137

Brenner, E., & Smeets, J. B. (1996). Size illusion influences how we lift but not how we grasp an object. *Experimental Brain Research*, *111*(3), 473-476.

Breveglieri, R., Kutz, D. F., Fattori, P., Gamberini, M., & Galletti, C. (2002). Somatosensory cells in the parieto-occipital area V6A of the macaque. *Neuroreport*, *13*(16), 2113-2116.

Brodmann, K. (1909). *Vergleichende Lokalisationslehre der Großhirnrinde in ihren Prinzipien dargestellt auf Grund des Zellenbaues*. Leipzig : Barth.

Brown, L. E., Halpert, B. A., & Goodale, M. A. (2005). Peripheral vision for perception and action. *Experimental Brain Research*, *165*(1), 97-106. doi: 10.1007/s00221-005-2285-y

Brown, L. E., Rosenbaum, D. A., & Sainburg, R. L. (2003). Limb position drift : Implications for control of posture and movement. *Journal of Neurophysiology*, *90*(5), 3105-3118. doi: 10.1152/jn.00013.2003

Buckner, R. L., Krienen, F. M., Castellanos, A., Diaz, J. C., & Yeo, B. T. T. (2011). The organization of the human cerebellum estimated by intrinsic functional connectivity. *Journal of Neurophysiology*, *106*(5), 2322-2345. doi: 10.1152/jn.00339.2011

Buneo, C. A., & Andersen, R. A. (2006). The posterior parietal cortex : Sensorimotor interface for the planning and online control of visually guided movements. *Neuropsychologia*, *44*(13), 2594-2606. doi: 10.1016/j.neuropsychologia.2005.10.011

Buneo, C. A., & Andersen, R. A. (2012). Integration of target and hand position signals in the posterior parietal cortex : Effects of workspace and hand vision. *Journal of Neurophysiology*, *108*(1), 187-199. doi: 10.1152/jn.00137.2011

Buneo, C. A., Jarvis, M. R., Batista, A. P., & Andersen, R. A. (2002). Direct visuomotor transformations for reaching. *Nature*, *416*(6881), 632-636. doi: 10.1038/416632a

Burnod, Y., Baraduc, P., Battaglia-Mayer, A., Guigon, E., Koechlin, E., Ferraina, S., ... Caminiti, R. (1999). Parieto-frontal coding of reaching : An integrated framework. *Experimental Brain Research*, *129*(3), 325-346.

Burns, J. K., & Blohm, G. (2010). Multi-sensory weights depend on contextual noise in reference frame transformations. *Frontiers in human neuroscience*, *4*, 221. doi: 10.3389/fnhum.2010.00221

Butler, J. S., Smith, S. T., Campos, J. L., & Bülthoff, H. H. (2010). Bayesian integration of visual and vestibular signals for heading. *Journal of Vision*, *10*(11), 23. doi: 10.1167/10.11.23

Buxbaum, L. J., & Coslett, H. B. (1998). Spatio-motor representaions in reaching : Evidence for subtypes of optic ataxia. *Cognitive Neuropsychology*, *15*(3), 279-312. doi: 10.1080/026432998381186

Calton, J. L., Dickinson, A. R., & Snyder, L. H. (2002). Non-spatial, motor-specific activation in posterior parietal cortex. *Nature Neuroscience*, *5*(6), 580-588. doi: 10.1038/nn862

Cameron, B. D., de la Malla, C., & López-Moliner, J. (2015). Why do movements drift in the dark ? Passive versus active mechanisms of error accumulation. *Journal of Neurophysiology*, *114*(1), 390-399. doi: 10.1152/jn.00032.2015

Carey, D. P., Coleman, R. J., & Della Sala, S. (1997). Magnetic misreaching. *Cortex ; a Journal Devoted to the Study of the Nervous System and Behavior*, *33*(4), 639-652.

Cavina-Pratesi, C., Connolly, J. D., & Milner, A. D. (2013). Optic ataxia as a model to investigate the role of the posterior parietal cortex in visually guided action : Evidence from studies of patient M.H. *Frontiers in Human Neuroscience*, *7*. doi: 10.3389/fnhum.2013.00336

Chambers, C., Fernandes, H., & Kording, K. (2017). Policies or Knowledge : Priors differ between perceptual and sensorimotor tasks. *bioRxiv*, 132829. doi: 10.1101/132829

Chang, S. W. C., Dickinson, A. R., & Snyder, L. H. (2008). Limb-specific representation for reaching in the posterior parietal cortex. *The Journal of neuroscience : the official journal of the Society for Neuroscience*, *28*(24), 6128-6140. doi: 10.1523/JNEUROSCI.1442-08.2008

Chang, S. W. C., & Snyder, L. H. (2010). Idiosyncratic and systematic aspects of spatial representations in the macaque parietal cortex. *Proceedings of the National Academy of Sciences of the United States of America*, *107*(17), 7951-7956. doi: 10.1073/pnas.0913209107

Ciavarro, M., Ambrosini, E., Tosoni, A., Committeri, G., Fattori, P., & Galletti, C. (2013). rTMS of medial parieto-occipital cortex interferes with attentional reorienting during attention and reaching tasks. *Journal of Cognitive Neuroscience*, *25*(9), 1453-1462. doi: 10.1162/jocn_a_00409

Cloutman, L. L. (2013). Interaction between dorsal and ventral processing streams : Where, when and how ? *Brain and Language*, *127*(2), 251-263. doi: 10.1016/j.bandl.2012.08.003

Clower, D. M., West, R. A., Lynch, J. C., & Strick, P. L. (2001). The inferior parietal lobule is the target of output from the superior colliculus, hippocampus, and cerebellum. *The Journal of Neuroscience : The Official Journal of the Society for Neuroscience*, *21*(16), 6283-6291.

Cohen, D. A., Prud'homme, M. J., & Kalaska, J. F. (1994). Tactile activity in primate primary somatosensory cortex during active arm movements : Correlation with receptive field properties. *Journal of Neurophysiology*, *71*(1), 161-172.

Cohen, Y. E. (2009). Multimodal activity in the parietal cortex. *Hearing Research*, *258*(1-2), 100-105. doi: 10.1016/j.heares.2009.01.011

Cohen, Y. E., & Andersen, R. A. (2002). A common reference frame for movement plans in the posterior parietal cortex. *Nature Reviews. Neuroscience*, *3*(7), 553-562. doi: 10.1038/nrn873

Colby, C. L., & Duhamel, J. R. (1996). Spatial representations for action in parietal cortex. *Brain Research. Cognitive Brain Research*, *5*(1-2), 105-115.

Colby, C. L., Duhamel, J. R., & Goldberg, M. E. (1995). Oculocentric spatial representation in parietal cortex. *Cerebral Cortex (New York, N.Y. : 1991)*, *5*(5), 470-481.

Colby, C. L., Gattass, R., Olson, C. R., & Gross, C. G. (1988). Topographical organization of cortical afferents to extrastriate visual area PO in the macaque : A dual tracer study. *The Journal of Comparative Neurology*, *269*(3), 392-413. doi: 10.1002/cne.902690307

Colby, C. L., & Goldberg, M. E. (1999). Space and attention in parietal cortex. *Annual Review of Neuroscience*, *22*, 319-349. doi: 10.1146/annurev.neuro.22.1.319

Cooke, J. D., & Diggles, V. A. (1984). Rapid error correction during human arm movements : Evidence for central monitoring. *Journal of Motor Behavior*, *16*(4), 348-363.

Cordo, P. (1990). Kinesthetic control of a multijoint movement sequence. *Journal of Neurophysiology*, *63*(1), 161-172. doi: 10.1152/jn.1990.63.1.161

Crawford, J. R., & Garthwaite, P. H. (2002). Investigation of the single case in neuropsychology : Confidence limits on the abnormality of test scores and test score differences. *Neuropsychologia*, *40*(8), 1196-1208.

Crawford, J. R., & Howell, D. C. (1998). Comparing an Individual's Test Score Against Norms Derived from Small Samples. *The Clinical Neuropsychologist*, *12*(4), 482-486. doi: 10.1076/clin.12.4.482.7241

Culham, J. C., Cavina-Pratesi, C., & Singhal, A. (2006). The role of parietal cortex in visuomotor control : What have we learned from neuroimaging ? *Neuropsychologia*, *44*(13), 2668-2684. doi: 10.1016/j.neuropsychologia.2005.11.003

Danckert, J., & Goodale, M. A. (2001). Superior performance for visually guided pointing in the lower visual field. *Experimental Brain Research*, *137*(3-4), 303-308.

de Vignemont, F., Ehrsson, H. H., & Haggard, P. (2005). Bodily illusions modulate tactile perception. *Current biology : CB*, *15*(14), 1286-1290. doi: 10.1016/j.cub.2005.06.067

Deneve, S., & Pouget, A. (2004). Bayesian multisensory integration and cross-modal spatial links. *Journal of physiology, Paris*, *98*(1-3), 249-258. doi: 10.1016/j.jphysparis.2004.03.011

Desmurget, M., Epstein, C. M., Turner, R. S., Prablanc, C., Alexander, G. E., & Grafton, S. T. (1999). Role of the posterior parietal cortex in updating reaching movements to a visual target. *Nature Neuroscience*, *2*(6), 563-567. doi: 10.1038/9219

Desmurget, M., & Grafton, S. T. (2000). Forward modeling allows feedback control for fast reaching movements. *Trends in Cognitive Sciences*, *4*(11), 423-431.

Desmurget, M., Gréa, H., Grethe, J. S., Prablanc, C., Alexander, G. E., & Grafton, S. T. (2001). Functional anatomy of nonvisual feedback loops during reaching : A positron emission tomography study. *The Journal of Neuroscience : The Official Journal of the Society for Neuroscience*, *21*(8), 2919-2928.

Desmurget, M., Rossetti, Y., Jordan, M., Meckler, C., & Prablanc, C. (1997). Viewing the hand prior to movement improves accuracy of pointing performed toward the unseen contralateral hand. *Experimental Brain Research*, *115*(1), 180-186.

Desmurget, M., Rossetti, Y., Prablanc, C., Stelmach, G. E., & Jeannerod, M. (1995). Representation of hand position prior to movement and motor variability. *Canadian Journal of Physiology and Pharmacology*, *73*(2), 262-272.

Dijkerman, H. C., & de Haan, E. H. F. (2007). Somatosensory processes subserving perception and action. *The Behavioral and brain sciences*, *30*(2), 189-201 ; discussion 201-239. doi: 10.1017/S0140525X07001392

Dijkerman, H. C., McIntosh, R. D., Anema, H. A., de Haan, E. H. F., Kappelle, L. J., & Milner, A. D. (2006). Reaching errors in optic ataxia are linked to eye position rather than head or body position. *Neuropsychologia*, *44*(13), 2766-2773. doi: 10.1016/j.neuropsychologia.2005.10.018

Distler, C., Boussaoud, D., Desimone, R., & Ungerleider, L. G. (1993). Cortical connections of

inferior temporal area TEO in macaque monkeys. *The Journal of Comparative Neurology*, *334*(1), 125-150. doi: 10.1002/cne.903340111

Duhamel, J. R., Colby, C. L., & Goldberg, M. E. (1992). The updating of the representation of visual space in parietal cortex by intended eye movements. *Science (New York, N.Y.)*, *255*(5040), 90-92.

Duhamel, J. R., Colby, C. L., & Goldberg, M. E. (1998). Ventral intraparietal area of the macaque : Congruent visual and somatic response properties. *Journal of Neurophysiology*, *79*(1), 126-136. doi: 10.1152/jn.1998.79.1.126

Elliott, D., Garson, R. G., Goodman, D., & Chua, R. (1991). Discrete vs. continuous visual control of manual aiming. *Human Movement Science*, *10*(4), 393-418. doi: 10.1016/0167-9457(91)90013-N

Elliott, D. B., Vale, A., Whitaker, D., & Buckley, J. G. (2009). Does my step look big in this ? A visual illusion leads to safer stepping behaviour. *PloS One*, *4*(2), e4577. doi: 10.1371/journal.pone.0004577

Ernst, M. O. (2006). A Bayesian view on multimodal cue integration. In G. Knoblich, I. M. Thornton, M. Grosjean, & M. Shiffrar (Eds.), *Human Body Perception From the Inside Out* (p. 105-131). Oxford University Press.

Ernst, M. O., & Banks, M. S. (2002). Humans integrate visual and haptic information in a statistically optimal fashion. *Nature*, *415*(6870), 429-433. doi: 10.1038/415429a

Ernst, M. O., Banks, M. S., & Bülthoff, H. H. (2000). Touch can change visual slant perception. *Nature Neuroscience*, *3*(1), 69-73. doi: 10.1038/71140

Ernst, M. O., & Bülthoff, H. H. (2004). Merging the senses into a robust percept. *Trends in Cognitive Sciences*, *8*(4), 162-169. doi: 10.1016/j.tics.2004.02.002

Eskandar, E. N., & Assad, J. A. (1999). Dissociation of visual, motor and predictive signals in parietal cortex during visual guidance. *Nature Neuroscience*, *2*(1), 88-93. doi: 10.1038/4594

Eskandar, E. N., & Assad, J. A. (2002). Distinct nature of directional signals among parietal cortical areas during visual guidance. *Journal of Neurophysiology*, *88*(4), 1777-1790. doi: 10.1152/jn.2002.88.4.1777

Fattori, P., Breveglieri, R., Bosco, A., Gamberini, M., & Galletti, C. (02 01, 2017). Vision for Prehension in the Medial Parietal Cortex. *Cerebral Cortex (New York, N.Y. : 1991)*, *27*(2), 1149-1163. doi: 10.1093/cercor/bhv302

Fattori, P., Kutz, D. F., Breveglieri, R., Marzocchi, N., & Galletti, C. (2005). Spatial tuning of reaching activity in the medial parieto-occipital cortex (area V6A) of macaque monkey. *The European Journal of Neuroscience*, *22*(4), 956-972. doi: 10.1111/j.1460-9568.2005.04288.x

Fernandes, H. L., Stevenson, I. H., Vilares, I., & Kording, K. P. (2014). The generalization of prior uncertainty during reaching. *The Journal of Neuroscience : The Official Journal of the Society for Neuroscience*, *34*(34), 11470-11484. doi: 10.1523/JNEUROSCI.3882-13.2014

Ferraina, S., Garasto, M. R., Battaglia-Mayer, A., Ferraresi, P., Johnson, P. B., Lacquaniti, F., & Caminiti, R. (1997). Visual control of hand-reaching movement : Activity in parietal area 7m. *The European Journal of Neuroscience*, *9*(5), 1090-1095.

Fetsch, C. R., Pouget, A., DeAngelis, G. C., & Angelaki, D. E. (2011). Neural correlates of reliability-based cue weighting during multisensory integration. *Nature Neuroscience*, *15*(1), 146-154. doi: 10.1038/nn.2983

Filimon, F. (2010). Human cortical control of hand movements : Parietofrontal networks for reaching, grasping, and pointing. *The Neuroscientist : A Review Journal Bringing Neurobiology, Neurology and Psychiatry*, *16*(4), 388-407. doi: 10.1177/1073858410375468

Filimon, F., Nelson, J. D., Huang, R.-S., & Sereno, M. I. (2009). Multiple parietal reach regions in humans : Cortical representations for visual and proprioceptive feedback during

on-line reaching. *The Journal of Neuroscience : The Official Journal of the Society for Neuroscience*, *29*(9), 2961-2971. doi: 10.1523/JNEUROSCI.3211-08.2009

Flanders, M., Tillery, S. I. H., & Soechting, J. F. (1992). *Early stages in a sensorimotor transformation.* /core/journals/behavioral-and-brain-sciences/article/early-stages-in-a-sensorimotor-transformation/E29673428D0DB9CA425C5EA91B7131D4. doi: 10.1017/S0140525X00068813

Frey, S. H., Vinton, D., Norlund, R., & Grafton, S. T. (2005). Cortical topography of human anterior intraparietal cortex active during visually guided grasping. *Brain Research. Cognitive Brain Research*, *23*(2-3), 397-405. doi: 10.1016/j.cogbrainres.2004.11.010

Galletti, C., Fattori, P., Battaglini, P. P., Shipp, S., & Zeki, S. (1996). Functional demarcation of a border between areas V6 and V6A in the superior parietal gyrus of the macaque monkey. *The European Journal of Neuroscience*, *8*(1), 30-52.

Galletti, C., Fattori, P., Kutz, D. F., & Gamberini, M. (1999). Brain location and visual topography of cortical area V6A in the macaque monkey. *The European Journal of Neuroscience*, *11*(2), 575-582.

Garcin, R., Rondot, P., & de Recondo, J. (1967). Ataxie optique localisée aux deux hémichamps visuels homonymes gauches. *Revue de Neurologie (Paris)*, *116*, 707-714.

Gaveau, V., Pélisson, D., Blangero, A., Urquizar, C., Prablanc, C., Vighetto, A., & Pisella, L. (2008). Saccade control and eye-hand coordination in optic ataxia. *Neuropsychologia*, *46*(2), 475-486. doi: 10.1016/j.neuropsychologia.2007.08.028

Gharbawie, O. A., Stepniewska, I., & Kaas, J. H. (2011). Cortical connections of functional zones in posterior parietal cortex and frontal cortex motor regions in new world monkeys. *Cerebral Cortex (New York, N.Y. : 1991)*, *21*(9), 1981-2002. doi: 10.1093/cercor/bhq260

Ghazanfar, A. A., & Schroeder, C. E. (2006). Is neocortex essentially multisensory ? *Trends in Cognitive Sciences*, *10*(6), 278-285. doi: 10.1016/j.tics.2006.04.008

Ghez, C., Favilla, M., Ghilardi, M. F., Gordon, J., Bermejo, R., & Pullman, S. (1997). Discrete and continuous planning of hand movements and isometric force trajectories. *Experimental Brain Research*, *115*(2), 217-233.

Ghez, C., Gordon, J., & Ghilardi, M. F. (1995). Impairments of reaching movements in patients without proprioception. II. Effects of visual information on accuracy. *Journal of Neurophysiology*, *73*(1), 361-372.

Ghilardi, M. F., Gordon, J., & Ghez, C. (1995). Learning a visuomotor transformation in a local area of work space produces directional biases in other areas. *Journal of Neurophysiology*, *73*(6), 2535-2539.

Gilman, S. (2002). Joint position sense and vibration sense : Anatomical organisation and assessment. *Journal of Neurology, Neurosurgery, and Psychiatry*, *73*(5), 473-477. doi: 10.1136/jnnp.73.5.473

Gleiss, S., & Kayser, C. (2012). Audio-visual detection benefits in the rat. *PloS One*, *7*(9), e45677. doi: 10.1371/journal.pone.0045677

Glickstein, M. (2000). How are visual areas of the brain connected to motor areas for the sensory guidance of movement ? *Trends in Neurosciences*, *23*(12), 613-617.

Goble, D. J., & Brown, S. H. (2008). Upper limb asymmetries in the matching of proprioceptive versus visual targets. *Journal of Neurophysiology*, *99*(6), 3063-3074. doi: 10.1152/jn.90259.2008

Godfroy-Cooper, M., Sandor, P. M. B., Miller, J. D., & Welch, R. B. (2015). The interaction of vision and audition in two-dimensional space. *Frontiers in Neuroscience*, *9*, 311. doi: 10.3389/fnins.2015.00311

Goodale, M. A., Meenan, J. P., Bülthoff, H. H., Nicolle, D. A., Murphy, K. J., & Racicot, C. I. (1994). Separate neural pathways for the visual analysis of object shape in perception and prehension. *Current biology : CB*, *4*(7), 604-610.

Goodale, M. A., & Milner, A. D. (1992). Separate visual pathways for perception and action.

Trends in neurosciences, *15*(1), 20-25.

Goodale, M. A., Pelisson, D., & Prablanc, C. (1986). Large adjustments in visually guided reaching do not depend on vision of the hand or perception of target displacement. *Nature*, *320*(6064), 748-750. doi: 10.1038/320748a0

Gordon, A. M., & Soechting, J. F. (1995). Use of tactile afferent information in sequential finger movements. *Experimental Brain Research*, *107*(2), 281-292.

Gordon, J., Ghilardi, M. F., & Ghez, C. (1995). Impairments of reaching movements in patients without proprioception. I. Spatial errors. *Journal of Neurophysiology*, *73*(1), 347-360.

Graziano, M. S., Cooke, D. F., & Taylor, C. S. (2000). Coding the location of the arm by sight. *Science (New York, N.Y.)*, *290*(5497), 1782-1786.

Gréa, H., Pisella, L., Rossetti, Y., Desmurget, M., Tilikete, C., Grafton, S., ... Vighetto, A. (2002). A lesion of the posterior parietal cortex disrupts on-line adjustments during aiming movements. *Neuropsychologia*, *40*(13), 2471-2480.

Grefkes, C., Ritzl, A., Zilles, K., & Fink, G. R. (2004). Human medial intraparietal cortex subserves visuomotor coordinate transformation. *NeuroImage*, *23*(4), 1494-1506. doi: 10.1016/j.neuroimage.2004.08.031

Grefkes, C., Weiss, P. H., Zilles, K., & Fink, G. R. (2002). Crossmodal processing of object features in human anterior intraparietal cortex : An fMRI study implies equivalencies between humans and monkeys. *Neuron*, *35*(1), 173-184.

Hadders-Algra, M. (2013). Typical and atypical development of reaching and postural control in infancy. *Developmental Medicine and Child Neurology*, *55 Suppl 4*, 5-8. doi: 10.1111/dmcn.12298

Hairston, W. D., Wallace, M. T., Vaughan, J. W., Stein, B. E., Norris, J. L., & Schirillo, J. A. (2003). Visual localization ability influences cross-modal bias. *Journal of Cognitive Neuroscience*, *15*(1), 20-29. doi: 10.1162/089892903321107792

Helms Tillery, S. I., Flanders, M., & Soechting, J. F. (1994). Errors in kinesthetic transformations for hand apposition. *Neuroreport*, *6*(1), 177-181.

Holm, S. (1979). A Simple Sequentially Rejective Multiple Test Procedure. *Scandinavian Journal of Statistics*, *6*(2), 65-70.

Holmes, G. (1918). Disturbances of visual orientation. *The British Journal of Ophthalmology*, *2*(9), 449-468.

Holmes, N. P., & Spence, C. (2004). The body schema and the multisensory representation(s) of peripersonal space. *Cognitive processing*, *5*(2), 94-105. doi: 10.1007/s10339-004-0013-3

Hwang, E. J., Hauschild, M., Wilke, M., & Andersen, R. A. (2012). Inactivation of the parietal reach region causes optic ataxia, impairing reaches but not saccades. *Neuron*, *76*(5), 1021-1029. doi: 10.1016/j.neuron.2012.10.030

Jackson, S. R., Newport, R., Mort, D., & Husain, M. (2005). Where the eye looks, the hand follows ; limb-dependent magnetic misreaching in optic ataxia. *Current biology : CB*, *15*(1), 42-46. doi: 10.1016/j.cub.2004.12.063

Jackson, S. R., & Shaw, A. (2000). The Ponzo illusion affects grip-force but not grip-aperture scaling during prehension movements. *Journal of Experimental Psychology. Human Perception and Performance*, *26*(1), 418-423.

Jacobs, R. A. (1999). Optimal integration of texture and motion cues to depth. *Vision Research*, *39*(21), 3621-3629.

Jacobs, R. A. (2002). What determines visual cue reliability ? *Trends in Cognitive Sciences*, *6*(8), 345-350.

Jacobs, R. A., & Fine, I. (1999). Experience-dependent integration of texture and motion cues to depth. *Vision Research*, *39*(24), 4062-4075.

Jeannerod, M. (1986). Mechanisms of visuomotor coordination : A study in normal and brain-damaged subjects. *Neuropsychologia*, *24*(1), 41-78.

Jeannerod, M., & Rossetti, Y. (1993). Visuomotor coordination as a dissociable visual function : Experimental and clinical evidence. *Bailliere's Clinical Neurology*, *2*(2), 439-460.

Johnson, H., Van Beers, R. J., & Haggard, P. (2002). Action and awareness in pointing tasks. *Experimental Brain Research*, *146*(4), 451-459. doi: 10.1007/s00221-002-1200-z

Johnson, P. B., Ferraina, S., Bianchi, L., & Caminiti, R. (1996). Cortical networks for visual reaching : Physiological and anatomical organization of frontal and parietal lobe arm regions. *Cerebral Cortex (New York, N.Y. : 1991)*, *6*(2), 102-119.

Jones, S. A. H., Byrne, P. A., Fiehler, K., & Henriques, D. Y. P. (2012). Reach endpoint errors do not vary with movement path of the proprioceptive target. *Journal of Neurophysiology*, *107*(12), 3316-3324. doi: 10.1152/jn.00901.2011

Jones, S. A. H., Cressman, E. K., & Henriques, D. Y. P. (2010). Proprioceptive localization of the left and right hands. *Experimental brain research*, *204*(3), 373-383. doi: 10.1007/s00221-009-2079-8

Kalaska, J. F., Caminiti, R., & Georgopoulos, A. P. (1983). Cortical mechanisms related to the direction of two-dimensional arm movements : Relations in parietal area 5 and comparison with motor cortex. *Experimental Brain Research*, *51*(2), 247-260.

Kalaska, J. F., Cisek, P., & Gosselin-Kessiby, N. (2003). Mechanisms of selection and guidance of reaching movements in the parietal lobe. *Advances in Neurology*, *93*, 97-119.

Kandel, E. R., Schwartz, J. H., Jessell, T. M., Siegelbaum, S. A., & Hudspeth, A. J. (2013). *Principles of Neural Science, Fifth Edition*. McGraw Hill Professional.

Karnath, H.-O., & Perenin, M.-T. (2005). Cortical control of visually guided reaching : Evidence from patients with optic ataxia. *Cerebral Cortex (New York, N.Y. : 1991)*, *15*(10), 1561-1569. doi: 10.1093/cercor/bhi034

Kawato, M. (1999). Internal models for motor control and trajectory planning. *Current Opinion in Neurobiology*, *9*(6), 718-727.

Kawato, M., & Gomi, H. (1992). A computational model of four regions of the cerebellum based on feedback-error learning. *Biological Cybernetics*, *68*(2), 95-103.

Kayser, C., & Shams, L. (2015). Multisensory causal inference in the brain. *PLoS biology*, *13*(2), e1002075. doi: 10.1371/journal.pbio.1002075

Khan, A. Z., Blangero, A., Rossetti, Y., Salemme, R., Luauté, J., Deubel, H., ... Pisella, L. (2009). Parietal Damage Dissociates Saccade Planning from Presaccadic Perceptual Facilitation. *Cerebral Cortex*, *19*(2), 383-387. doi: 10.1093/cercor/bhn088

Khan, A. Z., Crawford, J. D., Blohm, G., Urquizar, C., Rossetti, Y., & Pisella, L. (2007). Influence of initial hand and target position on reach errors in optic ataxic and normal subjects. *Journal of Vision*, *7*(5), 8.1-16. doi: 10.1167/7.5.8

Khan, A. Z., Pisella, L., Rossetti, Y., Vighetto, A., & Crawford, J. D. (2005). Impairment of gaze-centered updating of reach targets in bilateral parietal-occipital damaged patients. *Cerebral cortex (New York, N.Y. : 1991)*, *15*(10), 1547-1560. doi: 10.1093/cercor/bhi033

Khan, A. Z., Pisella, L., Vighetto, A., Cotton, F., Luauté, J., Boisson, D., ... Rossetti, Y. (2005). Optic ataxia errors depend on remapped, not viewed, target location. *Nature Neuroscience*, *8*(4), 418-420. doi: 10.1038/nn1425

Khan, A. Z., Prost-Lefebvre, M., Salemme, R., Blohm, G., Rossetti, Y., Tilikete, C., & Pisella, L. (2016). The Attentional Fields of Visual Search in Simultanagnosia and Healthy Individuals : How Object and Space Attention Interact. *Cerebral Cortex (New York, N.Y. : 1991)*, *26*(3), 1242-1254. doi: 10.1093/cercor/bhv059

Kim, S. S., Gomez-Ramirez, M., Thakur, P. H., & Hsiao, S. S. (2015). Multimodal interactions between proprioceptive and cutaneous signals in primary somatosensory cortex. *Neuron*, *86*(2), 555-566. doi: 10.1016/j.neuron.2015.03.020

Knill, D. C. (2005). Reaching for visual cues to depth : The brain combines depth cues differently for motor control and perception. *Journal of Vision*, *5*(2), 103-115. doi: 10.1167/5.2.2

Knill, D. C., & Pouget, A. (2004). The Bayesian brain : The role of uncertainty in neural coding

and computation. *Trends in Neurosciences*, *27*(12), 712-719. doi: 10.1016/j.tins.2004.10.007

Koch, G., Cercignani, M., Pecchioli, C., Versace, V., Oliveri, M., Caltagirone, C., ... Bozzali, M. (2010). In vivo definition of parieto-motor connections involved in planning of grasping movements. *NeuroImage*, *51*(1), 300-312. doi: 10.1016/j.neuroimage.2010.02.022

Koenigs, M., Barbey, A. K., Postle, B. R., & Grafman, J. (2009). Superior parietal cortex is critical for the manipulation of information in working memory. *The Journal of Neuroscience : The Official Journal of the Society for Neuroscience*, *29*(47), 14980-14986. doi: 10.1523/JNEUROSCI.3706-09.2009

Körding, K. P., Beierholm, U., Ma, W. J., Quartz, S., Tenenbaum, J. B., & Shams, L. (2007). Causal inference in multisensory perception. *PloS One*, *2*(9), e943. doi: 10.1371/journal.pone.0000943

Körding, K. P., & Wolpert, D. M. (2004). Bayesian integration in sensorimotor learning. *Nature*, *427*(6971), 244-247. doi: 10.1038/nature02169

Koyama, M., Hasegawa, I., Osada, T., Adachi, Y., Nakahara, K., & Miyashita, Y. (2004). Functional magnetic resonance imaging of macaque monkeys performing visually guided saccade tasks : Comparison of cortical eye fields with humans. *Neuron*, *41*(5), 795-807.

Lackner, J. R., & Dizio, P. (1994). Rapid adaptation to Coriolis force perturbations of arm trajectory. *Journal of Neurophysiology*, *72*(1), 299-313.

Lackner, J. R., & Shenker, B. (1985). Proprioceptive influences on auditory and visual spatial localization. *The Journal of Neuroscience : The Official Journal of the Society for Neuroscience*, *5*(3), 579-583.

Lacquaniti, F., Guigon, E., Bianchi, L., Ferraina, S., & Caminiti, R. (1995). Representing spatial information for limb movement : Role of area 5 in the monkey. *Cerebral Cortex (New York, N.Y. : 1991)*, *5*(5), 391-409.

Lakens, D. (2016). Equivalence Tests : A Practical Primer for t-Tests, Correlations, and Meta-Analyses. *PsyArXiv*. doi: 10.1177/1948550617697177

Lalanne, C., & Lorenceau, J. (2004). Crossmodal integration for perception and action. *Journal of Physiology, Paris*, *98*(1-3), 265-279. doi: 10.1016/j.jphysparis.2004.06.001

Larish, D. D., Volp, C. M., & Wallace, S. A. (1984). An empirical note on attaining a spatial target after distorting the initial conditions of movement via muscle vibration. *Journal of Motor Behavior*, *16*(1), 76-83.

Livingstone, M., & Hubel, D. (1988). Segregation of form, color, movement, and depth : Anatomy, physiology, and perception. *Science (New York, N.Y.)*, *240*(4853), 740-749.

Macefield, V. G. (2005). Physiological characteristics of low-threshold mechanoreceptors in joints, muscle and skin in human subjects. *Clinical and Experimental Pharmacology & Physiology*, *32*(1-2), 135-144. doi: 10.1111/j.1440-1681.2005.04143.x

Mamassian, P. (2008). Overconfidence in an objective anticipatory motor task. *Psychological Science*, *19*(6), 601-606. doi: 10.1111/j.1467-9280.2008.02129.x

Manto, M., Godaux, E., & Jacquy, J. (1994). Cerebellar hypermetria is larger when the inertial load is artificially increased. *Annals of Neurology*, *35*(1), 45-52. doi: 10.1002/ana.410350108

Marconi, B., Genovesio, A., Battaglia-Mayer, A., Ferraina, S., Squatrito, S., Molinari, M., ... Caminiti, R. (2001). Eye-hand coordination during reaching. I. Anatomical relationships between parietal and frontal cortex. *Cerebral Cortex (New York, N.Y. : 1991)*, *11*(6), 513-527.

Martin, J. H., Cooper, S. E., Hacking, A., & Ghez, C. (2000). Differential effects of deep cerebellar nuclei inactivation on reaching and adaptive control. *Journal of Neurophysiology*, *83*(4), 1886-1899. doi: 10.1152/jn.2000.83.4.1886

McCarley, J. S., Kramer, A. F., & DiGirolamo, G. J. (2003). Differential effects of the Müller-Lyer illusion on reflexive and voluntary saccades. *Journal of Vision*, *3*(11), 751-760. doi:

10.1167/3.11.9

McGuire, L. M. M., & Sabes, P. N. (2009). Sensory transformations and the use of multiple reference frames for reach planning. *Nature Neuroscience*, *12*(8), 1056-1061. doi: 10.1038/nn.2357

McIntyre, J., Stratta, F., & Lacquaniti, F. (1997). Viewer-centered frame of reference for pointing to memorized targets in three-dimensional space. *Journal of Neurophysiology*, *78*(3), 1601-1618. doi: 10.1152/jn.1997.78.3.1601

McIntyre, J., Stratta, F., & Lacquaniti, F. (1998). Short-term memory for reaching to visual targets : Psychophysical evidence for body-centered reference frames. *The Journal of Neuroscience : The Official Journal of the Society for Neuroscience*, *18*(20), 8423-8435.

Medendorp, W. P., Goltz, H. C., Crawford, J. D., & Vilis, T. (2005). Integration of target and effector information in human posterior parietal cortex for the planning of action. *Journal of Neurophysiology*, *93*(2), 954-962. doi: 10.1152/jn.00725.2004

Meredith, M. A., Nemitz, J. W., & Stein, B. E. (1987). Determinants of multisensory integration in superior colliculus neurons. I. Temporal factors. *The Journal of Neuroscience : The Official Journal of the Society for Neuroscience*, *7*(10), 3215-3229.

Meredith, M. A., & Stein, B. E. (1986). Visual, auditory, and somatosensory convergence on cells in superior colliculus results in multisensory integration. *Journal of Neurophysiology*, *56*(3), 640-662. doi: 10.1152/jn.1986.56.3.640

Meredith, M. A., & Stein, B. E. (1996). Spatial determinants of multisensory integration in cat superior colliculus neurons. *Journal of Neurophysiology*, *75*(5), 1843-1857. doi: 10.1152/jn.1996.75.5.1843

Miall, R. C., Christensen, L. O. D., Cain, O., & Stanley, J. (2007). Disruption of state estimation in the human lateral cerebellum. *PLoS biology*, *5*(11), e316. doi: 10.1371/journal.pbio.0050316

Milner, A. D., & Goodale, M. A. (1995). *The visual brain in action*. Oxford University Press.

Milner, A. D., Paulignan, Y., Dijkerman, H. C., Michel, F., & Jeannerod, M. (1999). A paradoxical improvement of misreaching in optic ataxia : New evidence for two separate neural systems for visual localization. *Proceedings. Biological Sciences / The Royal Society*, *266*(1434), 2225-2229. doi: 10.1098/rspb.1999.0912

Mishkin, M., Ungerleider, L. G., & Macko, K. A. (1983). Object vision and spatial vision : Two cortical pathways. *Trends in Neurosciences*, *6*, 414-417. doi: 10.1016/0166-2236(83)90190-X

Moberg, E. (1983). The role of cutaneous afferents in position sense, kinaesthesia, and motor function of the hand. *Brain : A Journal of Neurology*, *106 (Pt 1)*, 1-19.

Mountcastle, V. B. (2005). *The Sensory Hand : Neural Mechanisms of Somatic Sensation*. Harvard University Press.

Mountcastle, V. B., LaMotte, R. H., & Carli, G. (1972). Detection thresholds for stimuli in humans and monkeys : Comparison with threshold events in mechanoreceptive afferent nerve fibers innervating the monkey hand. *Journal of Neurophysiology*, *35*(1), 122-136. doi: 10.1152/jn.1972.35.1.122

Mountcastle, V. B., Lynch, J. C., Georgopoulos, A., Sakata, H., & Acuna, C. (1975). Posterior parietal association cortex of the monkey : Command functions for operations within extrapersonal space. *Journal of Neurophysiology*, *38*(4), 871-908. doi: 10.1152/jn.1975.38.4.871

Mullette-Gillman, O. A., Cohen, Y. E., & Groh, J. M. (2009). Motor-related signals in the intraparietal cortex encode locations in a hybrid, rather than eye-centered reference frame. *Cerebral Cortex (New York, N.Y. : 1991)*, *19*(8), 1761-1775. doi: 10.1093/cercor/bhn207

Mulliken, G. H., Musallam, S., & Andersen, R. A. (2008). Forward estimation of movement state in posterior parietal cortex. *Proceedings of the National Academy of Sciences of the United States of America*, *105*(24), 8170-8177. doi: 10.1073/pnas.0802602105

Murata, A., Gallese, V., Luppino, G., Kaseda, M., & Sakata, H. (2000). Selectivity for the shape, size, and orientation of objects for grasping in neurons of monkey parietal area AIP. *Journal of Neurophysiology*, *83*(5), 2580-2601. doi: 10.1152/jn.2000.83.5.2580

Murray, J. D., Jaramillo, J., & Wang, X.-J. (2017). Working Memory and Decision-Making in a Frontoparietal Circuit Model. *The Journal of Neuroscience : The Official Journal of the Society for Neuroscience*, *37*(50), 12167-12186. doi: 10.1523/JNEUROSCI.0343-17.2017

Nougier, V., Bard, C., Fleury, M., Teasdale, N., Cole, J., Forget, R., ... Lamarre, Y. (1996). Control of single-joint movements in deafferented patients : Evidence for amplitude coding rather than position control. *Experimental Brain Research*, *109*(3), 473-482.

O'Reilly, J. X., Jbabdi, S., & Behrens, T. E. J. (2012). How can a Bayesian approach inform neuroscience ? *The European Journal of Neuroscience*, *35*(7), 1169-1179. doi: 10.1111/j.1460-9568.2012.08010.x

Paillard, J., & Brouchon, M. (1968). Active and passive movements in the calibration of position sense. In F. SJ (Ed.), *The Neuropsychology of Spatially Oriented Behaviour* (p. 37-55). Homewood, IL : Dorsey Press.

Paillard, J., Michel, F., & Stelmach, G. (1983). Localization without content. A tactile analogue of 'blind sight'. *Archives of Neurology*, *40*(9), 548-551.

Pasalar, S., Ro, T., & Beauchamp, M. S. (2010). TMS of posterior parietal cortex disrupts visual tactile multisensory integration. *The European Journal of Neuroscience*, *31*(10), 1783-1790. doi: 10.1111/j.1460-9568.2010.07193.x

Patterson, J. R., Brown, L. E., Wagstaff, D. A., & Sainburg, R. L. (2017). Limb position drift results from misalignment of proprioceptive and visual maps. *Neuroscience*, *346*, 382-394. doi: 10.1016/j.neuroscience.2017.01.040

Pélisson, D., Prablanc, C., Goodale, M. A., & Jeannerod, M. (1986). Visual control of reaching movements without vision of the limb. *Experimental Brain Research*, *62*(2), 303-311. doi: 10.1007/BF00238849

Perenin, M. T., & Vighetto, A. (1988). Optic ataxia : A specific disruption in visuomotor mechanisms. I. Different aspects of the deficit in reaching for objects. *Brain : a journal of neurology*, *111 (Pt 3)*, 643-674.

Petrides, M., & Pandya, D. N. (1984). Projections to the frontal cortex from the posterior parietal region in the rhesus monkey. *The Journal of Comparative Neurology*, *228*(1), 105-116. doi: 10.1002/cne.902280110

Pisella, L., Gréa, H., Tilikete, C., Vighetto, A., Desmurget, M., Rode, G., ... Rossetti, Y. (2000). An 'automatic pilot' for the hand in human posterior parietal cortex : Toward reinterpreting optic ataxia. *Nature Neuroscience*, *3*(7), 729-736. doi: 10.1038/76694

Pisella, L., Sergio, L., Blangero, A., Torchin, H., Vighetto, A., & Rossetti, Y. (2009). Optic ataxia and the function of the dorsal stream : Contributions to perception and action. *Neuropsychologia*, *47*(14), 3033-3044. doi: 10.1016/j.neuropsychologia.2009.06.020

Pitzalis, S., Sereno, M. I., Committeri, G., Fattori, P., Galati, G., Tosoni, A., & Galletti, C. (2013). The human homologue of macaque area V6A. *NeuroImage*, *82*, 517-530. doi: 10.1016/j.neuroimage.2013.06.026

Pointer, J. S. (1986). The cortical magnification factor and photopic vision. *Biological Reviews of the Cambridge Philosophical Society*, *61*(2), 97-119.

Polit, A., & Bizzi, E. (1979). Characteristics of motor programs underlying arm movements in monkeys. *Journal of Neurophysiology*, *42*(1 Pt 1), 183-194. doi: 10.1152/jn.1979.42.1.183

Pouget, A., Ducom, J. C., Torri, J., & Bavelier, D. (2002). Multisensory spatial representations in eye-centered coordinates for reaching. *Cognition*, *83*(1), B1-11.

Prablanc, C., Desmurget, M., & Gréa, H. (2003). Neural control of on-line guidance of hand reaching movements. *Progress in Brain Research*, *142*, 155-170. doi: 10.1016/S0079-6123(03)42012-8

Prablanc, C., Echallier, J. E., Jeannerod, M., & Komilis, E. (1979). Optimal response of eye

and hand motor systems in pointing at a visual target. II. Static and dynamic visual cues in the control of hand movement. *Biological Cybernetics*, *35*(3), 183-187.

Prablanc, C., & Martin, O. (1992). Automatic control during hand reaching at undetected two-dimensional target displacements. *Journal of Neurophysiology*, *67*(2), 455-469. doi: 10.1152/jn.1992.67.2.455

Prablanc, C., Pélisson, D., & Goodale, M. A. (1986). Visual control of reaching movements without vision of the limb. I. Role of retinal feedback of target position in guiding the hand. *Experimental Brain Research*, *62*(2), 293-302.

Prado, J., Clavagnier, S., Otzenberger, H., Scheiber, C., Kennedy, H., & Perenin, M.-T. (2005). Two cortical systems for reaching in central and peripheral vision. *Neuron*, *48*(5), 849-858. doi: 10.1016/j.neuron.2005.10.010

Previc, F. H. (1990). Functional specialization in the lower and upper visual fields in humans : Its ecological origins and neurophysiological implications. *Behavioral and Brain Sciences*, *13*(3), 519-542. doi: 10.1017/S0140525X00080018

Prevosto, V., Graf, W., & Ugolini, G. (2011). Proprioceptive pathways to posterior parietal areas MIP and LIPv from the dorsal column nuclei and the postcentral somatosensory cortex. *The European Journal of Neuroscience*, *33*(3), 444-460. doi: 10.1111/j.1460-9568 .2010.07541.x

Prud'homme, M. J., Cohen, D. A., & Kalaska, J. F. (1994). Tactile activity in primate primary somatosensory cortex during active arm movements : Cytoarchitectonic distribution. *Journal of Neurophysiology*, *71*(1), 173-181. doi: 10.1152/jn.1994.71.1.173

Quian Quiroga, R., Snyder, L. H., Batista, A. P., Cui, H., & Andersen, R. A. (2006). Movement intention is better predicted than attention in the posterior parietal cortex. *The Journal of Neuroscience : The Official Journal of the Society for Neuroscience*, *26*(13), 3615-3620. doi: 10.1523/JNEUROSCI.3468-05.2006

Raiguel, S. E., Xiao, D. K., Marcar, V. L., & Orban, G. A. (1999). Response latency of macaque area MT/V5 neurons and its relationship to stimulus parameters. *Journal of Neurophysiology*, *82*(4), 1944-1956. doi: 10.1152/jn.1999.82.4.1944

Rao, A. K., & Gordon, A. M. (2001). Contribution of tactile information to accuracy in pointing movements. *Experimental Brain Research*, *138*(4), 438-445.

Redon, C., Hay, L., & Velay, J. L. (1991). Proprioceptive control of goal-directed movements in man, studied by means of vibratory muscle tendon stimulation. *Journal of Motor Behavior*, *23*(2), 101-108. doi: 10.1080/00222895.1991.9942027

Reichenbach, A., Thielscher, A., Peer, A., Bülthoff, H. H., & Bresciani, J.-P. (2009). Seeing the hand while reaching speeds up on-line responses to a sudden change in target position. *The Journal of Physiology*, *587*(Pt 19), 4605-4616. doi: 10.1113/jphysiol.2009.176362

Ren, L., Blohm, G., & Crawford, J. D. (2007). Comparing limb proprioception and oculomotor signals during hand-guided saccades. *Experimental Brain Research*, *182*(2), 189-198. doi: 10.1007/s00221-007-0981-5

Revol, P., Rossetti, Y., Vighetto, A., Rode, G., Boisson, D., & Pisella, L. (2003). Pointing errors in immediate and delayed conditions in unilateral optic ataxia. *Spatial Vision*, *16*(3-4), 347-364.

Rincon-Gonzalez, L., Naufel, S. N., Santos, V. J., & Helms Tillery, S. (2012). Interactions between tactile and proprioceptive representations in haptics. *Journal of Motor Behavior*, *44*(6), 391-401. doi: 10.1080/00222895.2012.746281

Rincon-Gonzalez, L., Warren, J. P., Meller, D. M., & Tillery, S. H. (2011). Haptic interaction of touch and proprioception : Implications for neuroprosthetics. *IEEE transactions on neural systems and rehabilitation engineering : a publication of the IEEE Engineering in Medicine and Biology Society*, *19*(5), 490-500. doi: 10.1109/TNSRE.2011.2166808

Rizzolatti, G., Luppino, G., & Matelli, M. (1998). The organization of the cortical motor system : New concepts. *Electroencephalography and Clinical Neurophysiology*, *106*(4), 283-296.

Roland, P. E. (1993). *Brain Activation.* Wiley.

Rossetti, Y., Desmurget, M., & Prablanc, C. (1995). Vectorial coding of movement : Vision, proprioception, or both ? *Journal of neurophysiology*, *74*(1), 457-463.

Rossetti, Y., Pisella, L., & Vighetto, A. (2003). Optic ataxia revisited : Visually guided action versus immediate visuomotor control. *Experimental Brain Research*, *153*(2), 171-179. doi: 10.1007/s00221-003-1590-6

Rossetti, Y., Revol, P., McIntosh, R., Pisella, L., Rode, G., Danckert, J., ... Milner, A. D. (2005). Visually guided reaching : Bilateral posterior parietal lesions cause a switch from fast visuomotor to slow cognitive control. *Neuropsychologia*, *43*(2), 162-177. doi: 10.1016/j.neuropsychologia.2004.11.004

Rossetti, Y., Rode, G., & Boisson, D. (1995). Implicit processing of somaesthetic information : A dissociation between where and how ? *Neuroreport*, *6*(3), 506-510.

Rossetti, Y., Stelmach, G., Desmurget, M., Prablanc, C., & Jeannerod, M. (1994). The effect of viewing the static hand prior to movement onset on pointing kinematics and variability. *Experimental Brain Research*, *101*(2), 323-330.

Rossit, S., McAdam, T., McLean, D. A., Goodale, M. A., & Culham, J. C. (2013). fMRI reveals a lower visual field preference for hand actions in human superior parieto-occipital cortex (SPOC) and precuneus. *Cortex ; a Journal Devoted to the Study of the Nervous System and Behavior*, *49*(9), 2525-2541. doi: 10.1016/j.cortex.2012.12.014

Rowland, B. A., Quessy, S., Stanford, T. R., & Stein, B. E. (2007). Multisensory integration shortens physiological response latencies. *The Journal of Neuroscience : The Official Journal of the Society for Neuroscience*, *27*(22), 5879-5884. doi: 10.1523/JNEUROSCI.4986-06.2007

Sadato, N. (2005). How the blind "see" Braille : Lessons from functional magnetic resonance imaging. *The Neuroscientist : A Review Journal Bringing Neurobiology, Neurology and Psychiatry*, *11*(6), 577-582. doi: 10.1177/1073858405277314

Sainburg, R. L., Ghilardi, M. F., Poizner, H., & Ghez, C. (1995). Control of limb dynamics in normal subjects and patients without proprioception. *Journal of Neurophysiology*, *73*(2), 820-835. doi: 10.1152/jn.1995.73.2.820

Sakata, H., Taira, M., Murata, A., & Mine, S. (1995). Neural mechanisms of visual guidance of hand action in the parietal cortex of the monkey. *Cerebral Cortex (New York, N.Y. : 1991)*, *5*(5), 429-438.

Sarlegna, F. R., Blouin, J., Bresciani, J.-P., Bourdin, C., Vercher, J.-L., & Gauthier, G. M. (2003). Target and hand position information in the online control of goal-directed arm movements. *Experimental Brain Research*, *151*(4), 524-535. doi: 10.1007/s00221-003-1504-7

Sarlegna, F. R., Gauthier, G. M., Bourdin, C., Vercher, J.-L., & Blouin, J. (2006). Internally driven control of reaching movements : A study on a proprioceptively deafferented subject. *Brain Research Bulletin*, *69*(4), 404-415. doi: 10.1016/j.brainresbull.2006.02.005

Schmidt, R. A. (1975). A Schema Theory of Discrete Motor Skill Learning. *Psychological Review*, *82*(4), 225–260.

Schuirmann, D. J. (1987). A comparison of the two one-sided tests procedure and the power approach for assessing the equivalence of average bioavailability. *Journal of Pharmacokinetics and Biopharmaceutics*, *15*(6), 657-680.

Sereno, M. I., Pitzalis, S., & Martinez, A. (2001). Mapping of contralateral space in retinotopic coordinates by a parietal cortical area in humans. *Science (New York, N.Y.)*, *294*(5545), 1350-1354. doi: 10.1126/science.1063695

Shadmehr, R., Smith, M. A., & Krakauer, J. W. (2010). Error correction, sensory prediction, and adaptation in motor control. *Annual Review of Neuroscience*, *33*, 89-108. doi: 10.1146/annurev-neuro-060909-153135

Shams, L., & Beierholm, U. R. (2010). Causal inference in perception. *Trends in Cognitive*

Sciences, *14*(9), 425-432. doi: 10.1016/j.tics.2010.07.001

Sheliga, B. M., & Miles, F. A. (2003). Perception can influence the vergence responses associated with open-loop gaze shifts in 3D. *Journal of Vision*, *3*(11), 654-676. doi: 10.1167/3.11.2

Singh-Curry, V., & Husain, M. (2009). The functional role of the inferior parietal lobe in the dorsal and ventral stream dichotomy. *Neuropsychologia*, *47*(6), 1434-1448. doi: 10.1016/j.neuropsychologia.2008.11.033

Sirigu, A., Duhamel, J. R., Cohen, L. G., Pillon, B., Dubois, B., & Agid, Y. (1996). The mental representation of hand movements after parietal cortex damage. *Science (New York, N.Y.)*, *273*(5281), 1564-1568.

Smeets, J. B., Erkelens, C. J., & Denier van der Gon, J. J. (1990). Adjustments of fast goal-directed movements in response to an unexpected inertial load. *Experimental Brain Research*, *81*(2), 303-312.

Smeets, J. B., van den Dobbelsteen, J. J., de Grave, D. D. J., van Beers, R. J., & Brenner, E. (2006). Sensory integration does not lead to sensory calibration. *Proceedings of the National Academy of Sciences of the United States of America*, *103*(49), 18781-18786. doi: 10.1073/pnas.0607687103

Snyder, L. H., Batista, A. P., & Andersen, R. A. (1997). Coding of intention in the posterior parietal cortex. *Nature*, *386*(6621), 167-170. doi: 10.1038/386167a0

Sober, S. J., & Sabes, P. N. (2003). Multisensory integration during motor planning. *The Journal of neuroscience : the official journal of the Society for Neuroscience*, *23*(18), 6982-6992.

Sober, S. J., & Sabes, P. N. (2005). Flexible strategies for sensory integration during motor planning. *Nature neuroscience*, *8*(4), 490-497. doi: 10.1038/nn1427

Soechting, J. F., & Flanders, M. (1992). Moving in three-dimensional space : Frames of reference, vectors, and coordinate systems. *Annual Review of Neuroscience*, *15*, 167-191. doi: 10.1146/annurev.ne.15.030192.001123

Soechting, J. F., & Lacquaniti, F. (1983). Modification of trajectory of a pointing movement in response to a change in target location. *Journal of Neurophysiology*, *49*(2), 548-564. doi: 10.1152/jn.1983.49.2.548

Sparks, D. L., & Hartwich-Young, R. (1989). The deep layers of the superior colliculus. *Reviews of Oculomotor Research*, *3*, 213-255.

Spijkers, W., & Lochner, P. (1994). Partial visual feedback and spatial end-point accuracy of discrete aiming movements. *Journal of Motor Behavior*, *26*(3), 283-295. doi: 10.1080/00222895.1994.9941684

Spijkers, W., & Spellerberg, S. (1995). On-line visual control of aiming movements ? *Acta Psychologica*, *90*(1-3), 333-348.

Stark, A., & Zohary, E. (2008). Parietal mapping of visuomotor transformations during human tool grasping. *Cerebral Cortex (New York, N.Y. : 1991)*, *18*(10), 2358-2368. doi: 10.1093/cercor/bhm260

Stein, B. E., & Meredith, M. A. (1993). *The Merging of the Senses*. MIT Press.

Stein, B. E., & Stanford, T. R. (2008). Multisensory integration : Current issues from the perspective of the single neuron. *Nature Reviews. Neuroscience*, *9*(4), 255-266. doi: 10.1038/nrn2331

Stein, J. F., & Glickstein, M. (1992). Role of the cerebellum in visual guidance of movement. *Physiological Reviews*, *72*(4), 967-1017. doi: 10.1152/physrev.1992.72.4.967

Stepniewska, I. (2003). The pulvinar complex. In *The Primate Visual System* (p. 53-80). Boca Raton : CRC Press.

Steyvers, M., Verschueren, S. M., Levin, O., Ouamer, M., & Swinnen, S. P. (2001). Proprioceptive control of cyclical bimanual forearm movements across different movement frequencies as revealed by means of tendon vibration. *Experimental Brain Research*, *140*(3), 326-334.

Taghizadeh, B., & Gail, A. (2014). Spatial task context makes short-latency reaches prone to induced Roelofs illusion. *Frontiers in Human Neuroscience*, *8*, 673. doi: 10.3389/

fnhum.2014.00673

Talbot, W. H., Darian-Smith, I., Kornhuber, H. H., & Mountcastle, V. B. (1968). The sense of flutter-vibration : Comparison of the human capacity with response patterns of mechanoreceptive afferents from the monkey hand. *Journal of Neurophysiology*, *31*(2), 301-334.

Tosoni, A., Pitzalis, S., Committeri, G., Fattori, P., Galletti, C., & Galati, G. (2015). Resting-state connectivity and functional specialization in human medial parieto-occipital cortex. *Brain Structure & Function*, *220*(6), 3307-3321. doi: 10.1007/s00429-014-0858-x

Trillenberg, P., Sprenger, A., Petersen, D., Kömpf, D., Heide, W., & Helmchen, C. (2007). Functional dissociation of saccade and hand reaching control with bilateral lesions of the medial wall of the intraparietal sulcus : Implications for optic ataxia. *NeuroImage*, *36 Suppl 2*, T69-76. doi: 10.1016/j.neuroimage.2007.03.038

Tuthill, J. C., & Azim, E. (2018). Proprioception. *Current biology : CB*, *28*(5), R194-R203. doi: 10.1016/j.cub.2018.01.064

Ungerleider, L. G., & Mishkin, M. (1982). Two cortical visual systems. In *Analysis of visual behavior* (pp. 549–586). Cambridge, MA : MIT Press. (OCLC : 1014738427)

van Beers, R. J., Sittig, A. C., & Denier van der Gon, J. J. (1996). How humans combine simultaneous proprioceptive and visual position information. *Experimental brain research*, *111*(2), 253-261.

van Beers, R. J., Sittig, A. C., & Denier van der Gon, J. J. (1998). The precision of proprioceptive position sense. *Experimental brain research*, *122*(4), 367-377.

van Beers, R. J., Sittig, A. C., & Denier van der Gon, J. J. (1999a). Integration of proprioceptive and visual position-information : An experimentally supported model. *Journal of neurophysiology*, *81*(3), 1355-1364.

van Beers, R. J., Sittig, A. C., & Denier van der Gon, J. J. (1999b). Localization of a seen finger is based exclusively on proprioception and on vision of the finger. *Experimental brain research*, *125*(1), 43-49.

van Beers, R. J., van Mierlo, C. M., Smeets, J. B., & Brenner, E. (2011). Reweighting visual cues by touch. *Journal of Vision*, *11*(10). doi: 10.1167/11.10.20

van Beers, R. J., Wolpert, D. M., & Haggard, P. (2002). When feeling is more important than seeing in sensorimotor adaptation. *Current biology : CB*, *12*(10), 834-837.

van der Meulen, J. H., Gooskens, R. H., Denier van der Gon, J. J., Gielen, C. C., & Wilhelm, K. (1990). Mechanisms underlying accuracy in fast goal-directed arm movements in man. *Journal of Motor Behavior*, *22*(1), 67-84.

van Donkelaar, P. (1999). Pointing movements are affected by size-contrast illusions. *Experimental Brain Research*, *125*(4), 517-520.

Vaziri, S., Diedrichsen, J., & Shadmehr, R. (2006). Why does the brain predict sensory consequences of oculomotor commands ? Optimal integration of the predicted and the actual sensory feedback. *The Journal of Neuroscience : The Official Journal of the Society for Neuroscience*, *26*(16), 4188-4197. doi: 10.1523/JNEUROSCI.4747-05.2006

Verstynen, T., & Sabes, P. N. (2011). How each movement changes the next : An experimental and theoretical study of fast adaptive priors in reaching. *The Journal of Neuroscience : The Official Journal of the Society for Neuroscience*, *31*(27), 10050-10059. doi: 10.1523/JNEUROSCI.6525-10.2011

Vesia, M., & Crawford, J. D. (2012). Specialization of reach function in human posterior parietal cortex. *Experimental Brain Research*, *221*(1), 1-18. doi: 10.1007/s00221-012-3158-9

Vesia, M., Prime, S. L., Yan, X., Sergio, L. E., & Crawford, J. D. (2010). Specificity of human parietal saccade and reach regions during transcranial magnetic stimulation. *The Journal of Neuroscience : The Official Journal of the Society for Neuroscience*, *30*(39), 13053-13065. doi: 10.1523/JNEUROSCI.1644-10.2010

Vesia, M., Yan, X., Henriques, D. Y., Sergio, L. E., & Crawford, J. D. (2008). Transcranial magnetic stimulation over human dorsal-lateral posterior parietal cortex disrupts integra-

tion of hand position signals into the reach plan. *Journal of Neurophysiology*, *100*(4), 2005-2014. doi: 10.1152/jn.90519.2008

Vighetto, A. (1980). *Étude neuropsychologique et psychophysique de l'ataxie optique* (Thèse Médecine). Université Claude Bernard Lyon 1.

Vilares, I., Howard, J. D., Fernandes, H. L., Gottfried, J. A., & Kording, K. P. (2012). Differential representations of prior and likelihood uncertainty in the human brain. *Current biology : CB*, *22*(18), 1641-1648. doi: 10.1016/j.cub.2012.07.010

Vindras, P., Blangero, A., Ota, H., Reilly, K. T., Rossetti, Y., & Pisella, L. (2016). The Pointing Errors in Optic Ataxia Reveal the Role of "Peripheral Magnification" of the PPC. *Frontiers in Integrative Neuroscience*, *10*. doi: 10.3389/fnint.2016.00027

Vindras, P., & Viviani, P. (1998). Frames of reference and control parameters in visuomanual pointing. *Journal of Experimental Psychology. Human Perception and Performance*, *24*(2), 569-591.

von Bonin, G., & Bailey, P. (1947). *The Neocortex of Macaca Mulatta*. University of Illinois Press.

von Holst, E. (1954). Relations between the central Nervous System and the peripheral organs. *The British Journal of Animal Behaviour*, *2*(3), 89-94. doi: 10.1016/S0950-5601(54)80044-X

von von Economo, C. F., & Koskinas, G. N. (1925). *Die Cytoarchitektonik der Hirnrinde des erwachsenen Menschen*. J. Springer.

Wallace, M. T., Meredith, M. A., & Stein, B. E. (1998). Multisensory integration in the superior colliculus of the alert cat. *Journal of Neurophysiology*, *80*(2), 1006-1010.

Wallace, M. T., Wilkinson, L. K., & Stein, B. E. (1996). Representation and integration of multiple sensory inputs in primate superior colliculus. *Journal of Neurophysiology*, *76*(2), 1246-1266.

Wann, J. P., & Ibrahim, S. F. (1992). Does limb proprioception drift ? *Experimental Brain Research*, *91*(1), 162-166.

Warren, J. P., Santello, M., & Helms Tillery, S. I. (2011). Effects of fusion between tactile and proprioceptive inputs on tactile perception. *PloS One*, *6*(3), e18073. doi: 10.1371/journal.pone.0018073

Watkins, S., Shams, L., Tanaka, S., Haynes, J.-D., & Rees, G. (2006). Sound alters activity in human V1 in association with illusory visual perception. *NeuroImage*, *31*(3), 1247-1256. doi: 10.1016/j.neuroimage.2006.01.016

Weber, D. J., London, B. M., Hokanson, J. A., Ayers, C. A., Gaunt, R. A., Torres, R. R., ... Miller, L. E. (2011). Limb-state information encoded by peripheral and central somatosensory neurons : Implications for an afferent interface. *IEEE transactions on neural systems and rehabilitation engineering : a publication of the IEEE Engineering in Medicine and Biology Society*, *19*(5), 501-513. doi: 10.1109/TNSRE.2011.2163145

Weerakkody, N. S., Mahns, D. A., Taylor, J. L., & Gandevia, S. C. (2007). Impairment of human proprioception by high-frequency cutaneous vibration. *The Journal of Physiology*, *581*(Pt 3), 971-980. doi: 10.1113/jphysiol.2006.126854

Weerakkody, N. S., Taylor, J. L., & Gandevia, S. C. (2009). The effect of high-frequency cutaneous vibration on different inputs subserving detection of joint movement. *Experimental Brain Research*, *197*(4), 347-355. doi: 10.1007/s00221-009-1921-3

Westwood, D. A., McEachern, T., & Roy, E. A. (2001). Delayed grasping of a Müller-Lyer figure. *Experimental Brain Research*, *141*(2), 166-173. doi: 10.1007/s002210100865

Wichmann, F. A., & Hill, N. J. (2001a). The psychometric function : I. Fitting, sampling, and goodness of fit. *Perception & Psychophysics*, *63*(8), 1293-1313.

Wichmann, F. A., & Hill, N. J. (2001b). The psychometric function : II. Bootstrap-based confidence intervals and sampling. *Perception & Psychophysics*, *63*(8), 1314-1329.

Wilson, E. T., Wong, J., & Gribble, P. L. (2010). Mapping proprioception across a 2D horizontal

workspace. *PloS One*, *5*(7), e11851. doi: 10.1371/journal.pone.0011851

Wise, S. P., Boussaoud, D., Johnson, P. B., & Caminiti, R. (1997). Premotor and parietal cortex : Corticocortical connectivity and combinatorial computations. *Annual Review of Neuroscience*, *20*, 25-42. doi: 10.1146/annurev.neuro.20.1.25

Wolpert, D. M., & Ghahramani, Z. (2000). Computational principles of movement neuroscience. *Nature Neuroscience*, *3 Suppl*, 1212-1217. doi: 10.1038/81497

Wolpert, D. M., Ghahramani, Z., & Jordan, M. I. (1995). An internal model for sensorimotor integration. *Science (New York, N.Y.)*, *269*(5232), 1880-1882.

Wolpert, D. M., Goodbody, S. J., & Husain, M. (1998). Maintaining internal representations : The role of the human superior parietal lobe. *Nature Neuroscience*, *1*(6), 529-533. doi: 10.1038/2245

Wolpert, D. M., & Miall, R. C. (1996). Forward Models for Physiological Motor Control. *Neural Networks : The Official Journal of the International Neural Network Society*, *9*(8), 1265-1279.

Wolpert, D. M., Miall, R. C., & Kawato, M. (1998). Internal models in the cerebellum. *Trends in Cognitive Sciences*, *2*(9), 338-347.

Wong, J. D., Wilson, E. T., Kistemaker, D. A., & Gribble, P. L. (2014). Bimanual proprioception : Are two hands better than one ? *Journal of Neurophysiology*, *111*(6), 1362-1368. doi: 10.1152/jn.00537.2013

Zaidel, A., Turner, A. H., & Angelaki, D. E. (2011). Multisensory calibration is independent of cue reliability. *The Journal of Neuroscience : The Official Journal of the Society for Neuroscience*, *31*(39), 13949-13962. doi: 10.1523/JNEUROSCI.2732-11.2011

Zelaznik, H. N., & Lantero, D. (1996). The role of vision in repetitive circle drawing. *Acta Psychologica*, *92*(1), 105-118.

Zhang, H., Daw, N. D., & Maloney, L. T. (2013). Testing whether humans have an accurate model of their own motor uncertainty in a speeded reaching task. *PLoS computational biology*, *9*(5), e1003080. doi: 10.1371/journal.pcbi.1003080

Zhang, H., Morvan, C., & Maloney, L. T. (2010). Gambling in the visual periphery : A conjoint-measurement analysis of human ability to judge visual uncertainty. *PLoS computational biology*, *6*(12), e1001023. doi: 10.1371/journal.pcbi.1001023

Zhong, Y.-M., & Rockland, K. S. (2003). Inferior parietal lobule projections to anterior inferotemporal cortex (area TE) in macaque monkey. *Cerebral Cortex (New York, N.Y. : 1991)*, *13*(5), 527-540.

Zhou, Y.-D., & Fuster, J. M. (2004). Somatosensory cell response to an auditory cue in a haptic memory task. *Behavioural Brain Research*, *153*(2), 573-578. doi: 10.1016/j.bbr.2003.12.024

Zmigrod, S. (2014). The role of the parietal cortex in multisensory and response integration : Evidence from transcranial direct current stimulation (tDCS). *Multisensory Research*, *27*(2), 161-172.